Polynomial Preserving Recovery

Xiaotong Niu, Nan Qiao, Qianyu Xu, Yifei Xu, Yijia Xu

September 11, 2025

1 Preliminary

Polynomial Preserving Recovery, which is proposed by Zhiming Zhang and Naga in 2005, is one great kind of post-processing method to recover the gradient at a vertex by local least-squares fitting to the finite element solution in an associated patch and then taking gradient of the least-squares fitted polynomial. In this section, it focuses on the preliminary of Polynomial Preserving Recovery (PPR) method with the briefly introduction of its progress.[2]

- Mapping each node (x, y) to the coordinate of (ξ, η)

$$(x, y) \to (\xi, \eta) = \frac{(x, y) - (x_0, y_0)}{h} \tag{1}$$

  then we can obtain $x - x_0 = h\xi$ and $y - y_0 = h\eta$.

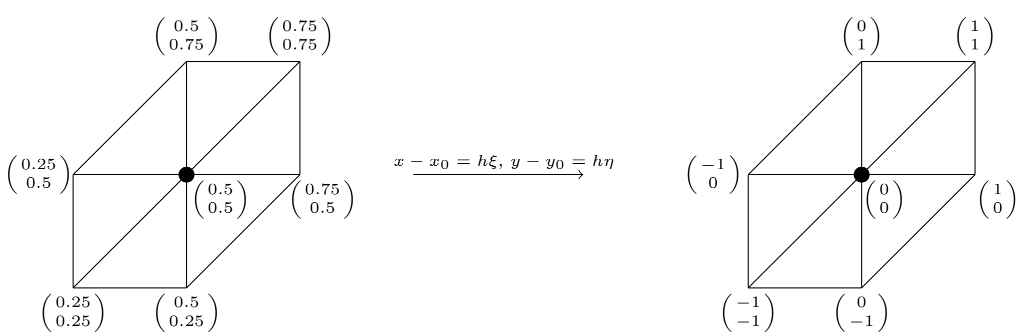

(a) Coordinate of (x, y) (b) Coordinate of (ξ, η)

Figure 1: Coordinate system mapping

In the reference coordinate,

- Fit a quadratic polynomial

$$P_z(\xi, \eta) = (1, \xi, \eta, \xi^2, \xi\eta, \eta^2)(a_1, a_2, a_3, a_4, a_5, a_6)^T \tag{2}$$

- Suppose there exist a point z, which is the origin in the reference patch, then recover gradient at that point. Denote $\vec{e}$ with the number of nodes, $\vec{\xi}$ with the horizontal coordinate of each node and $\vec{\eta}$ with the vertical one on account of the origin node in the reference coordinate.

  An example of Regular Interior,

$$\begin{aligned} \vec{e} &= (1,1,1,1,1,1,1)^T \\ \vec{\xi} &= (0,1,1,0,-1,-1,0)^T \\ \vec{\eta} &= (0,0,1,1,0,-1,-1)^T \end{aligned} \tag{3}$$

- Set matrix A

$$A = (\vec{e}, \vec{\xi}, \vec{\eta}, \vec{\xi}^2, \vec{\xi}\vec{\eta}, \vec{\eta}^2) \tag{4}$$

- Evaluate the coefficient, applying the least square fitting procedure we obtained

$$\begin{aligned} A\vec{x} =& \vec{b} \\ A^T A\vec{x} =& A^T\vec{b} \\ (A^T A)^{-1}(A^T A)\vec{x} =& (A^T A)^{-1}A^T\vec{b} \\ \vec{x} =& (A^T A)^{-1}A^T\vec{b} \end{aligned} \tag{5}$$

- $\vec{b}$ represents
  - an exact function u
  - a FEM solution u_h
  - partial derivative function $\frac{\partial u}{\partial x}$

Change the coordinate to (x, y) through $x - x_0 = h\xi$ and $y - y_0 = h\eta$.

- According to the basic pattern of binary equation

$$\begin{aligned} P_z(x,y) &= \hat{a}_1 + \hat{a}_2 x + \hat{a}_3 y + \hat{a}_4 x^2 + \hat{a}_5 xy + \hat{a}_6 y^2 \\ &= (1, x, y, x^2, xy, y^2)(\hat{a}_1, \hat{a}_2, \hat{a}_3, \hat{a}_4, \hat{a}_5, \hat{a}_6)^T \end{aligned} \tag{6}$$

- Based on $(\hat{a}_1, \hat{a}_2, \hat{a}_3, \hat{a}_4, \hat{a}_5, \hat{a}_6)^T = (a_1, ha_2, ha_3, h^2a_4, h^2a_5, h^2a_6)^T$, the polynomial will be shown as $P_z(x, y)$.

- Deducing the partial derivative of $P_z(x, y)$ with respect to x and y, we can obtain the recovered gradient at the vertex z, which is written as $G_h u(z)$.

- Use a computer algebra system Mathematica to perform Taylor expansion and the result will be depicted as a second order finite difference scheme approximating $\nabla u(z)$.

2 Examples

We manually calculate the gradient recovery on the Regular and Chevron both paid attention on the interior points and boundary points according to the method we mentioned in previous section. By this way, we use gradient recovery to post-process the finite element solution u_h.

2.1 Interior Point

Given a point u_0 as the origin worked on, the patch is comprised of the elements including u_0, which is defined as layer 1.

- **Regular Pattern**

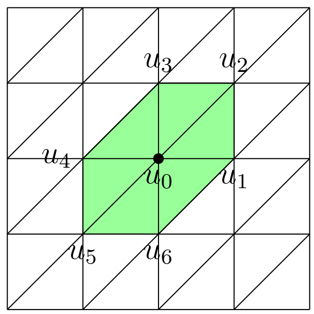

Figure 2: Regular Interior

In the Regular Interior Figure 2, we denote,

$$\vec{e} = (1,1,1,1,1,1,1)^T, \vec{\xi} = (0,1,1,0,-1,-1,0)^T \tag{7}$$

$$\vec{\eta} = (0,0,1,1,0,-1,-1)^T, A = (\vec{e}, \vec{\xi}, \vec{\eta}, \vec{\xi}^2, \vec{\xi}\vec{\eta}, \vec{\eta}^2) \tag{8}$$

Then we obtain the matrix in Matlab,

$$A = \begin{bmatrix} 1 & 0 & 0 & 0 & 0 & 0 \\ 1 & 1 & 0 & 1 & 0 & 0 \\ 1 & 1 & 1 & 1 & 1 & 1 \\ 1 & 0 & 1 & 0 & 0 & 1 \\ 1 & -1 & 0 & 1 & 0 & 0 \\ 1 & -1 & -1 & 1 & 1 & 1 \\ 1 & 0 & -1 & 0 & 0 & 1 \end{bmatrix}$$

A is a 9×6 matrix. However, according to the linear algebra we learned, the inverse matrix should be obtained from square matrix. Accordingly multiply the A by A^T, represent it as $A' * A$ in Matlab, then the matrix turns into a 6×6 square matrix like in this example and we can achieve the inverse matrix.

$$A_1 = (A^T A)^{-1} A^T = \frac{1}{6h} \begin{bmatrix} 6 & 0 & 0 & 0 & 0 & 0 & 0 \\ 0 & 2 & 1 & -1 & -2 & -1 & 1 \\ 0 & -1 & 1 & 2 & 1 & -1 & -2 \\ -6 & 3 & 0 & 0 & 3 & 0 & 0 \\ 6 & -3 & 3 & -3 & -3 & 3 & -3 \\ -6 & 0 & 0 & 3 & 0 & 0 & 3 \end{bmatrix}$$

So the binomial equation will be found as,

$$\begin{aligned} P_2(x,y) =& u_0 + \frac{1}{6h}(2u_1 + u_2 - u_3 - 2u_4 - u_5 + u_6)x + \frac{1}{6h}(-u_1 + u_2 + 2u_3 + u_4 - u_5 - 2u_6)y \\ &+ \frac{1}{6h^2}(-6u_0 + 3u_2 + 3u_5)x^2 + \frac{1}{6h^2}(6u_0 - 3u_1 + 3u_2 - 3u_3 - 3u_4 + 3u_5 - 3u_6)xy \\ &+ \frac{1}{6h^2}(-6u_0 + 3u_3 + 3u_6)y^2 \end{aligned} \tag{9}$$

Take the partial derivative to x and y, we can obtain,

$$\begin{aligned} \frac{\partial P_2(x,y)}{\partial x} =& \frac{1}{6h}(2u_1 + u_2 - u_3 - 2u_4 - u_5 + u_6) + \frac{1}{3h^2}(-6u_0 + 3u_2 + 3u_5)x + \frac{1}{6h^2}(6u_0 - 3u_1 \\ &+ 3u_2 - 3u_3 - 3u_4 + 3u_5 - 3u_6)y \end{aligned} \tag{10}$$

$$\begin{aligned} \frac{\partial P_2(x,y)}{\partial y} =& \frac{1}{6h}(-u_1 + u_2 + 2u_3 + u_4 - u_5 - 2u_6) + \frac{1}{3h^2}(-6u_0 + 3u_3 + 3u_6)y + \frac{1}{6h^2}(6u_0 - 3u_1 \\ &+ 3u_2 - 3u_3 - 3u_4 + 3u_5 - 3u_6)x \end{aligned} \tag{11}$$

Eventually, we get the recovered gradient at the origin,

$$\nabla P_2(0,0) = \frac{1}{6h} \begin{pmatrix} 2u_1 + u_2 - u_3 - 2u_4 - u_5 + u_6 \\ -u_1 + u_2 + 2u_3 + u_4 - u_5 - 2u_6 \end{pmatrix} \tag{12}$$

Taylor expansion result in,

$$G_h u(z) = \begin{pmatrix} u_x(z) + \dfrac{h^2}{6}\left(u_{xyy}(z) + u_{xxy}(z) + u_{xxx}(z)\right) + O(h^4) \\ u_y(z) + \dfrac{h^2}{6}\left(u_{yyy}(z) + u_{xyy}(z) + u_{xxy}(z)\right) + O(h^4) \end{pmatrix} \tag{13}$$

which means it is second order finite difference scheme approximating $\nabla u(z)$.

- **Chevron Pattern**

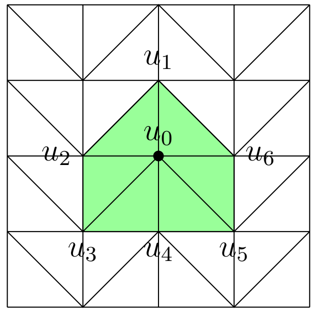

Figure 3: Chevron Interior

According to the matrix, the binary equation reveals that,

$$\begin{aligned}P_2(x,y) =&\frac{1}{6}(8u_0+2u_2-2u_3+4u_4-3u_5+2u_6)+\frac{1}{6h}(-6u_2+6u_6)x+\frac{1}{6h}(-2u_0+6u_1+u_2\\&-u_3-u_4-u_5+u_6)y+\frac{1}{6h^2}(-6u_0+3u_3+3u_6)x^2+\frac{1}{6h^2}(6u_0-3u_2+3u_3-6u_4+3u_5\\&+3u_6)xy+\frac{1}{6h^2}(-6u_0+6u_1-3u_2+3u_3+3u_5+3u_6)y^2\end{aligned} \tag{14}$$

It implies that,

$$\frac{\partial P_2(x,y)}{\partial x} =\frac{1}{6h}(-6u_2+6u_6)+\frac{1}{3h^2}(-6u_0+3u_3+3u_6)x+\frac{1}{6h^2}(6u_0-3u_2+3u_3-6u_4+3u_5+3u_6)y \tag{15}$$

$$\begin{aligned}\frac{\partial P_2(x,y)}{\partial y} =&\frac{1}{6h}(-2u_0+6u_1+u_2-u_3-u_4-u_5+u_6)+\frac{1}{3h^2}(-6u_0+6u_1-3u_2+3u_3+3u_5+3u_6)y\\&+\frac{1}{6h^2}(6u_0-3u_2+3u_3-6u_4+3u_5+3u_6)y\end{aligned} \tag{16}$$

By the partial equation, the recovered gradient on $(0,0)$ is,

$$\nabla P_2(0,0) =\frac{1}{6h}\begin{pmatrix} -6u_2+6u_6 \\ -2u_0+6u_1+u_2-u_3-4u_4-u_5+u_6 \end{pmatrix} \tag{17}$$

Taylor expansion results in,

$$G_h u(z) = \begin{pmatrix} u_x(z)+\frac{h^2}{6}\left(u_{xyy}(z)+u_{xxy}(z)+u_{xxx}(z)\right)+O\left(h^4\right) \\ u_y(z)+\frac{h^2}{6}\left(u_{yyy}(z)+u_{xyy}(z)+u_{xxy}(z)\right)+O\left(h^4\right) \end{pmatrix} \tag{18}$$

2.2 Boundary Point

Without the consideration of boundary strategy, the performance on boundary will be worse [2]. To improve the accuracy of PPR on boundary, two boundary strategies are promoted. For the first one, extending layer 2, only use the interior points on layer 1. For the second one, we also focus on the boundary points on layer 1.

- **Regular Case 1**

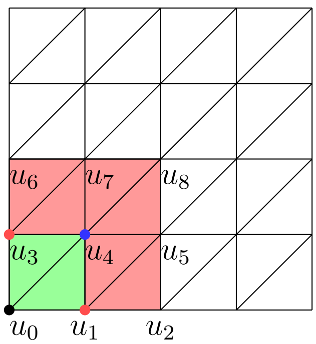

Figure 4: Regular Case 1

According to the matrix in Matlab, the binary equation of the Regular Pattern on the bottom left corner point is,

$$\begin{aligned}P_z(x,y) =& \frac{1}{36}(29u_0 + 8u_1 - 1u_2 + 8u_3 - 4u_4 - 4u_5 - u_6 - 4u_7 + 5u_8)\\ &+ \frac{1}{36h}(-27u_0 + 24u_1 + 3u_2 - 18u_3 + 24u_4 - 6u_5 - 9u_6 + 24u_7 - 15u_8)x\\ &+ \frac{1}{36h}(-27u_0 - 18u_1 - 9u_2 + 24u_3 + 24u_4 + 24u_5 + 3u_6 - 6u_7 - 15u_8)y\\ &+ \frac{1}{36h^2}(6u_0 - 12u_1 + 6u_2 + 6u_3 - 12u_4 + 6u_5 + 6u_6 - 12u_7 + 6u_8)x^2\\ &+ \frac{1}{36h^2}(9u_0 - 9u_2 - 9u_6 + 9u_8)xy\\ &+ \frac{1}{36h^2}(6u_0 + 6u_1 + 6u_2 - 12u_3 - 12u_4 - 12u_5 + 6u_6 + 6u_7 + 6u_8)y^2 \end{aligned} \tag{19}$$

Then deduce the partial x and partial y of $P_z(x, y)$,

$$\begin{aligned}\frac{\partial P_z(x,y)}{\partial x} =& \frac{1}{36h}(-27u_0 + 24u_1 + 3u_2 - 18u_3 + 24u_4 - 6u_5 - 9u_6 + 24u_7 - 15u_8)\\ &+ \frac{1}{18h^2}(6u_0 - 12u_1 + 6u_2 + 6u_3 - 12u_4 + 6u_5 + 6u_6 - 12u_7 + 6u_8)x\\ &+ \frac{1}{36h^2}(9u_0 - 9u_2 - 9u_6 + 9u_8)y \end{aligned} \tag{20}$$

$$
\begin{aligned}
\frac{\partial P_z(x,y)}{\partial y} =& \frac{1}{36h}(-27u_0 - 18u_1 - 9u_2 + 24u_3 + 24u_4 + 24u_5 + 3u_6 - 6u_7 - 15u_8) \\
&+ \frac{1}{36h^2}(9u_0 - 9u_2 - 9u_6 + 9u_8)x \\
&+ \frac{1}{18h^2}(6u_0 + 6u_1 + 6u_2 - 12u_3 - 12u_4 - 12u_5 + 6u_6 + 6u_7 + 6u_8)y
\end{aligned} \tag{21}
$$

Thus, we can get the recovered gradient at original node z,

$$
\nabla P_z(0,0) = \frac{1}{36h}\begin{pmatrix} -27u_0 + 24u_1 + 3u_2 - 18u_3 + 24u_4 - 6u_5 - 9u_6 + 24u_7 - 15u_8 \\ -27u_0 - 18u_1 - 9u_2 + 24u_3 + 24u_4 + 24u_5 + 3u_6 - 6u_7 - 15u_8 \end{pmatrix} \tag{22}
$$

Taylor expansion results in,

$$
G_h u(z) = \begin{pmatrix} u_x(z) + \frac{h^2}{6}\left(-u_{xyy}(z) - 6u_{xxy}(z) - 2u_{xxx}(z)\right) + O(h^3) \\ u_y(z) + \frac{h^2}{6}\left(-2u_{yyy}(z) - 6u_{xyy}(z) - u_{xxy}(z)\right) + O(h^3) \end{pmatrix} \tag{23}
$$

which means it is second order finite difference scheme approximating $\nabla u(z)$.

- **Regular Case 2**

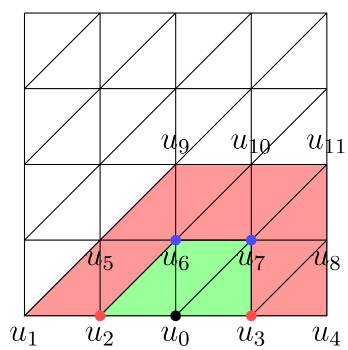

Figure 5: Regular Case 2

The equation will be indicated as,

$$\begin{aligned}P_z(x,y) =&\frac{1}{560}(232u_0 - 8u_1 + 172u_2 + 172u_3 - 8u_4 - 60u_5 + 60u_6 + 60u_7 - 60u_8 - 20u_9 \\ &+ 40u_{10} - 20u_{11}) \\ &+ \frac{1}{560h}(-104u_1 - 52u_2 + 52u_3 + 104u_4 - 24u_5 - 8u_6 + 8u_7 + 24u_8 + 20u_9 \\ &- 20u_{11})x \\ &+ \frac{1}{560h}(-218u_0 - 66u_1 - 167u_2 - 219u_3 - 170u_4 + 317u_5 + 259u_6 + 251u_7 \\ &+ 293u_8 - 95u_9 - 110u_{10} - 75u_{11})y \\ &+ \frac{1}{560h^2}(-60u_0 + 60u_1 - 30u_2 - 30u_3 + 60u_4 + 30u_5 - 30u_6 - 30u_7 + 30u_8 \\ &+ 10u_9 - 20u_{10} + 10u_{11})x^2 \\ &+ \frac{1}{560h^2}(60u_0 + 12u_1 + 66u_2 - 6u_3 - 132u_4 - 78u_5 + 14u_6 + 46u_7 + 18u_8 \\ &- 110u_9 + 20u_{10} + 90u_{11})xy \\ &+ \frac{1}{560h^2}(46u_0 + 30u_1 + 33u_2 + 69u_3 + 102u_4 - 111u_5 - 137u_6 - 153u_7 - 159u_8 \\ &+ 145u_9 + 90u_{10} + 45u_{11})y^2 \end{aligned} \tag{24}$$

Then we can derive the partial equation of x and y,

$$\begin{aligned}\frac{\partial P_z(x,y)}{\partial x} =&\frac{1}{560h}(-104u_1 - 52u_2 + 52u_3 + 104u_4 - 24u_5 - 8u_6 + 8u_7 + 24u_8 + 20u_9 \\ &- 20u_{11}) \\ &+ \frac{1}{280h^2}(-60u_0 + 60u_1 - 30u_2 - 30u_3 + 60u_4 + 30u_5 - 30u_6 - 30u_7 + 30u_8 \\ &+ 10u_9 - 20u_{10} + 10u_{11})x \\ &+ \frac{1}{560h^2}(60u_0 + 12u_1 + 66u_2 - 6u_3 - 132u_4 - 78u_5 + 14u_6 + 46u_7 + 18u_8 \\ &- 110u_9 + 20u_{10} + 90u_{11})y \end{aligned} \tag{25}$$

$$\begin{aligned}\frac{\partial P_z(x,y)}{\partial y} =&\frac{1}{560h}(-218u_0 - 66u_1 - 167u_2 - 219u_3 - 170u_4 + 317u_5 + 259u_6 + 251u_7 \\ &+ 293u_8 - 95u_9 - 110u_{10} - 75u_{11}) \\ &+ \frac{1}{560h^2}(60u_0 + 12u_1 + 66u_2 - 6u_3 - 132u_4 - 78u_5 + 14u_6 + 46u_7 + 18u_8 \\ &- 110u_9 + 20u_{10} + 90u_{11})x \\ &+ \frac{1}{280h^2}(46u_0 + 30u_1 + 33u_2 + 69u_3 + 102u_4 - 111u_5 - 137u_6 - 153u_7 \\ &- 159u_8 + 145u_9 + 90u_{10} + 45u_{11})y \end{aligned} \tag{26}$$

Finally, plug $(0, 0)$ into the partial equation, the recovered gradient will demonstrate as,

$$G_h u(z) = \frac{1}{560h} \begin{pmatrix} -104u_1 - 52u_2 + 52u_3 + 104u_4 - 24u_5 - 8u_6 + 8u_7 + 24u_8 + 20u_9 - 20u_{11} \\ -218u_0 - 66u_1 - 167u_2 - 219u_3 - 170u_4 + 317u_5 + 259u_6 + 251u_7 + 293u_8 - 95u_9 - 110u_{10} - 75u_{11} \end{pmatrix} \tag{27}$$

Taylor expansion results in,

$$G_h u(z) = \begin{pmatrix} u_x(z) + \frac{h^2}{420}\left(-30u_{xyy}(z) - 30u_{xxy}(z) + 229u_{xxx}(z)\right) + O(h^3) \\ u_y(z) + \frac{h^2}{840}\left(-280u_{yyy}(z) - 390u_{xyy}(z) + 690u_{xxy}(z) + 171u_{xxx}(z)\right) + O(h^3) \end{pmatrix} \tag{28}$$

which means it is second order finite difference scheme approximating $\nabla u(z)$.

- **Regular Case 3**

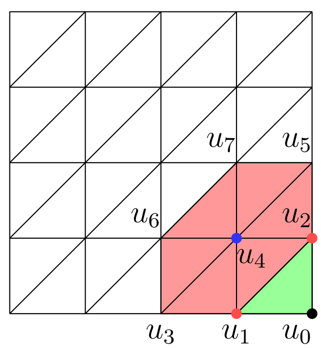

Figure 6: Regular Case 3

The binomial equation will imply to,

$$\begin{aligned} P_z(x, y) =& \frac{1}{42}(38u_0 + 6u_1 + 6u_2 - 2u_3 - 8u_4 - 2u_5 + 2u_6 + 2u_7) \\ &+ \frac{1}{42h}(44u_0 - 38u_1 + 11u_2 - 6u_3 - 38u_4 + 8u_5 + 27u_6 - 8u_7)x \\ &+ \frac{1}{42h}(-44u_0 - 11u_1 + 38u_2 - 8u_3 + 38u_4 + 6u_5 + 8u_6 - 27u_7)y \\ &+ \frac{1}{42h^2}(12u_0 - 18u_1 + 3u_2 + 6u_3 - 18u_4 + 6u_5 + 15u_6 u_7)x^2 \\ &+ \frac{1}{42h^2}(-18u_0 + 6u_1 + 6u_2 + 12u_3 + 6u_4 + 12u_5 - 12u_6 - 12u_7)xy \\ &+ \frac{1}{42h^2}(12u_0 + 3u_1 - 18u_2 + 6u_3 - 18u_4 + 6u_5 - 6u_6 + 15u_7)y^2 \end{aligned} \tag{29}$$

Evaluate $\frac{\partial P_z(x,y)}{\partial x}$ and $\frac{\partial P_z(x,y)}{\partial y}$

$$\begin{aligned}\frac{\partial P_z(x,y)}{\partial x} =& \frac{1}{42h}(44u_0 - 38u_1 + 11u_2 - 6u_3 - 38u_4 + 8u_5 + 27u_6 - 8u_7) \\ &+ \frac{1}{21h^2}(12u_0 - 18u_1 + 3u_2 + 6u_3 - 18u_4 + 6u_5 + 15u_6u_7)x \\ &+ \frac{1}{42h^2}(-18u_0 + 6u_1 + 6u_2 + 12u_3 + 6u_4 + 12u_5 - 12u_6 - 12u_7)y \end{aligned} \tag{30}$$

$$\begin{aligned}\frac{\partial P_z(x,y)}{\partial y} =& \frac{1}{42h}(-44u_0 - 11u_1 + 38u_2 - 8u_3 + 38u_4 + 6u_5 + 8u_6 - 27u_7) \\ &+ \frac{1}{42h^2}(-18u_0 + 6u_1 + 6u_2 + 12u_3 + 6u_4 + 12u_5 - 12u_6 - 12u_7)x \\ &+ \frac{1}{21h^2}(12u_0 + 3u_1 - 18u_2 + 6u_3 - 18u_4 + 6u_5 - 6u_6 + 15u_7)y \end{aligned} \tag{31}$$

Thus, the partial equation on $(0,0)$, the gradient recovery will be presented like below,

$$G_h u(z) = \frac{1}{42h}\begin{pmatrix} 44u_0 - 38u_1 + 11u_2 - 6u_3 - 38u_4 + 8u_5 + 27u_6 - 8u_7 \\ -44u_0 - 11u_1 + 38u_2 - 8u_3 + 38u_4 + 6u_5 + 8u_6 - 27u_7 \end{pmatrix} \tag{32}$$

Taylor expansion results in,

$$G_h u(z) = \begin{pmatrix} u_x(z) + \dfrac{h^2}{42}\left(8u_{xyy}(z) + 27u_{xxy}(z) - 14u_{xxx}(z)\right) + O(h^3) \\ u_y(z) + \dfrac{h^2}{42}\left(-14u_{yyy}(z) + 27u_{xyy}(z) + 8u_{xxy}(z)\right) + O(h^3) \end{pmatrix} \tag{33}$$

which means it is second order finite difference scheme approximating $\nabla u(z)$.

- **Chevron Case 1**

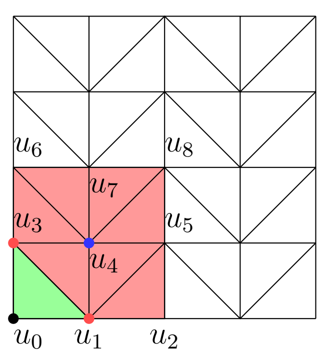

Figure 7: Chevron Case 1

Multiplied the coefficients with "1, x, y, x^2, xy, y^2", the equation is like,

$$
\begin{aligned}
P_z(x,y) =& \frac{1}{36}(29u_0 + 8u_1 - 1u_2 + 8u_3 - 4u_4 - 4u_5 - u_6 - 4u_7 + 5u_8) \\
&+ \frac{1}{36h}(-27u_0 + 24u_1 + 3u_2 - 18u_3 + 24u_4 - 6u_5 - 9u_6 + 24u_7 - 15u_8)x \\
&+ \frac{1}{36h}(-27u_0 - 18u_1 - 9u_2 + 24u_3 + 24u_4 + 24u_5 + 3u_6 - 6u_7 - 15u_8)y \\
&+ \frac{1}{36h^2}(6u_0 - 12u_1 + 6u_2 + 6u_3 - 12u_4 + 6u_5 + 6u_6 - 12u_7 + 6u_8)x^2 \\
&+ \frac{1}{36h^2}(9u_0 - 9u_2 - 9u_6 + 9u_8)xy \\
&+ \frac{1}{36h^2}(6u_0 + 6u_1 + 6u_2 - 12u_3 - 12u_4 - 12u_5 + 6u_6 + 6u_7 + 6u_8)y^2
\end{aligned} \tag{34}
$$

Calculated the ∂x and ∂y,

$$
\begin{aligned}
\frac{\partial P_z(x,y)}{\partial x} =& \frac{1}{36h}(-27u_0 + 24u_1 + 3u_2 - 18u_3 + 24u_4 - 6u_5 - 9u_6 + 24u_7 - 15u_8) \\
&+ \frac{1}{18h^2}(6u_0 - 12u_1 + 6u_2 + 6u_3 - 12u_4 + 6u_5 + 6u_6 - 12u_7 + 6u_8)x \\
&+ \frac{1}{36h^2}(9u_0 - 9u_2 - 9u_6 + 9u_8)y
\end{aligned} \tag{35}
$$

$$
\begin{aligned}
\frac{\partial P_z(x,y)}{\partial y} =& \frac{1}{36h}(-27u_0 - 18u_1 - 9u_2 + 24u_3 + 24u_4 + 24u_5 + 3u_6 - 6u_7 - 15u_8) \\
&+ \frac{1}{36h^2}(9u_0 - 9u_2 - 9u_6 + 9u_8)x \\
&+ \frac{1}{18h^2}(6u_0 + 6u_1 + 6u_2 - 12u_3 - 12u_4 - 12u_5 + 6u_6 + 6u_7 + 6u_8)y
\end{aligned} \tag{36}
$$

With the help of $(0,0)$, the recovered gradient indicates,

$$
G_h u(z) = \frac{1}{36h}\begin{pmatrix} -27u_0 + 24u_1 + 3u_2 - 18u_3 + 24u_4 - 6u_5 - 9u_6 + 24u_7 - 15u_8 \\ -27u_0 - 18u_1 - 9u_2 + 24u_3 + 24u_4 + 24u_5 + 3u_6 - 6u_7 - 15u_8 \end{pmatrix} \tag{37}
$$

Taylor expansion results in,

$$
G_h u(z) = \begin{pmatrix} u_x(z) + \dfrac{h^2}{6}\left(-u_{xyy}(z) - 6u_{xxy}(z) - 2u_{xxx}(z)\right) + O(h^3) \\ u_y(z) + \dfrac{h^2}{6}\left(-2u_{yyy}(z) - 6u_{xyy}(z) - u_{xxy}(z)\right) + O(h^3) \end{pmatrix} \tag{38}
$$

which means it is second order finite difference scheme approximating $\nabla u(z)$.

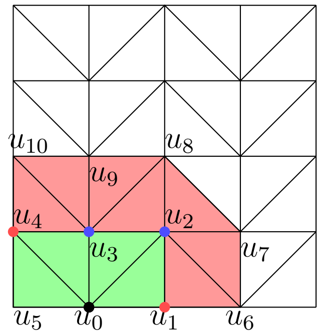

Figure 8: Chevron Case 2

- **Chevron Case 2**

  Binomial equation getting from Matlab and manual calculation,

$$
\begin{aligned}
P_z(x,y) =& \frac{1}{2100}(812u_0 + 658u_1 + 154u_2 + 266u_3 - 42u_4 + 546u_5 + 84u_6 - 378u_7 + 70u_8 \\
&+ 140u_9 - 210u_{10}) + \frac{1}{2100h}(56u_0 + 454u_1 + 277u_2 + 233u_3 - 321u_4 - 852u_5 \\
&+ 342u_6 - 189u_7 - 140u_8 + 170u_9 - 30u_{10})x + \frac{1}{2100h}(-756u_0 - 579u_1 + 1098u_2 + 1242u_3 \\
&+ 1146u_4 - 1173u_5 - 642u_6 + 714u_7 - 735u_8 - 270u_9 - 45u_{10})y \\
&+ \frac{1}{2100h^2}(-210u_0 - 240u_1 - 195u_2 - 255u_3 + 135u_4 + 270u_5 + 180u_6 + 315u_7 \\
&- 150u_9 + 150u_{10})x^2 + \frac{1}{2100h^2}(42u_0 - 222u_1 - 36u_2 - 144u_3 - 72u_4 + 486u_5 - 306u_6 \\
&+ 252u_7 + 420u_8 - 60u_9 - 360u_{10})xy + \frac{1}{2100h^2}(210u_0 + 165u_1 - 555u_2 - 645u_3 - 585u_4 \\
&+ 405u_5 + 270u_6 - 315u_7 + 525u_8 + 300u_9 + 225u_{10})y^2 \qquad (39)
\end{aligned}
$$

  The derivations of the partial equations from $P_z(x,y)$ display as,

$$
\begin{aligned}
\frac{\partial P_z(x,y)}{\partial x} =& \frac{1}{2100h}(56u_0 + 454u_1 + 277u_2 + 233u_3 - 321u_4 - 852u_5 + 342u_6 - 189u_7 - 140u_8 \\
&+ 170u_9 - 30u_{10}) + \frac{1}{2100h^2}(-210u_0 - 240u_1 - 195u_2 - 255u_3 + 135u_4 + 270u_5 \\
&+ 180u_6 + 315u_7 - 150u_9 + 150u_10)2x + \frac{1}{2100h^2}(42u_0 - 222u_1 - 36u_2 - 144u_3 - 72u_4 \\
&+ 486u_5 - 306u_6 + 252u_7 + 420u_8 - 60u_9 - 360u_{10})y \qquad (40)
\end{aligned}
$$

$$
\begin{aligned}
\frac{\partial P_z(x,y)}{\partial y} =& \frac{1}{2100h}(-756u_0 - 579u_1 + 1098u_2 + 1242u_3 + 1146u_4 - 1173u_5 - 642u_6 + 714u_7 - 735u_8 \\
&- 270u_9 - 45u_{10}) + \frac{1}{2100h^2}(42u_0 - 222u_1 - 36u_2 - 144u_3 - 72u_4 + 486u_5 - 306u_6 \\
&+ 252u_7 + 420u_8 - 60u_9 - 360u_{10})x + \frac{1}{2100h^2}(210u_0 + 165u_1 - 555u_2 - 645u_3 - 585u_4 \\
&+ 405u_5 + 270u_6 - 315u_7 + 525u_8 + 300u_9 + 225u_{10})2y
\end{aligned} \tag{41}
$$

The recovered gradient derives to the following equation based on the coordinate of the origin,

$$
G_h u(z) = \frac{1}{2100h}
\begin{pmatrix}
56u_0 + 454u_1 + 277u_2 + 233u_3 - 321u_4 - 852u_5 + 342u_6 - 189u_7 - 140u_8 + 170u_9 - 30u_{10} \\
-756u_0 - 579u_1 + 1098u_2 + 1242u_3 + 1146u_4 - 1173u_5 - 642u_6 + 714u_7 - 735u_8 - 270u_9 - 45u_{10}
\end{pmatrix} \tag{42}
$$

Taylor expansion results in,

$$
G_h u(z) = \begin{pmatrix}
u_x(z) + \frac{h^2}{2100}\left(-110u_{xyy}(z) - 570u_{xxy}(z) + 503u_{xxx}(z)\right) + O(h^3) \\
u_y(z) + \frac{h^2}{1050}\left(-350u_{yyy}(z) - 345u_{xyy}(z) + 885u_{xxy}(z) + 36u_{xxx}(z)\right) + O(h^3)
\end{pmatrix} \tag{43}
$$

which means it is second order finite difference scheme approximating $\nabla u(z)$.

- **Chevron Case 3**

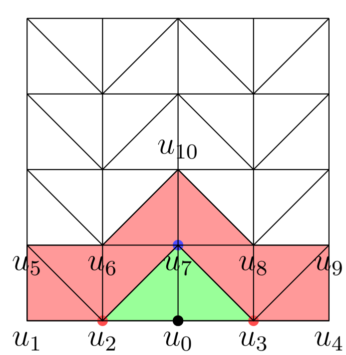

Figure 9: Chevron Case 3

Binary equation based on the matrix in Matlab presents as,

$$
\begin{aligned}
P_z(x,y) =& \frac{1}{140}(48u_0 + 8u_1 + 38u_2 + 38u_3 + 8u_4 - 20u_5 + 10u_6 + 20u_7 - 10u_8 - 20u_9) \\
&+ \frac{1}{140h}(-28u_1 - 14u_2 + 14u_3 + 28u_4)x \\
&+ \frac{1}{140h}(-32u_0 - 52u_1 - 37u_2 - 37u_3 - 52u_4 + 46u_5 + 61u_6 + 66u_7 + 61u_8 + 46u_9 - 70u_{10})y \\
&+ \frac{1}{140h^2}(-10u_0 + 10u_1 - 5u_2 - 5u_3 + 10u_4 + 10u_5 - 5u_6 - 10u_7 - 5u_8 + 10u_9)x^2 \\
&+ \frac{1}{140h^2}(28u_1 + 14u_2 - 14u_3 - 28u_4 - 28u_5 - 14u_6 + 14u_8 + 28u_9)xy \\
&+ \frac{1}{140h^2}(4u_0 + 24u_1 + 9u_2 + 9u_3 + 24u_4 - 18u_5 - 33u_6 - 38u_7 - 33u_8 - 18u_9 + 70u_{10})y^2
\end{aligned}
\tag{44}
$$

Partial equations will be presented below,

$$
\begin{aligned}
\frac{\partial P_z(x,y)}{\partial x} =& \frac{1}{140h}(-28u_1 - 14u_2 + 14u_3 + 28u_4) \\
&+ \frac{1}{140h^2}(-10u_0 + 10u_1 - 5u_2 - 5u_3 + 10u_4 + 10u_5 - 5u_6 - 10u_7 - 5u_8 + 10u_9)x \\
&+ \frac{1}{140h^2}(28u_1 + 14u_2 - 14u_3 - 28u_4 - 28u_5 - 14u_6 + 140u_8 + 28u_9)y
\end{aligned}
\tag{45}
$$

$$
\begin{aligned}
\frac{\partial P_z(x,y)}{\partial y} =& \frac{1}{140h}(-32u_0 - 52u_1 - 37u_2 - 37u_3 - 52u_4 + 46u_5 + 61u_6 + 66u_7 + 61u_8 + 46u_9 - 70u_{10}) \\
&+ \frac{1}{140h^2}(28u_1 + 144u_2 - 14u_3 - 28u_3 - 28u_4 - 28u_5 - 14u_6 + 14u_8 + 28u_9)x \\
&+ \frac{1}{140h^2}(4u_0 + 24u_1 + 9u_2 + 9u_3 + 24u_4 - 18u_5 - 33u_6 - 38u_7 - 33u_8 - 18u_9 + 70u_{10})y
\end{aligned}
\tag{46}
$$

The gradient recovery will be like the $\nabla u(z)$,

$$
G_h u(z) = \frac{1}{140h}
\begin{pmatrix}
-28u_1 - 14u_2 + 14u_3 + 28u_4 \\
-32u_0 - 52u_1 - 37u_2 - 37u_3 - 52u_4 + 46u_5 + 61u_6 + 66u_7 + 61u_8 + 46u_9 - 70u_{10}
\end{pmatrix}
\tag{47}
$$

Taylor expansion results in,

$$
G_h u(z) = \begin{pmatrix}
u_x(z) + \frac{17h^2}{30} u_{xxx}(z) + O(h^4) \\
u_y(z) + \frac{h^2}{12}\left(-4u_{yyy}(z) + 21u_{xyy}(z)\right) + O(h^3)
\end{pmatrix}
\tag{48}
$$

which means it is second order finite difference scheme approximating $\nabla u(z)$.

3 Analysis of Matlab Coding

In this section, we will demonstrate the process to find the patch node by Matlab. There are different ways to achieve the patch node. Moreover, we will discuss the comparison and choose the most efficient scheme.

3.1 Find Layer 1 Patch Nodes

We need at least 6 information of nodes to fit with $1, x, y, x^2, xy, y^2$. If the number of patch nodes exceeds 6, which means u_0 is an interior point, those patch nodes will form layer 1. For layer 1, there are two methods to reach our purpose. Those two means have different thoughts, which result in different efficiency.

- **'any':** In this method, we use the command 'any' to find all elements which contain u_0. These elements form a patch and then find all corresponding nodes about the patch. Then 'for loop' is used to traverse all nodes in the mesh.

```
for j = 1:numNode
%'2' in the command 'any', in our opinion, it means 2-D.
patchNode=elem (any(elem == j,2),:)
if size(patchNode,1) > 6
patchNode=unique(patchNode);
% Because of the different number of patchNode in every loop, we use
% cell to save them.
patchNode{j} = patchNode;
end
```

- **Sort elements:** Plug the sequence number of element into the nodes of its three vertices. Then 'for loop' is used to traverse all elements in the mesh.

```
for i = 1:numElem
PatchElem{elem(i,1)}(end+1) = i;
PatchElem{elem(i,2)}(end+1) = i;
PatchElem{elem(i,3)}(end+1) = i;
end
```

  Express the sequence number of element in the corresponding nodes. Using the command 'unique' to remove the repetitive patch nodes and save them in the cell.

```
for i = 1:numNode
patchNode = elem(PatchElem{i}(:),:);
patchNode = patchNode(:)';
patchNode = unique(patchNode);
PatchNode1{i} = patchNode;
end
layer1 = PatchNode1;
```

- **Comparison:**

  For ‘any’, the command is short. However, it traverses all elements in every ‘for loop’. When the mesh is complicated, there will be enormous number of nodes, which causes too much times of cycle. That will cost too much time to calculate.

  For ‘Sort elements’, it sorts the elements relative to the nodes directly, which saves more time than using the command ‘any’.

  Therefore, according to the analysis above, the method ‘Sort elements’ is better than ‘any’. Finally, we use the method ‘Sort elements’ to reach our destination.

3.2 Find Layer 2 Patch Nodes

Through previous judgment, if the number of patch nodes of the layer 1 is smaller than 6, we extend layer 2. For layer 2, we find the patch nodes of the first layer of u_0 in previous process, then extend the u_0 patch through finding their first layer nodes of every node. There also exist two methods during our exploration.

- **layer 1 nodes $\longrightarrow$ layer 2 elements $\longrightarrow$ layer 2 nodes:** In this method, relying on the experience of finding the layer 1 nodes, we first find the layer 2 elements through the layer 1, then switch these elements into layer 2 nodes.

```
for i = 1:numNode
% find the correspoding node of 1st layer
patchNode = elem(PatchElem{i}(:),:) ;
% transpose the matrix for convenient observation
patchNode = patchNode(:)';
% delete the repeated node
patchNode = unique(patchNode);
% the i-th row in PatchNode is patchNode
PatchNode(i) = {patchNode};
% judge the interior nodes
if length(patchNode) > 6
% fill the PatchNode cell for storing layer 2 nodes of every nodes
PatchNode(i) = {patchNode};
else
ExtendLayer2 = [];
for j = 1:length(PatchNode{i})
% find the layer 2 PatchElem
extendLayer2 = PatchElem{PatchNode{i}(j)};
ExtendLayer2 = [ExtendLayer2,extendLayer2];
ExtendLayer2 = unique(ExtendLayer2);
end
% switch the elements into nodes
extend2PatchNode = elem(ExtendLayer2(:),:);
```

```
extend2PatchNode = unique(extend2PatchNode);
extend2PatchNode = extend2PatchNode';
% unit the layer 1 and layer 2 nodes together
patchNode = [patchNode,extend2PatchNode];
patchNode = unique(patchNode);
PatchNode(i) = {patchNode};
end
end
```

- **layer 1 nodes $\longrightarrow$ layer 2 nodes:** As analyzing previous approach, we find a more straightforward way, which is find the layer 2 nodes directly from layer 1.

  Idea 1: In the approach, we expanded layer on the original foundation. 'for loop' is used for both attaining the nodes of every layer 2 patch node and fill it in a new cell.

```
for i = 1:(nx+1)*(ny+1)
if length(Patch_node{i}) > 6
layer2node{i} = Patch_node{i};
layer3node{i} = layer2node{i};
else
u = Patch_node{i};
for j = 1:length(Patch_node{i})
for k = 1:length(Patch_node{u(1,j)}(:)')
layer2node{i}(end + 1) = Patch_node{u(1,j)}(k);
%traverse every correspoinding layer2 node of every node
layer2node{i} = unique(layer2node{i});
end
end
end
```

  Idea 2: By exploration, we use the command $ExtendLayer2 = [ExtendLayer2, extendLayer2]$ instead of 'for loop' to improve efficiency.

```
for i = 1:numNode
if length(layer1{i}) > 6
PatchNode2{i} = layer1{i};
else
ExtendLayer2 = [];
for j = 1:length(layer1{i})
% extend layer2 from layer1's nodes to layer2's nodes
extendLayer2 = layer1{layer1{i}(j)};
% unit the layer 1 and layer 2 nodes together
ExtendLayer2 = [ExtendLayer2,extendLayer2];
% delete the repeated node
ExtendLayer2 = unique(ExtendLayer2);
```

```
end
PatchNode2{i} = ExtendLayer2;
end
end
layer2 = PatchNode2;
```

- **Comparison**:

  The second method is the improved version of the first method. We have obtained the layer 1 nodes of each nodes to find layer 2. Therefore we can directly call the layer 1 nodes rather than call the layer 1 elements. In the second method, there are two ideas. And the idea 2 is more efficient because it dose not use 'for loop'. Thus, the second method idea 2 is most efficient and we choose it in layer 3.

3.3 Find Layer 3 Patch Nodes

For some boundary points, although their layer 2 contain 6 nodes, the information is not enough to achieve the gradient recovery. So we need to extend layer 2 to layer 3. For example, Figure 10, in regular pattern, node u_0 below is such a point which needs to extend twice.

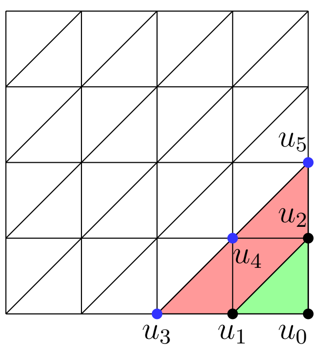

(a) Extend once

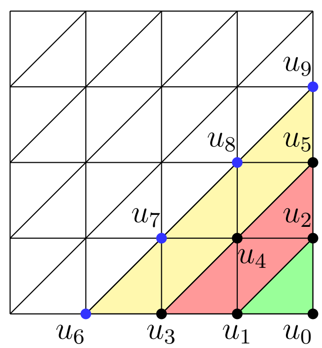

(b) Extend twice

Figure 10: Special Boundary Points

Thereby, if the number of patch nodes in layer 2 is less than 9, the patch should be extended again. Generally, the information of 9 patch nodes is enough to achieve gradient recovery on u_0.

```
for i = 1:numNode
if length(layer1{i}) > 6
PatchNode3{i} = layer1{i};
else
if length(layer2{i}) >= 9
PatchNode3{i} = layer2{i};
else
ExtendLayer3 =[];
```

```
for j = 1:length(layer2{i})
extendLayer3 = layer1{layer2{i}(j)};
ExtendLayer3 = [ExtendLayer3,extendLayer3];
ExtendLayer3 = unique(ExtendLayer3);
end
PatchNode3{i} = ExtendLayer3;
end
end
end
layer3 = PatchNode3;
```

Finally, layer 3 contains the complete patch nodes at every node in the mesh.

4 Analysis of Symmetry

According to the examples of gradient recovery, it is obvious to find some rules of symmetry. The symmetry is performed on patches, coefficients and Taylor Expansion.

4.1 Symmetry of Patch

This part displays symmetry of patches which are formed by both interior nodes and boundary nodes on five different patterns.

4.1.1 Regular Pattern

Regular Interior

- Interior: The patch is central symmetric about node z when z is an interior node in Regular Pattern (Figure 11). Meanwhile, the recovered gradient coefficients of two nodes which are central symmetric about z is opposite at the coordinate with respect to x and y.

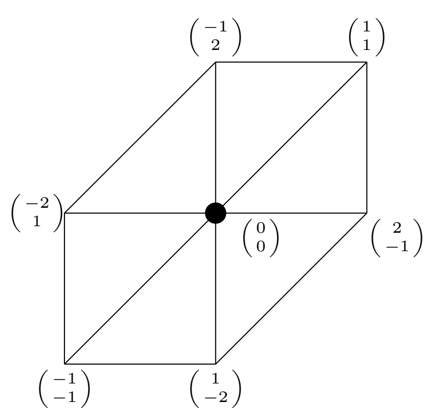

Figure 11: Regular Interior Symmetry

$$G_h u(z) = \frac{1}{6h} \begin{pmatrix} 2u_1 + u_2 - u_3 - 2u_4 - u_5 + u_6 \\ -u_1 + u_2 + 2u_3 + u_4 - u_5 - 2u_6 \end{pmatrix} \tag{49}$$

$$G_h u(z) = \begin{pmatrix} u_x(z) + \dfrac{h^2}{6}\left(u_{xyy}(z) + u_{xxy}(z) + u_{xxx}(z)\right) + O\left(h^4\right) \\ u_y(z) + \dfrac{h^2}{6}\left(u_{yyy}(z) + u_{xyy}(z) + u_{xxy}(z)\right) + O\left(h^4\right) \end{pmatrix} \tag{50}$$

Regular Boundary

- Boundary 1: The patch is a square when z is the first type of boundary node in Regular Pattern (Figure 12). Through observation of the recovered gradient coefficients at every node, we can find that on the diagonal, the coefficient with respect to x and y are same. Meanwhile, nodes which are symmetric by the diagonal also have rules. The coefficient with respect to x of one node is equal to the coefficient with respect to y of the vertices on the diagonal.

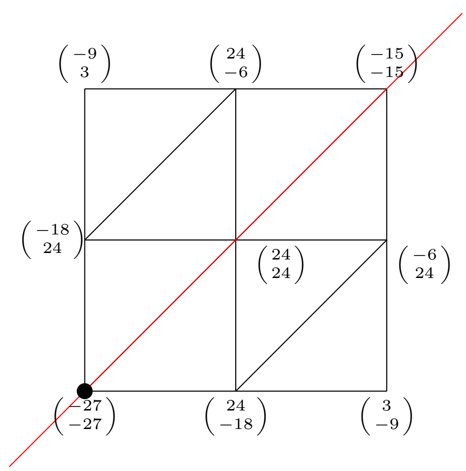

Figure 12: Regular Boundary 1 Symmetry

$$G_h u(z) = \frac{1}{36h} \begin{pmatrix} -27u_0 + 24u_1 + 3u_2 - 18u_3 + 24u_4 - 6u_5 - 9u_6 + 24u_7 - 15u_8 \\ -27u_0 - 18u_1 - 9u_2 + 24u_3 + 24u_4 + 24u_5 + 3u_6 - 6u_7 - 15u_8 \end{pmatrix} \tag{51}$$

$$G_h u(z) = \begin{pmatrix} u_x(z) + \dfrac{h^2}{6}\left(-u_{xyy}(z) - 6u_{xxy}(z) - 2u_{xxx}(z)\right) + O(h^3) \\ u_y(z) + \dfrac{h^2}{6}\left(-2u_{yyy}(z) - 6u_{xyy}(z) - u_{xxy}(z)\right) + O(h^3) \end{pmatrix} \tag{52}$$

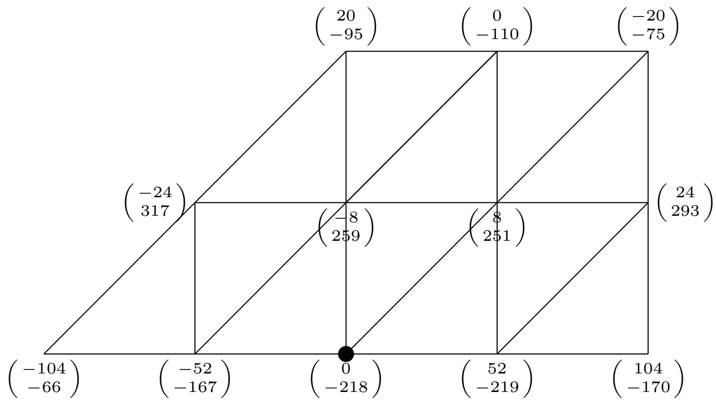

Figure 13: Regular Boundary 2 Symmetry

- Boundary 2: If z is the second type of boundary node in Regular Pattern, the patch is obvious not symmetry (Figure 13). Thus, the coefficient of recovered gradient at every vertex of the patch has no rule except the sums both with respect to x and y of them are zero.

$$G_h^x u(z) = \frac{1}{560h}(-104u_1 - 52u_2 + 52u_3 + 104u_4 - 24u_5 - 8u_6 + 8u_7 + 24u_8 + 20u_9 - 20u_{11}) \tag{53}$$

$$\begin{aligned} G_h^y u(z) = &\frac{1}{560h}(-218u_0 - 66u_1 - 167u_2 - 219u_3 - 170u_4 + 317u_5 + 259u_6 + 251u_7 + 293u_8 \\ &- 95u_9 - 110u_{10} - 75u_{11}) \end{aligned} \tag{54}$$

$$G_h u(z) = \begin{pmatrix} u_x(z) + \dfrac{h^2}{420}\left(-30u_{xyy}(z) - 30u_{xxy}(z) + 229u_{xxx}(z)\right) + O(h^3) \\ u_y(z) + \dfrac{h^2}{840}\left(-280u_{yyy}(z) - 390u_{xyy}(z) + 690u_{xxy}(z) + 171u_{xxx}(z)\right) + O(h^3) \end{pmatrix} \tag{55}$$

- Boundary 3: The patch resembles a diamond which has a axis of symmetry. The axis is represented as the line from u_0 to u_4 (Figure 6). Nodes which are symmetric by the diagonal also have rules. Some rules can be easily to find from the Figure 14 below. From the nodes which are symmetric by the axis, there recovered gradient coefficient with respect to x of one node is equal to the coefficients with respect to y of the other.

$$G_h u(z) = \frac{1}{42h}\begin{pmatrix} 44u_0 - 38u_1 + 11u_2 - 6u_3 - 38u_4 + 8u_5 + 27u_6 - 8u_7 \\ -44u_0 - 11u_1 + 38u_2 - 8u_3 + 38u_4 + 6u_5 + 8u_6 - 27u_7 \end{pmatrix} \tag{56}$$

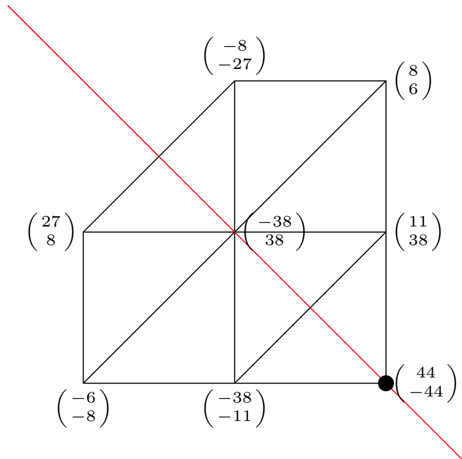

Figure 14: Regular Boundary 3 Symmetry

$$G_h u(z) = \begin{pmatrix} u_x(z) + \dfrac{h^2}{42}\left(8u_{xyy}(z) + 27u_{xxy}(z) - 14u_{xxx}(z)\right) + O(h^3) \\ u_y(z) + \dfrac{h^2}{42}\left(-14u_{yyy}(z) + 27u_{xyy}(z) + 8u_{xxy}(z)\right) + O(h^3) \end{pmatrix} \tag{57}$$

4.1.2 Chevron Pattern

Chevron Interior: If z is an interior point in Chevron Pattern, its patch (Figure 15) is a pentagon. The coefficients of the patch vertices which is symmetric about a vertical line from u_1 to u_4 (Figure 3) have a certain rule, the coefficients of these vertices are same.

- Chevron Interior 1

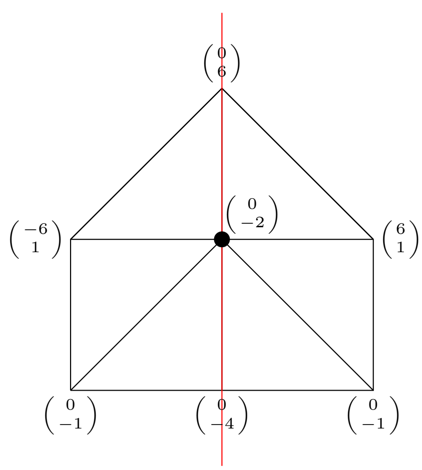

Figure 15: Chevron Interior 1 Symmetry

$$G_h u(z) = \frac{1}{6h} \begin{pmatrix} -6u_2 + 6u_6 \\ -2u_0 + 6u_1 + u_2 - u_3 - 4u_4 - u_5 + u_6 \end{pmatrix} \tag{58}$$

$$G_h u(z) = \begin{pmatrix} u_x(z) + \frac{h^2}{6} u_{xxx}(z) + O(h^4) \\ u_y(z) + \frac{h^2}{12} (2u_{yyy}(z) + u_{xxy}(z)) + O(h^3) \end{pmatrix} \tag{59}$$

- Chevron Interior 2

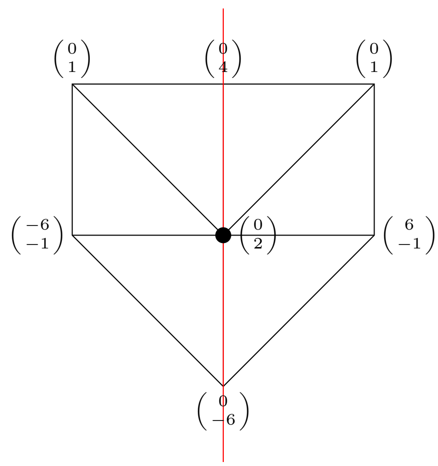

Figure 16: Chevron Interior 2 Symmetry

$$G_h u(z) = \frac{1}{12h} \begin{pmatrix} -6u_2 + 6u_3 \\ 2u_0 - 6u_1 - u_2 - u_3 + u_4 + 4u_5 + u_6 \end{pmatrix} \tag{60}$$

$$G_h u(z) = \begin{pmatrix} u_x(z) + \frac{h^2}{6} u_{xxx}(z) + O(h^4) \\ u_y(z) + \frac{h^2}{12} (2u_{yyy}(z) + u_{xxy}(z)) + O(h^3) \end{pmatrix} \tag{61}$$

Chevron Boundary:

- Boundary 1: When z is the first type of boundary node in Chevron Pattern, the patch of it is also a square (Figure 17). The first rule of the coefficients of recovered gradient is on the diagonal from u_0 to u_8 (Figure 7), the coefficient with respect to x and y are same. The second one is the coefficient with respect to x of one vertex is equal to the coefficient with

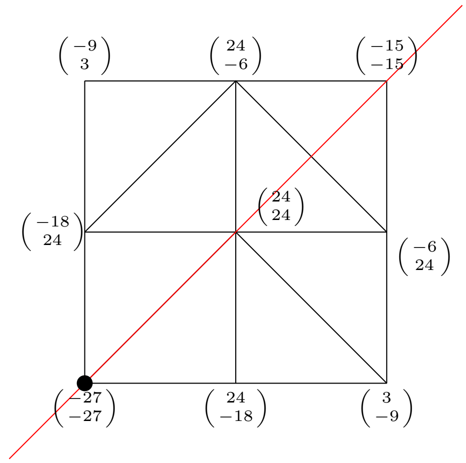

Figure 17: Chevron Boundary 1 Symmetry

respect to y of the other one if these two points are symmetric about the diagonal from u_2 to u_6 (Figure 7).

$$G_h u(z) = \frac{1}{36h} \begin{pmatrix} -27u_0 + 24u_1 + 3u_2 - 18u_3 + 24u_4 - 6u_5 - 9u_6 + 24u_7 - 15u_8 \\ -27u_0 - 18u_1 - 9u_2 + 24u_3 + 24u_4 + 24u_5 + 3u_6 - 6u_7 - 15u_8 \end{pmatrix} \tag{62}$$

$$G_h u(z) = \begin{pmatrix} u_x(z) + \frac{h^2}{6}\left(-u_{xyy}(z) - 6u_{xxy}(z) - 2u_{xxx}(z)\right) + O(h^3) \\ u_y(z) + \frac{h^2}{6}\left(-2u_{yyy}(z) - 6u_{xyy}(z) - u_{xxy}(z)\right) + O(h^3) \end{pmatrix} \tag{63}$$

- Boundary 2: It does not exhibit symmetry because of the asymmetric patch.

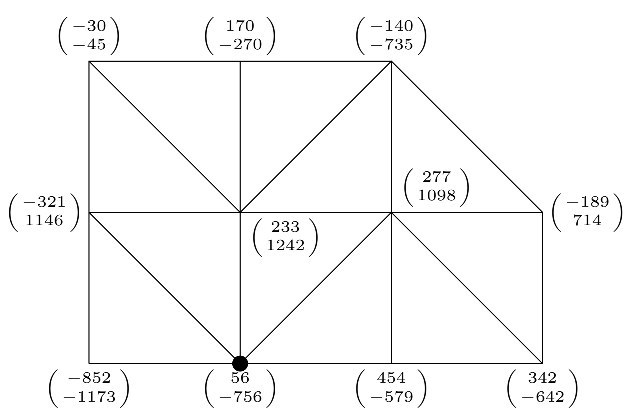

Figure 18: Chevron Boundary 2 Symmetry

$$G_h^x u(z) = \frac{1}{2100h}(56u_0 + 454u_1 + 277u_2 + 233u_3 - 321u_4 - 852u_5 + 342u_6 - 189u_7 - 140u_8 + 170u_9 - 30u_{10}) \tag{64}$$

$$G_h^y u(z) = \frac{1}{2100h}(-756u_0 - 579u_1 + 1098u_2 + 1242u_3 + 1146u_4 - 1173u_5 - 642u_6 + 714u_7 - 735u_8 - 270u_9 - 45u_{10}) \tag{65}$$

$$G_h u(z) = \begin{pmatrix} u_x(z) + \frac{h^2}{2100}\left(-110u_{xyy}(z) - 570u_{xxy}(z) + 503u_{xxx}(z)\right) + O(h^3) \\ u_y(z) + \frac{h^2}{1050}\left(-350u_{yyy}(z) - 345u_{xyy}(z) + 885u_{xxy}(z) + 36u_{xxx}(z)\right) + O(h^3) \end{pmatrix} \tag{66}$$

- Boundary 3: The recovered gradient coefficients represent the first and second rows respectively, where coefficients are completely symmetric in the first row and the coefficients with respect to x are opposite but are same with respect to y.

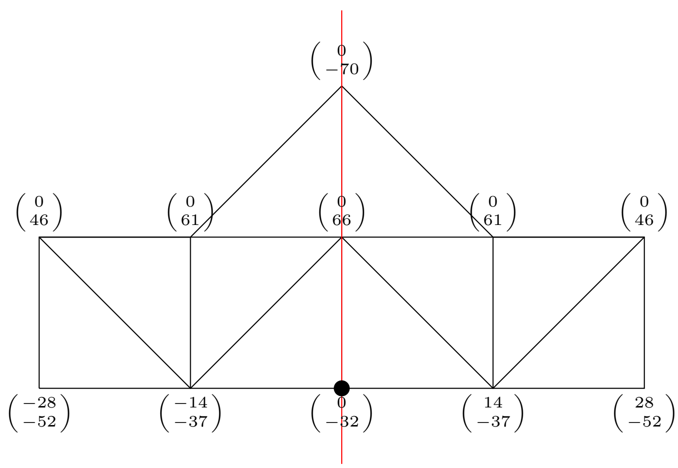

Figure 19: Chevron Boundary 3 Symmetry

$$G_h u(z) = \frac{1}{140h} \begin{pmatrix} -28u_1 - 14u_2 + 14u_3 + 28u_4 \\ -32u_0 - 52u_1 - 37u_2 - 37u_3 - 52u_4 + 46u_5 + 61u_6 + 66u_7 + 61u_8 + 46u_9 - 70u_{10} \end{pmatrix} \tag{67}$$

$$G_h u(z) = \begin{pmatrix} u_x(z) + \dfrac{17h^2}{30} u_{xxx}(z) + O(h^4) \\ u_y(z) + \dfrac{h^2}{12}\left(-4u_{yyy}(z) + 21u_{xyy}(z)\right) + O(h^3) \end{pmatrix} \tag{68}$$

4.1.3 Union-Jack Pattern

Union-Jack Interior

- Interior 1: The patch is central symmetric. Two vertices which are symmetric about z have opposite recovered gradient coefficients (Figure 20).

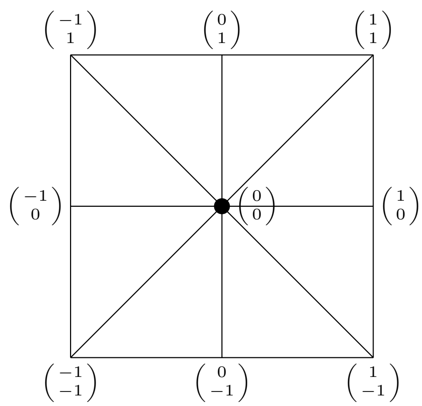

Figure 20: Union-Jack Interior 1 Symmetry

$$G_h u(z) = \frac{1}{6h} \begin{pmatrix} -u_1 + u_3 - u_4 + u_5 - u_6 + u_8 \\ -u_1 - u_2 - u_3 + u_6 + u_7 + u_8 \end{pmatrix} \tag{69}$$

$$G_h u(z) = \begin{pmatrix} u_x(z) + \dfrac{h^2}{6}(2u_{xyy}(z) + u_{xxx}(z)) + O(h^4) \\ u_y(z) + \dfrac{h^2}{6}\left(u_{yyy}(z) + 2u_{xxy}(z)\right) + O(h^4) \end{pmatrix} \tag{70}$$

- Interior 2: If two vertices are symmetric about the axis from u_8 to u_{10}, the coefficients of recovered gradient with respect to y are opposite (Figure 21).

$$\begin{aligned} G_h^x u(z) =& \frac{1}{73480h}(1892u_0 - 7832u_1 + 2332u_2 + 5456u_3 - 8162u_4 + 2002u_5 + 5126u_6 \\ &+ 1210u_7 - 8272u_8 + 5016u_9 + 1100u_{10} - 8162u_{11} + 2002u_{12} + 5126u_{13} \\ &+ 1210u_{14} - 7832u_{15} + 2332u_{16} + 5456u_{17}) \end{aligned} \tag{71}$$

$$\begin{aligned} G_h^y u(z) =& \frac{1}{73480h}(-5344u_1 - 4676u_2 - 4008u_3 - 2672u_4 - 2338u_5 - 2004u_6 - 1670u_7 \\ &+ 2672u_{11} + 2338u_{12} + 2004u_{13} + 1670u_{14} + 5344u_{15} + 4676u_{16} + 4008u_{17}) \end{aligned} \tag{72}$$

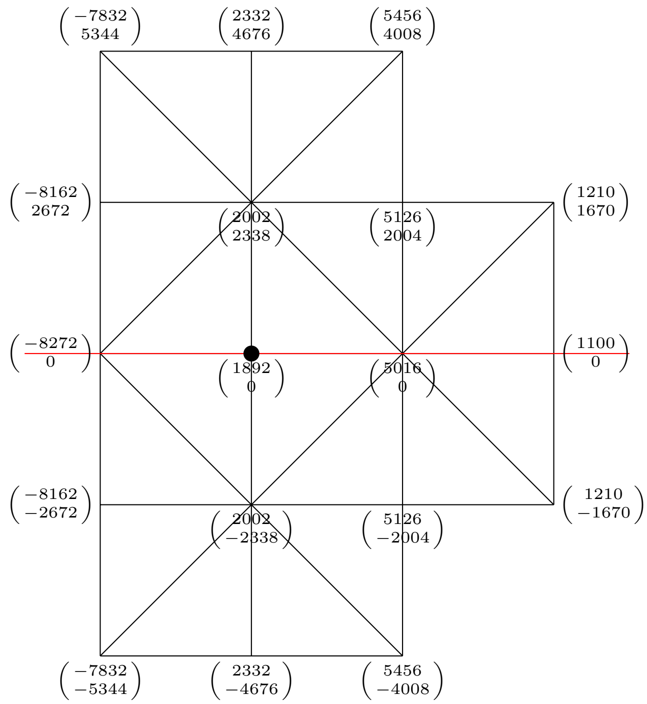

Figure 21: Union-Jack Interior 2 Symmetry

$$G_h u(z) = \begin{pmatrix} u_x(z) + \frac{h^2}{2100}\left(-110u_{xyy}(z) - 570u_{xxy}(z) + 503u_{xxx}(z)\right) + O(h^3) \\ u_y(z) + \frac{h^2}{1050}\left(-350u_{yyy}(z) + -345u_{xyy}(z) + 885u_{xxy}(z) + 36u_{xxx}(z)\right) + O(h^3) \end{pmatrix} \tag{73}$$

- Interior 3: Every vertex is central symmetric with z (Figure 22).

$$G_h^x u(z) = \frac{1}{34h}(-u_1 + u_3 - 2u_4 - u_5 + u_7 + 2u_8 - 2u_9 - u_{10} + u_{11} + 2u_{12} - 2u_{13} - u_{14} + u_{16} + 2u_{17} - u_{18} + u_{20}) \tag{74}$$

$$G_h^y u(z) = \frac{1}{34h}(-2u_1 - 2u_2 - 2u_3 - u_4 - u_5 - u_6 - u_7 - u_8 + u_{13} + u_{14} + u_{15} + u_{16} + u_{17} + 2u_{18} + 2u_{19} + 2u_{20}) \tag{75}$$

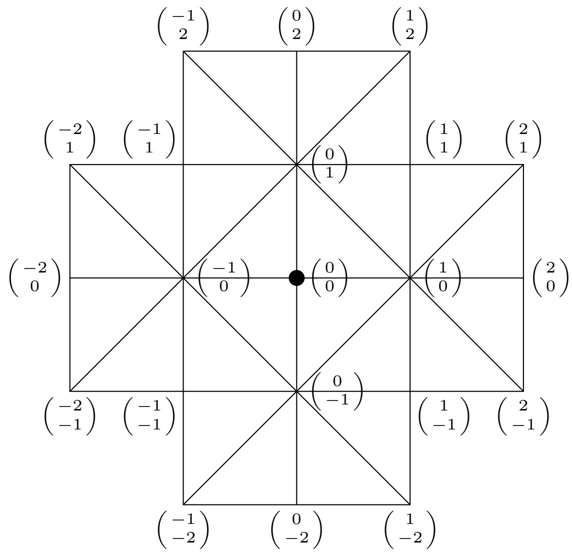

Figure 22: Union-Jack Interior 3 Symmetry

$$G_h u(z) = \begin{pmatrix} u_x(z) + \dfrac{h^2}{102}\left(54u_{xyy}(z) + 53u_{xxx}(z)\right) + O(h^4) \\ u_y(z) + \dfrac{h^2}{102}\left(53u_{yyy}(z) + 54u_{xxy}(z)\right) + O(h^4) \end{pmatrix} \tag{76}$$

- Interior 4: About the axis passes through u_4 and u_9, the opposite number of the recovered gradient coefficients with respect to x is the coefficient with respect to y with the symmetric vertex (Figure 23).

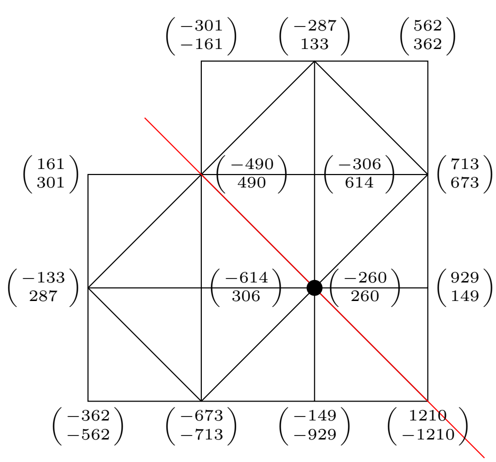

Figure 23: Union-Jack Interior 4 Symmetry

$$G_h^x u(z) = \frac{1}{6160h}(-260u_0 - 362u_1 - 673u_2 - 149u_3 + 1210u_4 - 133u_5 - 614u_6 + 929u_7$$
$$+161u_8 - 490u_9 - 306u_{10} + 713u_{11} - 301u_{12} - 287u_{13} + 562u_{14}) \tag{77}$$
$$G_h^y u(z) = \frac{1}{6160h}(260u_0 - 562u_1 - 713u_2 - 929u_3 - 1210u_4 + 287u_5 + 306u_6 + 149u_7 + 301u_8$$
$$+490u_9 + 614u_{10} + 673u_{11} - 161u_{12} + 133u_{13} + 362u_{14}) \tag{78}$$

$$G_h u(z) = \begin{pmatrix} u_x(z) + \frac{h^2}{9240}\left(-39u_{yyy}(z) + 5205u_{xyy}(z) + 1725u_{xxy}(z) - 2041u_{xxx}(z)\right) + O(h^3) \\ u_y(z) + \frac{h^2}{9240}\left(2041u_{yyy}(z) + 1725u_{xyy}(z) + 5205u_{xxy}(z) - 39u_{xxx}(z)\right) + O(h^3) \end{pmatrix} \tag{79}$$

Union-Jack Boundary

- Boundary 1: If two vertices which are symmetric about diagonal from u_0 to u_8, the recovered gradient coefficient with respect to x equals to the other's recovered gradient coefficient with respect to y. The recovered gradient coefficients with respect to y of vertices on the symmetric axis are 0 (Figure 24).

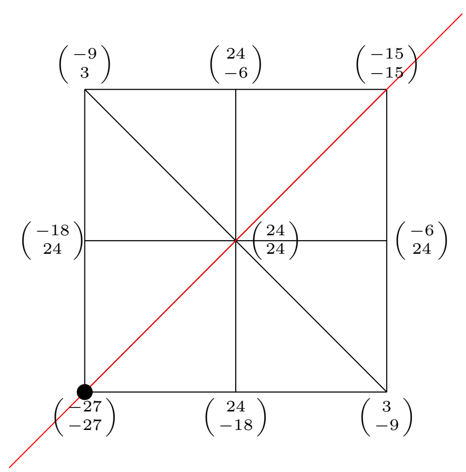

Figure 24: Union-Jack Boundary 1 Symmetry

$$G_h u(z) = \frac{1}{36h}\begin{pmatrix} -27u_0 + 24u_1 + 3u_2 - 18u_3 + 24u_4 - 6u_5 - 9u_6 + 24u_7 - 15u_8 \\ -27u_0 - 18u_1 - 9u_2 + 24u_3 + 24u_4 + 24u_5 + 3u_6 - 6u_7 - 15u_8 \end{pmatrix} \tag{80}$$

$$
G_h u(z) = \begin{pmatrix} u_x(z) + \frac{h^2}{6}\left(-u_{xyy}(z) - 6u_{xxy}(z) - 2u_{xxx}(z)\right) + O(h^3) \\ u_y(z) + \frac{h^2}{6}\left(-2u_{yyy}(z) - 6u_{xyy}(z) - u_{xxy}(z)\right) + O(h^3) \end{pmatrix} \tag{81}
$$

- Boundary 2: Among the second type, the patch is not symmetric. Thereby, the coefficient has no rules about symmetry (Figure 25).

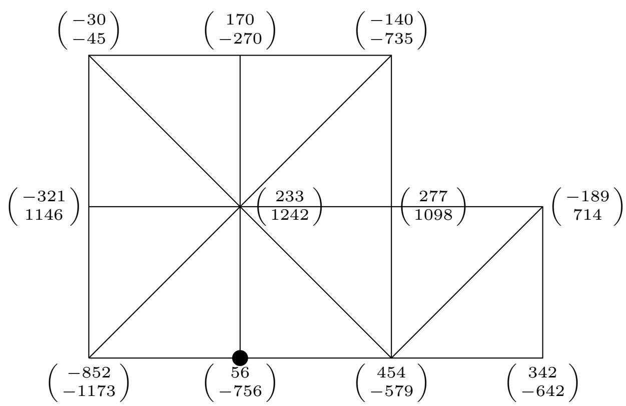

Figure 25: Union-Jack Boundary 2 Symmetry

$$
\begin{aligned}
G_h^x u(z) =& \frac{1}{2100h}(56u_0 - 852u_1 + 454u_2 + 342u_3 - 321u_4 + 233u_5 + 277u_6 - 189u_7 \\
& - 30u_8 + 170u_9 - 140u_{10}) \qquad (82) \\
G_h^y u(z) =& \frac{1}{2100h}(-756u_0 - 1173u_1 - 579u_2 - 642u_3 + 1146u_4 + 1242u_5 + 1098u_6 \\
& + 714u_7 - 45u_8 - 270u_9 - 735u_{10}) \qquad (83)
\end{aligned}
$$

$$
G_h u(z) = \begin{pmatrix} u_x(z) + \frac{h^2}{2100}\left(-110u_{xyy}(z) - 570u_{xxy}(z) + 503u_{xxx}(z)\right) + O(h^3) \\ u_y(z) + \frac{h^2}{1050}\left(-350u_{yyy}(z) - 345u_{xyy}(z) + 885u_{xxy}(z) + 36u_{yyy}(z)\right) + O(h^3) \end{pmatrix} \tag{84}
$$

- Boundary 3: About the third one, the patch is symmetric about the axis from u_0 to u_{12}. Due to the symmetry of the patch, the recovered gradient coefficients with respect to x have symmetry about the axis as well but the coefficients with respect to y are same (Figure 26).

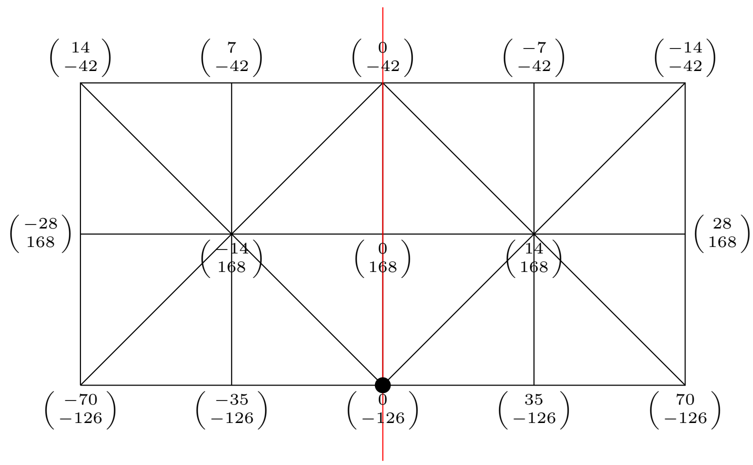

Figure 26: Union Jack Boundary 3 Symmetry

$$\begin{aligned} G_h^x u(z) =& \frac{1}{420h}(-70u_1 - 35u_2 + 35u_3 + 70u_4 - 28u_5 - 14u_6 + 14u_8 + 28u_9 + 14u_{10} \\ & + 7u_{11} - 7u_{13} - 14u_{14}) \end{aligned} \tag{85}$$

$$\begin{aligned} G_h^y u(z) =& \frac{1}{420h}(-126u_0 - 126u_1 - 126u_2 - 126u_3 - 126u_4 + 168u_5 + 168u_6 + 168u_7 \\ & + 168u_8 + 168u_9 - 42u_{10} - 42u_{11} - 42u_{12} - 42u_{13} - 42u_{14}) \end{aligned} \tag{86}$$

$$G_h u(z) = \begin{pmatrix} u_x(z) + \frac{h^2}{30}\left(-5u_{xyy}(z) + 17u_{xxx}(z)\right) + O(h^3) \\ u_y(z) + \frac{h^2}{3}\left(-u_{yyy}(z) + 3u_{xxy}(z)\right) + O(h^3) \end{pmatrix} \tag{87}$$

- Boundary 4: It is easy to see that when z is the solid dot below, the patch at node z is symmetric about the vertical line which through z (Figure 27). Meanwhile, the coefficients of each nodes have a rule as follow. Their recovered gradients with respect to x are opposite if they are symmetric about the vertical line that through z and the recovered gradient with respect to y are same.

$$\begin{aligned} G_h^x u(z) =& \frac{1}{4300h}(-774u_1 - 387u_2 + 387u_3 + 774u_4 - 172u_5 - 86u_6 + 86u_8 + 172u_9 \\ & +215u_{10} - 215u_{12}) \end{aligned} \tag{88}$$

$$\begin{aligned} G_h^y u(z) =& \frac{1}{4300h}(-1090u_0 - 1490u_1 - 1190u_2 - 1190u_3 - 1490u_4 + 1520u_5 + 1820u_6 + 1920u_7 \\ & +1820u_8 + 1520u_9 - 750u_{10} - 650u_{11} - 750u_{12}) \end{aligned} \tag{89}$$

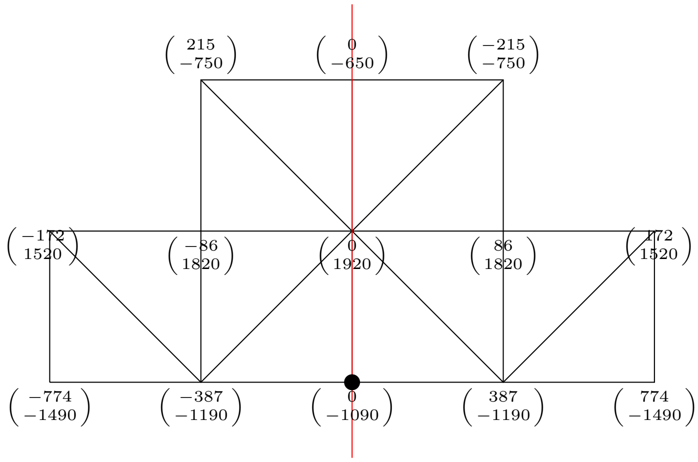

Figure 27: Union-Jack Boundary 4 Symmetry

$$G_h u(z) = \begin{pmatrix} u_x(z) + \dfrac{h^2}{150}\left(-15u_{xyy}(z) + 91u_{xxx}(z)\right) + O(h^3) \\ u_y(z) + \dfrac{h^2}{129}\left(-43u_{yyy}(z) + 192u_{xxy}(z)\right) + O(h^3) \end{pmatrix} \tag{90}$$

- Boundary 5: About the axis passes through u_0 and u_4, the opposite number of the recovered gradient coefficients with respect to x is the coefficient with respect to y of the symmetric vertex (Figure 28).

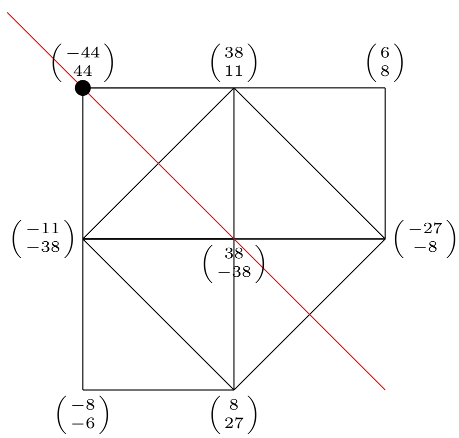

Figure 28: Union-Jack Boundary 5 Symmetry

$$G_h u(z) = \frac{1}{42h}\begin{pmatrix} -44u_0 - 8u_1 + 8u_2 - 11u_3 + 38u_4 - 27u_5 + 38u_6 + 6u_7 \\ 44u_0 - 6u_1 + 27u_2 - 38u_3 - 38u_4 - 8u_5 + 11u_6 + 8u_7 \end{pmatrix} \tag{91}$$

$$G_h u(z) = \begin{pmatrix} u_x(z) + \frac{h^2}{42}\left(8u_{xyy}(z) + 27u_{xxy}(z) - 14u_{xxx}(z)\right) + O(h^3) \\ u_y(z) + \frac{h^2}{42}\left(-14u_{yyy}(z) + 27u_{xyy}(z) + 8u_{xxy}(z)\right) + O(h^3) \end{pmatrix} \tag{92}$$

- Boundary 6: There are two rules. The first one is that the sum of the recovered gradient coefficient with respect to x on every row is zero. For the other rule, the coefficients with respect to y are same on the middle row (Figure 29).

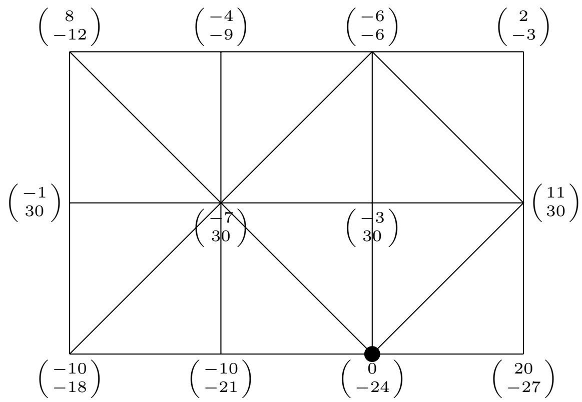

Figure 29: Union-Jack Boundary 6 Symmetry

$$G_h^x u(z) = \frac{1}{60h}(-10u_1 - 10u_2 + 20u_3 - u_4 - 7u_5 - 3u_6 + 11u_7 + 8u_8 - 4u_9 - 6u_{10} + 2u_{11}) \tag{93}$$

$$\begin{aligned} G_h^y u(z) = &\frac{1}{60h}(-24u_0 - 18u_1 - 21u_2 - 27u_3 + 30u_4 + 30u_5 + 30u_6 + 30u_7 - 12u_8 - 9u_9 \\ &- 6u_{10} - 3u_{11}) \end{aligned} \tag{94}$$

$$G_h u(z) = \begin{pmatrix} u_x(z) + \frac{h^2}{60}\left(-10u_{xyy}(z) + 30u_{xxy}(z) + 13u_{xxx}(z)\right) + O(h^3) \\ u_y(z) + \frac{h^2}{6}\left(-2u_{yyy}(z) + 3u_{xyy}(z) + 3u_{xxy}(z)\right) + O(h^3) \end{pmatrix} \tag{95}$$

4.1.4 Criss-cross Pattern

Criss-cross Interior

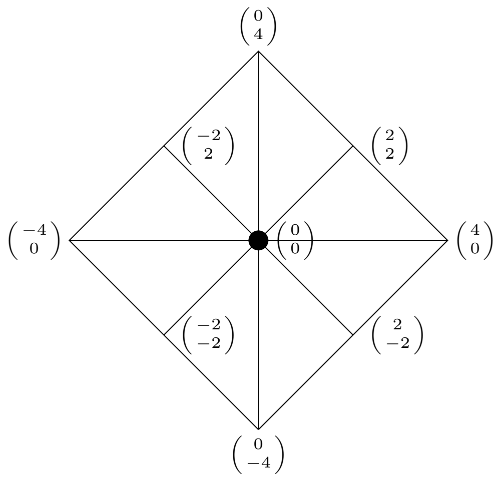

Figure 30: Criss-cross Interior 1 Symmetry

- Interior 1: Figure 30 shows as central symmetry, which u_1 and u_5, u_2 and u_6, u_3 and u_7, u_4 and u_8 are symmetric about u_0. It is proved by the coefficients obtained from gradient recovery.

$$G_h u(z) = \frac{1}{12h}\begin{pmatrix} 2u_2 + 4u_3 + 2u_4 - 2u_6 - 4u_7 - 2u_8 \\ 4u_1 + 2u_2 - 2u_4 - 4u_5 - 2u_6 + 2u_8 \end{pmatrix} \tag{96}$$

$$G_h u(z) = \begin{pmatrix} u_x(z) + \dfrac{h^2}{24}(u_{xyy}(z) + 3u_{xxx}(z)) + O(h^4) \\ u_y(z) + \dfrac{h^2}{24}(3u_{yyy}(z) + u_{xxy}(z)) + O(h^4) \end{pmatrix} \tag{97}$$

- Interior 2: Still demonstrated as central symmetry, if plug the patch into a coordinate system, the second case of Criss-cross Interior (Figure 31) is symmetric about $y = x$ and $y = -x$.

$$\begin{aligned} G_h^x u(z) =& \frac{1}{205020h}(-6030u_1 + 6030u_2 + 6030u_3 - 6030u_4 - 6030u_5 + 6030u_7 + 12060u_8 \\ &+ 18090u_9 + 12060u_{10} + 18090u_{11} + 12060u_{12} + 6030u_{13} - 6030u_{15} - 12060u_{16} \\ &- 18090u_{17} - 12060u_{18} - 18090u_{19} - 12060u_{20}) \qquad (98) \\ G_h^y u(z) =& \frac{1}{205020h}(6030u_1 + 6030u_2 - 6030u_3 - 6030u_4 + 18090u_5 + 12060u_6 + 18090u_7 \\ &+ 12060u_8 + 6030u_9 - 6030u_{11} - 12060u_{12} - 18090u_{13} - 12060u_{14} - 18090u_{15} \\ &- 12060u_{16} - 6030u_{17} + 6030u_{19} + 12060u_{20}) \qquad (99) \end{aligned}$$

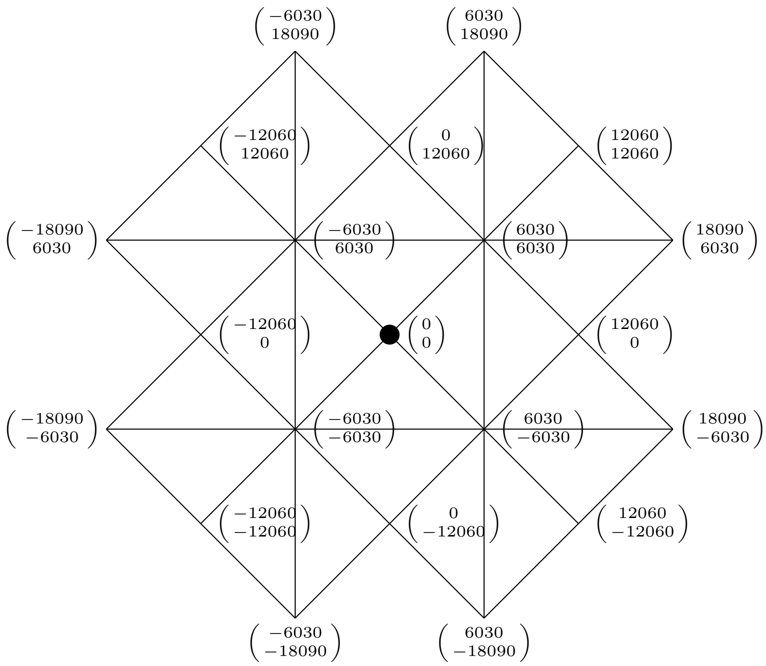

Figure 31: Criss-cross Interior 2 Symmetry

$$G_h u(z) = \begin{pmatrix} u_x(z) + \dfrac{h^2}{408}\left(105u_{xyy}(z) + 107u_{xxx}(z)\right) + O(h^4) \\ u_y(z) + \dfrac{h^2}{408}\left(107u_{yyy}(z) + 105u_{xxy}(z)\right) + O(h^4) \end{pmatrix} \tag{100}$$

- Interior 3: The patch depicted in Figure 32 is in a shape of house, which is symmetric about the midperpendicular of it. In one group, those two nodes changed the coordinate of x and y. The coefficients of the points on the midperpendicular line, the coordinates with respect to x and y are same.

$$\begin{aligned} G_h^x u(z) =& \frac{1}{4732h}(-216u_0 + 2378u_1 - 1431u_2 - 530u_3 - 1110u_4 + 943u_5 - 208u_6 - 747u_7 \\ & - 434u_8 + 822u_9 + 1611u_{10} - 1078u_{11}) \end{aligned} \tag{101}$$

$$\begin{aligned} G_h^y u(z) =& \frac{1}{4732h}(-216u_0 + 2378u_1 + 1611u_2 + 822u_3 - 434u_4 - 747u_5 - 208u_6 + 943u_7 \\ & - 1110u_8 - 530u_9 - 1431u_{10} - 1078u_{11}) \end{aligned} \tag{102}$$

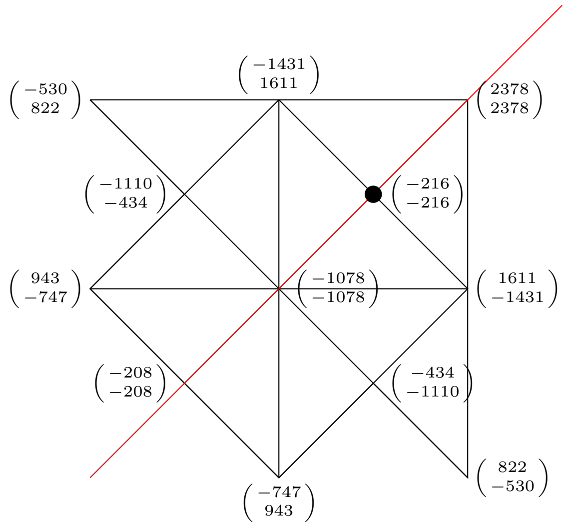

Figure 32: Criss-cross Interior 3 Symmetry

$$G_h u(z) = \begin{pmatrix} u_x(z) + \dfrac{h^2}{56784}\left(513u_{yyy}(z) + 15783u_{xyy}(z) + 8553u_{xxy}(z) + 1865u_{xxx}(z)\right) + O(h^3) \\ u_y(z) + \dfrac{h^2}{56784}\left(1865u_{yyy}(z) + 8553u_{xyy}(z) + 15783u_{xxy}(z) + 513u_{xxx}(z)\right) + O(h^3) \end{pmatrix} \tag{103}$$

- Interior 4: Before analyzing the symmetry of the patch, we separated the nodes of patch into two types, one of them on the red edge and another on the blue edge implied in Figure 33. The vertices on the red edge are symmetric about the central line from the vertex with $(17390, 0)$ to the one with $(110926, 0)$. The vertices on the blue edge are symmetric about the vertical line from a vertex related to the coefficient $(31561, 72765)$ to related to the coefficient $(31561, 72765)$.

$$\begin{aligned} G_h^x u(z) =& \frac{1}{957264h}(17390u_0 - 221408u_1 + 31561u_2 + 170681u_3 + 125097u_4 - 62678u_5 \\ &+ 110926u_6 - 62678u_7 + 125097u_8 + 170681u_9 + 31561u_{10} - 221408u_{11} \\ &- 249750u_{12} - 249750u_{13} + 142339u_{14} + 142339u_{15}) \end{aligned} \tag{104}$$

$$\begin{aligned} G_h^y u(z) =& \frac{1}{957264h}(135828u_1 + 72765u_2 + 82467u_3 + 37191u_4 + 9702u_5 - 9702u_7 - 37191u_8 \\ &- 82467u_9 - 72765u_{10} - 135828u_{11} - 45276u_{12} + 45276u_{13} + 27489u_{14} - 27489u_{15}) \end{aligned} \tag{105}$$

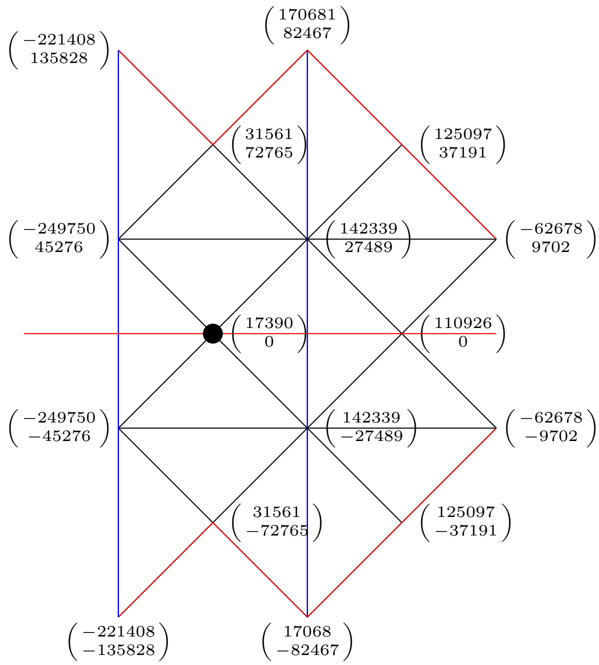

Figure 33: Criss-cross Interior 4 Symmetry

$$G_h u(z) = \begin{pmatrix} u_x(z) + \dfrac{h^2}{6468}\left(3998u_{xyy}(z) + 151u_{xxx}(z)\right) + O(h^3) \\ u_y(z) + \dfrac{h^2}{888}\left(265u_{yyy}(z) + 129u_{xxy}(z)\right) + O(h^3) \end{pmatrix} \tag{106}$$

Criss-cross Boundary

- Boundary 1: Suppose that u_0 with the coefficients of $(-330, -330)$ and u_5 with $(-12, -12)$, the coefficients of each vertex are symmetric about the diagonal from u_0 to u_5 (Figure 35).

$$G_h u(z) = \frac{1}{220h}\begin{pmatrix} -330u_0 - 75u_1 + 150u_2 + 365u_3 + 12u_4 + 5u_5 - 12u_6 - 39u_7 - 76u_8 \\ -330u_0 + 365u_1 + 150u_2 - 75u_3 - 76u_4 - 39u_5 - 12u_6 + 5u_7 + 12u_8 \end{pmatrix} \tag{107}$$

$$G_h u(z) = \begin{pmatrix} u_x(z) + \dfrac{h^2}{5280}\left(159u_{yyy}(z) - 27u_{xyy}(z) - 423u_{xxy}(z) - 1469u_{xxx}(z)\right) + O(h^3) \\ u_y(z) + \dfrac{h^2}{5280}\left(-1469u_{yyy}(z) - 423u_{xyy}(z) - 27u_{xxy}(z) + 159u_{xxx}(z)\right) + O(h^3) \end{pmatrix} \tag{108}$$

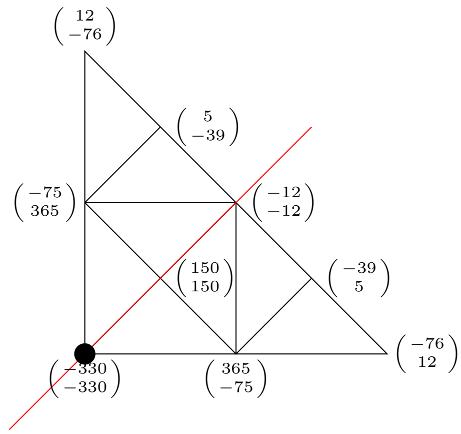

Figure 34: Criss-cross Boundary 1 Symmetry

- Boundary 2: Assume that u_0 with the coefficients of $(0, -30)$ and u_{10} with the coefficients of $(0, -28)$, the coefficients of each vertex are symmetric about the midperpendicular from u_0 to u_{10} of this triangular patch (Figure 34).

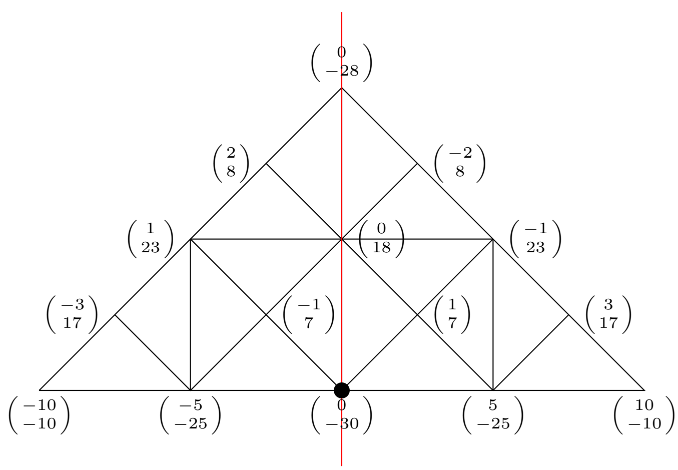

Figure 35: Criss-cross Boundary 2 Symmetry

$$G_h^x u(z) = \frac{1}{56h}(-5u_1 - u_2 + u_4 + 5u_5 - 10u_6 - 3u_7 + u_8 + 2u_9 - 2u_{11} - u_{12} + 3u_{13} + 10u_{14}) \tag{109}$$

$$\begin{aligned} G_h^y u(z) = &\frac{1}{56h}(-30u_0 - 25u_1 + 7u_2 + 18u_3 + 7u_4 - 25u_5 - 10u_6 + 17u_7 + 23u_8 + 8u_9 \\ &- 28u_{10} + 8u_{11} + 23u_{12} + 17u_{13} - 10u_{14}) \end{aligned} \tag{110}$$

$$G_h u(z) = \begin{pmatrix} u_x(z) + \dfrac{h^2}{84}\left(-3u_{xyy}(z) + 47u_{xxx}(z)\right) + O(h^3) \\ u_y(z) + \dfrac{h^2}{84}\left(-25u_{yyy}(z) + 69u_{xxy}(z)\right) + O(h^3) \end{pmatrix} \tag{111}$$

- Boundary 3: The patch shown in Figure 36 is not a graph with symmetry, so the coefficients of the vertices have no symmetry.

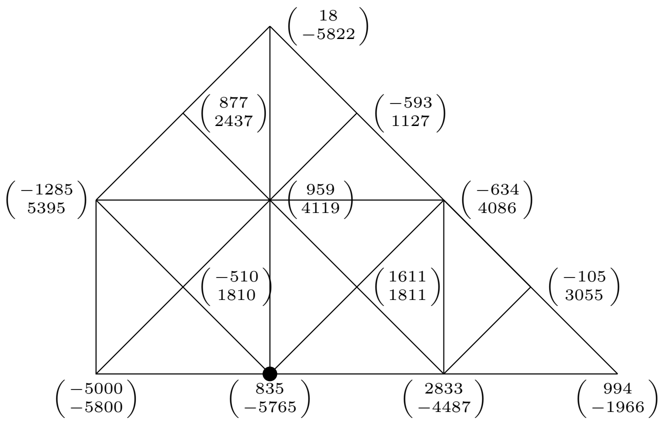

Figure 36: Criss-cross Boundary 3 Symmetry

$$\begin{aligned} G_h^x u(z) =& \frac{1}{10640h}(835u_0 - 5000u_1 - 510u_2 + 959u_3 + 1611u_4 + 2833u_5 - 1285u_6 + 877u_7 \\ &+ 18u_8 - 593u_9 - 634u_{10} - 105u_{11} + 994u_{12}) \end{aligned} \tag{112}$$

$$\begin{aligned} G_h^y u(z) =& \frac{1}{10640h}(-5765u_0 - 5800u_1 + 1810u_2 + 4119u_3 + 1811u_4 - 4487u_5 + 5395u_6 + 2437u_7 \\ &- 5822u_8 + 1127u_9 + 4086u_{10} + 3055u_{11} - 1966u_{12}) \end{aligned} \tag{113}$$

$$G_h u(z) = \begin{pmatrix} u_x(z) + \dfrac{h^2}{63840}\left(267u_{yyy}(z) - 2331u_{xyy}(z) - 5379u_{xxy}(z) + 16163u_{xxx}(z)\right) + O(h^3) \\ u_y(z) + \dfrac{h^2}{63840}\left(-20113u_{yyy}(z) + 4911u_{xyy}(z) + 44121u_{xxy}(z) - 5577u_{xxx}(z)\right) + O(h^3) \end{pmatrix} \tag{114}$$

4.1.5 Cartesian Pattern

- Interior: Assume that the top right node is u_8 and the bottom left is u_1, the coefficients of the nodes are symmetric about the diagonal from u_1 to u_8 (Figure 37).

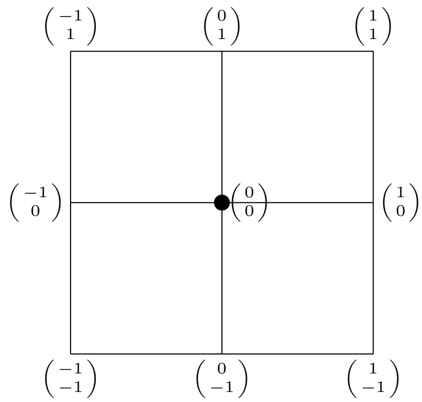

Figure 37: Cartesian Interior Symmetry

$$G_h u(z) = \frac{1}{6h} \begin{pmatrix} -u_1 + u_3 - u_4 + u_5 - u_6 + u_8 \\ -u_1 - u_2 - u_3 + u_6 + u_7 + u_8 \end{pmatrix} \tag{115}$$

$$G_h u(z) = \begin{pmatrix} u_x(z) + \dfrac{h^2}{6}\left(2u_{xyy}(z) + u_{xxx}(z)\right) + O(h^4) \\ u_y(z) + \dfrac{h^2}{6}\left(u_{yyy}(z) + 2u_{xxy}(z)\right) + O(h^4) \end{pmatrix} \tag{116}$$

- Boundary 1: Suppose that u_0 with the coefficients of $(-9,-9)$ and u_8 with the coefficients of $(-5,-5)$, the coefficients of each vertex are symmetric about the diagonal of the square patch from u_0 to u_8. And the coefficients of nodes on the diagonal are same with respect to x and y (Figure 38).

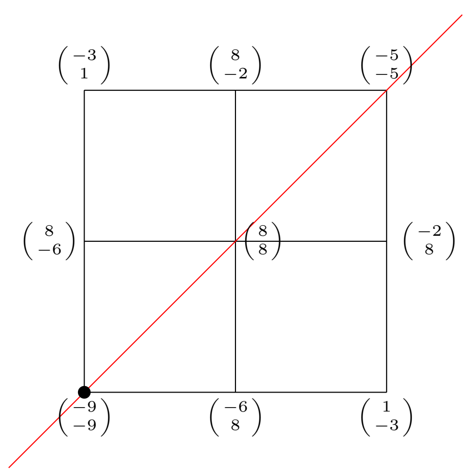

Figure 38: Cartesian Boundary 1 Symmetry

$$G_h u(z) = \frac{1}{12h} \begin{pmatrix} -9u_0 + 8u_1 + u_2 - 6u_3 + 8u_4 - 2u_5 - 3u_6 + 8u_7 - 5u_8 \\ -9u_0 - 6u_1 - 3u_2 + 8u_3 + 8u_4 + 8u_5 + u_6 - 2u_7 - 5u_8 \end{pmatrix} \tag{117}$$

$$G_h u(z) = \begin{pmatrix} u_x(z) + \frac{h^2}{6}\left(-u_{xyy}(z) - 6u_{xxy}(z) + u_{xxy}(z) + 2u_{xxx}(z)\right) + O(h^3) \\ u_y(z) + \frac{h^2}{6}\left(-2u_{yyy}(z) - 6u_{xyy}(z) - u_{xxy}(z)\right) + O(h^3) \end{pmatrix} \tag{118}$$

- Boundary 2: For Cartesian boundary 2, the recovered gradient coefficients with respect to y are same of all nodes on the same rows. The other rule is, about the axis from u_0 to u_{12}, the coefficients with respect to y are opposite numbers.

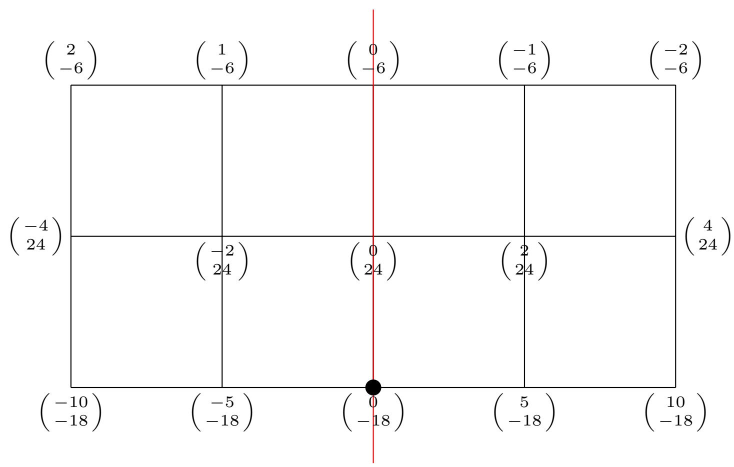

Figure 39: Cartesian Boundary 2 Symmetry

$$\begin{aligned} G_h^x u(z) = \frac{1}{60h}(&-10u_1 - 5u_2 + 5u_3 + 10u_4 - 4u_5 - 2u_6 + 2u_8 + 4u_9 + 2u_{10} \\ &+ u_{11} - u_{13} - 2u_{14}) \end{aligned} \tag{119}$$

$$\begin{aligned} G_h^y u(z) = \frac{1}{60h}(&-18u_0 - 18u_1 - 18u2 - 18u_3 - 18u_4 + 24u_5 + 24u_6 + 24u_7 \\ &+ 24u_8 + 24u_9 - 6u_{10} - 6u_{11} - 6u_{12} - 6u_{13} - 6u_{14}) \end{aligned} \tag{120}$$

$$G_h u(z) = \begin{pmatrix} u_x(z) + \frac{h^2}{30}\left(-5u_{xyy}(z) + 17u_{xxx}(z)\right) + O(h^3) \\ u_y(z) + \frac{h^2}{3}\left(-1u_{yyy}(z) + 3u_{xxy}(z)\right) + O(h^3) \end{pmatrix} \tag{121}$$

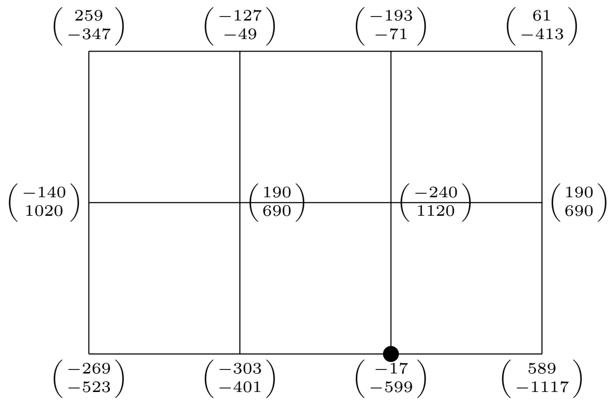

Figure 40: Cartesian Boundary 3 Symmetry

- Boundary 3: Considering the node regarded as the original node $(-17, -590)$, the patch has no symmetry according to this asymmetric patch.

$$\begin{aligned} G_h^x u(z) =& \frac{1}{6160h}(-17u_0 - 269u_1 - 303u_2 + 589u_3 - 140u_4 + 190u_5 - 240u_6 + 190u_7 \\ &+ 259u_8 - 127u_9 - 193u_{10} + 61u_{11}) \end{aligned} \tag{122}$$

$$\begin{aligned} G_h^y u(z) =& \frac{1}{6160h}(-599u_0 - 523u_1 - 401u_2 - 1117u_3 + 1020u_4 + 690u_5 + 1120u_6 + 690u_7 \\ &- 347u_8 - 49u_9 - 71u_{10} - 413u_{11}) \end{aligned} \tag{123}$$

$$G_h u(z) = \begin{pmatrix} u_x(z) + \dfrac{h^2}{9240}\left(-39u_{yyy}(z) + 5205u_{xyy}(z) + 1725u_{xxy}(z) + 2041u_{xxx}(z)\right) + O(h^3) \\ u_y(z) + \dfrac{h^2}{9240}\left(2041u_{yyy}(z) + 1725u_{xyy}(z) + 5205u_{xxy}(z) - 39u_{xxx}(z)\right) + O(h^3) \end{pmatrix} \tag{124}$$

4.2 Taylor Series

The coefficients of Taylor expansion are also regular, for central symmetric patch, the coefficient of h^2 of $G_h u(z)$ with respect to x and $G_h u(z)$ with respect to y are symmetric as well. Let the degree of the partial derivative of x is m and the degree of the partial derivative of y is n. For example, towards Regular Interior 1, the coefficient of $u_{x^m y^n}$ in $G_h u(z)$ with respect to x equals to the coefficient of $u_{y^m x^n}$. The rule doesn't exist when the patch is not symmetric.

Additionally, sometimes the patch is symmetric about some axis. When the axis of symmetry is horizontal or vertical, the coefficients are asymmetric. Plug into the coordinate system, when the patch is symmetric about $y = x$ or $y = -x$, although patch is not central symmetric, the coefficient still corresponds to the rules when is central symmetric.

Observing the Taylor expansion of every patch, the term after ux and uy is multiplied by x square which prove the recovered gradient is of second order precision.

Focusing on the remainder: $O(h^3)$ and $O(h^4)$,

- Central Symmetry: Both Taylor Expansion remainder of $G_h^x u(z)$ and $G_h^y u(z)$ are $O(h^4)$. Based on the rules mentioned about the coefficient of the patch nodes central symmetry, the sum of coefficient of h^3 is zero because the coefficients of u_{xxxx}, u_{xxxy}, u_{xxyy}, u_{xyyy} and u_{yyyy} are zero.

- Non-centrosymmetry: Both of the remainder of $G_h^x u(z)$ and $G_h^y u(z)$ are $O(h^3)$. Because the coefficients of u_{xxxx}, u_{xxxy}, u_{xxyy}, u_{xyyy} and u_{yyyy} are not all zero.

- Specially, for Chevron Interior case (Figure 15) and Chevron Boundary Case 3 (Figure 19), the coefficients with respect to x are zero, so the Taylor Expansion remainder of $G_h^x u(z)$ is $O(h^4)$.

5 Error in Boundary and Interior

It is mentioned above that gradient recovery techniques may deteriorate near boundary. Thus, boundary strategy is utilized to improve the accuracy of PPR method. This section will compare the error between the exact gradient and the recovered gradient at interior nodes and boundary nodes. Three principles are used to define the range of boundary, which are edge of domain, defined by h and defined by L. Following analysis is based on Regular Pattern and function $u = sinx \cdot siny$ and the domain is $[0, 1]^2$.

5.1 Three Types of Boundary

Considering error on boundary is the maximum value at every boundary nodes. Meanwhile, error in interior is the maximum value at every interior nodes. Thus, tables will be obtained below,which Error-bd represents error for boundary nodes and Error-in represents error for interior nodes

- Boundary 1: Edge of Domain

  Boundary nodes here are nodes on the domain edge. Table 1 is shown below.

Dofs	Error-bd	Error-in	Runtime
289	2.78e-03	1.12e-03	0.09
1089	6.82e-04	2.84e-04	0.08
4225	1.69e-04	7.14e-05	0.32
16641	4.19e-05	1.79e-05	3.31

Table 1: Error-in and Error-bd in Boundary 1

- Boundary 2: Defined by h

  Boundary points here are nodes in a range. The range is formed by the edge of domain and the edge of a square whose length of side is $(1 - 2h)$. Table 2 is shown below.

Dofs	Error-bd	Error-in	Runtime
289	2.78e-03	1.08e-03	0.10
1089	6.82e-04	2.79e-04	0.08
4225	1.69e-04	7.09e-05	0.32
16641	4.19e-05	1.79e-05	3.68

Table 2: Error-in and Error-bd in Boundary 2

- Boundary 3: Defined by L

  Boundary nodes are also the nodes in a range. Differently, the range here is formed by the edge of domain and the edge of a square whose length of side is $(1 - 2L)$. There we let $L = 0.1$. Table 3 is shown below.

Dofs	Error-bd	Error-in	Runtime
289	2.78e-03	1.08e-03	0.11
1089	6.82e-04	2.71e-04	0.08
4225	1.69e-04	6.82e-05	0.31
16641	4.19e-05	1.71e-05	3.51

Table 3: Error-in and Error-bd in Boundary 3

5.2 Comparison

- Comparison between Error-bd and Error-in

  Observing the three tables above, it is easy to find that under each DOF, interior error Error-in is always smaller than boundary error Error-bd. Therefore, it can conclude that even though the performance becomes better after boundary strategy, the accuracy on boundary is worse than the accuracy in interior.

- Comparison between three kinds of boundary

  Tables show that Error-bd of three kinds of boundary are the same. According to this rule, after processing data, it can find that the maximum error always obtained at a certain node on the edge of domain. Error-in of three kinds of interior are similar and it is slightly small in Boundary 3. In the data, it shows that maximum error appears at the different nodes but most of their places are closed to each other. However, if DOF becomes larger, the difference of Error-in between these three kinds of boundary principles will increase.

6 Hessian Recovery

Hessian Recovery [1] applies gradient recovery again based on PPR, which is also called PPR-PPR. The section is going to discuss how it works and introduce another way to perform it by utilizing the binomial equation in following parts. Meanwhile, those two methods refined by Regular and Cartesian Pattern are given some examples and comparisons between them will be presented below.

6.1 Preliminary

- Method 1

  In the previous section, we obtained the recovered gradient by PPR.

$$G_h u(z) = \begin{pmatrix} G_h^x u \\ G_h^y u \end{pmatrix} \tag{125}$$

  In order to gain more information of interior nodes and boundary nodes, it can further recover the gradient recovery. It means regarding $G_h^x u$ and $G_h^y u$ as new items and then applying gradient recovery on it. This process is defined as Method 1 in Hessian recovery.

$$H_h u(z) = (G_h(G_h^x u), G_h(G_h^y u)) = \begin{pmatrix} G_h^x(G_h^x u) & G_h^x(G_h^y u) \\ \\ G_h^y(G_h^x u) & G_h^y(G_h^y u) \end{pmatrix} \tag{126}$$

- Method 2

  For method 2 of Hessian Recovery, it is known that binary quadratic equation can be represented as

$$P_2(x,y) = a_1 + a_2 x + a_3 y + a_4 x^2 + a_5 xy + a_6 y^2$$

  Thereby, when conferring second partial derivative of the equation, only the the last three items are left and we can acquire:

$$(H_h^{xx} u)(z) = 2a_4 \tag{127}$$
$$(H_h^{xy} u)(z) = a_5 \tag{128}$$
$$(H_h^{yx} u)(z) = a_5 \tag{129}$$
$$(H_h^{yy} u)(z) = 2a_6 \tag{130}$$

  Then the recovered Hessian is gained at origin.

$$H_h u = \begin{pmatrix} H_h^{xx} & H_h^{xy} \\ H_h^{yx} & H_h^{yy} \end{pmatrix} = \begin{pmatrix} 2a_4 & a_5 \\ a_5 & 2a_6 \end{pmatrix} \tag{131}$$

6.2 Regular Pattern

In this part, Hessian Recovery will be explained through Regular Pattern with two methods. Then the result of Hessian Recovery and the Taylor Expansion of them will be performed.

6.2.1 Method 1

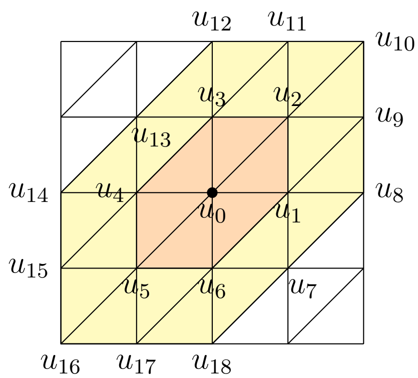

Figure 41: Regular Method 1

Following the gradient of Regular interior node and the principle of the first method of Hessian Recovery, we get the equation of Hessian Recovery below,

$$\begin{aligned}(H_h^{xx}u)(z_0) = \frac{1}{36}(&-12u_0 + 2u_1 - 4u_2 - 4u_3 + 2u_4 - 4u_5 - 4u_6 + 4u_7 + 4u_8 + 4u_9 + u_{10} \\ &- 2u_{11} + u_{12} + 4u_{13} + 4u_{14} + 4u_{15} + u_{16} - 2u_{17} + u_{18}) \end{aligned} \tag{132}$$

$$\begin{aligned}(H_h^{yx}u)(z_0) = \frac{1}{36}(&6u_0 - u_1 + 5u_2 - u_3 - u_4 + 5u_5 - u_6 - 5u_7 - 2u_8 + u_9 + u_{10} \\ &+ u_{11} - 2u_{12} - 5u_{13} - 2u_{14} + u_{15} + u_{16} + u_{17} - 2u_{18}) \end{aligned} \tag{133}$$

$$\begin{aligned}(H_h^{yy}u)(z_0) = \frac{1}{36}(&-12u_0 - 4u_1 - 4u_2 + 2u_3 - 4u_4 - 4u_5 + 2u_6 + 4u_7 + u_8 - 2u_9 + u_{10} \\ &+ 4u_{11} + 4u_{12} + 4u_{13} + u_{14} - 2u_{15} + u_{16} + 4u_{17} + 4u_{18}) \end{aligned} \tag{134}$$

$$\begin{aligned}(H_h^{xy}u)(z_0) = \frac{1}{36}(&6u_0 - u_1 + 5u_2 - u_3 - u_4 + 5u_5 - u_6 - 5u_7 - 2u_8 + u_9 + u_{10} \\ &+ u_{11} - 2u_{12} - 5u_{13} - 2u_{14} + u_{15} + u_{16} + u_{17} - 2u_{18}) \end{aligned} \tag{135}$$

Using Mathematica to perform the Taylor Expansion of H_hu at the node z_0, $(H_h^{xx}u)(z_0)$,

$(H_h^{yx}u)(z_0)$, $(H_h^{yy}u)(z_0)$ and $(H_h^{xy}u)(z_0)$ will be demonstrated as,

$$(H_h^{xx}u)(z_0) = u_{xx}(z) + \frac{h^2}{3}(u_{xxyy}(z) + u_{xxxy}(z) + u_{xxxx}(z)) + O(h^4) \tag{136}$$
$$(H_h^{yx}u)(z_0) = u_{yx}(z) + \frac{h^2}{3}(u_{xyyy}(z) + u_{xxyy}(z) + u_{xxxy}(z)) + O(h^4) \tag{137}$$
$$(H_h^{yy}u)(z_0) = u_{yy}(z) + \frac{h^2}{3}(u_{yyyy}(z) + u_{xyyy}(z) + u_{xxyy}(z)) + O(h^4) \tag{138}$$
$$(H_h^{xy}u)(z_0) = u_{xy}(z) + \frac{h^2}{3}(u_{xyyy}(z) + u_{xxyy}(z) + u_{xxxy}(z)) + O(h^4) \tag{139}$$

6.2.2 Method 2

Based on the previous gradient and second method principle, the equation of Hessian Recovery will be depicted,

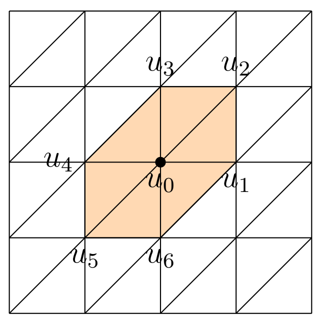

Figure 42: Regular Method 2

$$(H_h^{xx}u)(z_0) = -2u_0 + u_1 + u_4 \tag{140}$$
$$(H_h^{yx}u)(z_0) = 2u_0 - u_1 + u_2 - u_3 - u_4 + u_5 - u_6 \tag{141}$$
$$(H_h^{xy}u)(z_0) = 2u_0 - u_1 + u_2 - u_3 - u_4 + u_5 - u_6 \tag{142}$$
$$(H_h^{yy}u)(z_0) = -2u_0 + u_3 + u_6 \tag{143}$$

Using Mathematica to perform the Taylor Expansion of H_hu at the node z_0, $H_hu(z)$ will be displayed as following,

$$H_hu(z) = \begin{pmatrix} u_{xx}(z) + \frac{h^2}{12}u_{xxxx}(z) + O(h^4) \\ u_{yx}(z) + \frac{h^2}{12}\left(2u_{xyyy}(z) + 3u_{xxyy}(z) + 2u_{xxxy}(z)\right) + O(h^4) \\ u_{xy}(z) + \frac{h^2}{12}\left(2u_{xxxy}(z) + 3u_{xxyy}(z) + 2u_{xyyy}(z)\right) + O(h^4) \\ u_{yy}(z) + \frac{h^2}{12}u_{yyyy}(z) + O(h^4) \end{pmatrix} \tag{144}$$

6.3 Cartesian Pattern

In this part, the Hessian Recovery will be demonstrated by Cartesian Pattern. One of the interior nodes will be given an example of its results and Taylor Expansion.

6.3.1 Method 1

About Method 1, the patch is expanded by the other layer on the original basis with the patch of the Cartesian.

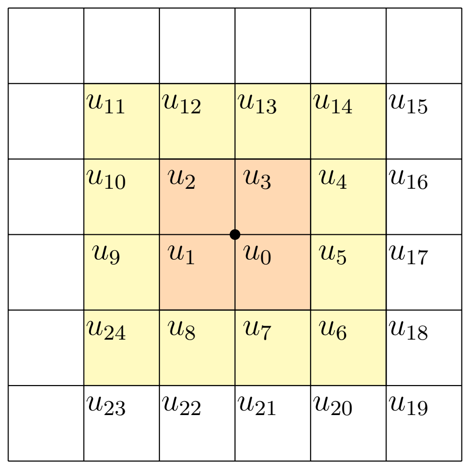

Figure 43: Cartesian Method 1

$$
\begin{aligned}
(H_h^{xx}u)(z_0) =& \frac{1}{36}(-6u_0 - 4u_1 - 4u_5 - 2u_9 + u_{11} + 2u_{12} + 3u_{13} + 2u_{14} + u_{15} - 2u_{17} \\
& + u_{19} + 2u_{20} + 3u_{21} + 2u_{22} + u_{23}) \qquad (145) \\
(H_h^{xy}u)(z_0) =& \frac{1}{36}(-u_2 + u_4 - u_6 + u_8 - u_{10} - u_{11} - u_{12} + u_{14} + u_{15} + u_{16} - u_{18} - u_{19} \\
& - u_{20} + u_{22} + u_{23} + u_{24}) \qquad (146) \\
(H_h^{yx}u)(z_0) =& \frac{1}{36}(-u_2 + u_4 - u_6 + u_8 - u_{10} - u_{11} - u_{12} + u_{14} + u_{15} + u_{16} - u_{18} - u_{19} \\
& - u_{20} + u_{22} + u_{23} + u_{24}) \qquad (147) \\
(H_h^{yy}u)(z_0) =& \frac{1}{36}(-6u_0 - 4u_3 - 4u_7 + 3u_9 + 2u_{10} + u_{11} - 2u_{13} + u_{15} + 2u_{16} + 3u_{17} \\
& + 2u_{18} + u_{19} - 2u_{21} + u_{23} + 2u_{24}) \qquad (148)
\end{aligned}
$$

The Taylor Expansions of $(H_h^{xx}u)(z_0)$, $(H_h^{xy}u)(z_0)$, $(H_h^{yy}u)(z_0)$ and $(H_h^{yx}u)(z_0)$ are as following;

$$(H_h^{xx}u)(z_0) = u_{xx}(z) + \frac{h^2}{3}(2u_{xxyy}(z) + u_{xxxx}(z)) + O(h^4) \tag{149}$$

$$(H_h^{xy}u)(z_0) = u_{xy}(z) + \frac{h^2}{2}(u_{xyyy}(z) + u_{xyyy}(z) + u_{xxxy}(z)) + O(h^4) \tag{150}$$

$$(H_h^{yy}u)(z_0) = u_{yy}(z) + \frac{h^2}{3}(u_{yyyy}(z) + 2u_{xxyy}(z)) + O(h^4) \tag{151}$$

$$(H_h^{yx}u)(z_0) = u_{yx}(z) + \frac{h^2}{2}(u_{xyyy}(z) + u_{xyyy}(z) + u_{xxxy}(z)) + O(h^4) \tag{152}$$

6.3.2 Method 2

Considering the Method 2, the patch is shown as the same way as the patch of the gradient recovery:

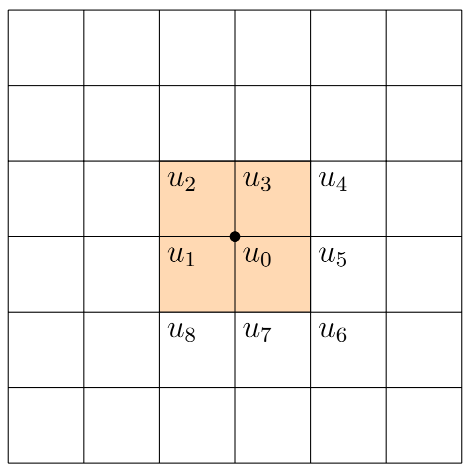

Figure 44: Cartesian Method 2

$$(H_h^{xx}u)(z_0) = \frac{1}{3}(-2u_0 + u_1 + u_2 - 2u_3 + u_4 + u_5 + u_6 - 2u_7 + u_8) \tag{153}$$

$$(H_h^{xy}u)(z_0) = \frac{1}{4}(-u_2 + u_4 - u_6 + u_8) \tag{154}$$

$$(H_h^{yy}u)(z_0) = \frac{1}{3}(-2u_0 - 2u_1 + u_2 + u_3 + u_4 - 2u_5 + u_6 + u_7 + u_8) \tag{155}$$

$$(H_h^{yx}u)(z_0) = \frac{1}{4}(-u_2 + u_4 - u_6 + u_8) \tag{156}$$

Using Mathematica to calculate the Taylor Expansion, $(H_h^{xx}u)(z_0)$, $(H_h^{xy}u)(z_0)$, $(H_h^{yy}u)(z_0)$ and $(H_h^{yx}u)(z_0)$ can be acquired and shown below:

$$(H_h^{xx}u)(z_0) = u_{xx}(z) + \frac{h^2}{12}(4u_{xxyy}(z) + u_{xxxx}(z)) + O(h^4) \tag{157}$$

$$(H_h^{xy}u)(z_0) = u_{xy}(z) + \frac{h^2}{6}(u_{xyyy}(z) + u_{xxxy}(z)) + O(h^4) \tag{158}$$

$$(H_h^{yy}u)(z_0) = u_{yy}(z) + \frac{h^2}{12}(u_{yyyy}(z) + 4u_{xxyy}(z)) + O(h^4) \tag{159}$$

$$(H_h^{xy}u)(z_0) = u_{xy}(z) + \frac{h^2}{6}(u_{xyyy}(z) + u_{xxxy}(z)) + O(h^4) \tag{160}$$

7 Convergence Rate of Operator

This section focuses on examining the accuracy of Gradient Operator (G_h) and Hessian Operator (H_h). And we use exact functions to test the accuracy. The following two parts using Cartesian Pattern and Regular Pattern display the accuracy of them.

7.1 Cartesian Pattern

- Smooth Function: $u = \sin(\pi x) \cdot \sin(\pi y)$

  The smooth function performs well when it is recovered by Gradient and Hessian Recovery operator. Tables 4 and 5, and figure show a second order finite difference scheme approximating both $\nabla u(z)$ and the second-order partial derivative of u.

Dofs	$\|G_h u - \nabla u\|_{\infty,\Omega_h}$	order	$\|G_h u - \nabla u\|_{\infty,\Omega_{1,h}}$	order
289	8.1490e-02	–	5.5555e-02	–
1089	2.0234e-02	2.01	1.3963e-02	1.99
4225	5.0496e-03	2.00	3.5621e-03	1.97
16641	1.2618e-03	2.00	8.9838e-04	1.99
66049	3.1542e-04	2.00	2.2461e-04	2.00
263169	7.8854e-05	2.00	5.6154e-05	2.00
1050625	1.9713e-05	2.00	1.4053e-05	2.00
4198401	4.9283e-06	2.00	3.5150e-06	2.00

Table 4: Convergence Rate for Smooth Function (G_h)

- Quadratic Polynomial: $u = x^2 + y^2$

  Quadratic polynomial function is fitted well, so it demonstrates error close to 10^{-14} in Gradient Recovery and 10^{-13} in Hessian Recovery. Since the fitting process cannot be more accurate, the error will increase while the number of degree of freedoms increases. Tables 6 and 7 represent both of operators converge at a rate of $O(h^2)$.

Dofs	$\|H_h u - \Delta u\|_{\infty,\Omega_h}$	order	$\|H_h u - \Delta u\|_{\infty,\Omega_{1,h}}$	order
289	1.8739e+00	–	1.5769e-01	–
1089	9.6086e-01	0.96	3.9582e-02	1.99
4225	4.8346e-01	0.99	9.9056e-03	2.00
16641	2.4211e-01	1.00	2.4770e-03	2.00
66049	1.2110e-01	1.00	6.1930e-04	2.00
263169	6.0557e-02	1.00	1.5483e-04	2.00
1050625	3.0279e-02	1.00	3.8707e-05	2.00
4198401	1.5140e-02	1.00	9.6798e-06	2.00

Table 5: Convergence Rate for Smooth Function (H_h)

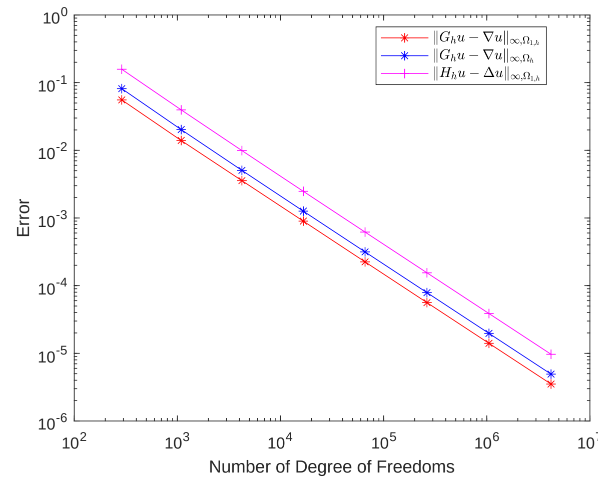

Dofs	$\|G_h u - \nabla u\|_{\infty,\Omega_h}$	order	$\|G_h u - \nabla u\|_{\infty,\Omega_{1,h}}$	order
289	3.7303e-14	–	8.8818e-16	–
1089	9.2371e-14	-1.31	1.7764e-15	-1.00
4225	1.8474e-13	-1.00	3.5527e-15	-1.00
16641	3.9790e-13	-1.11	7.1054e-15	-1.00
66049	8.2423e-13	-1.05	1.4211e-14	-1.00
263169	1.6485e-12	-1.00	2.8422e-14	-1.00
1050625	3.2969e-12	-1.00	5.6843e-14	-1.00
4198401	6.3665e-12	-0.95	1.1369e-13	-1.00

Table 6: Convergence Rate for Quadratic Polynomial (G_h)

Dofs	$\|H_h u - \Delta u\|_{\infty,\Omega_h}$	order	$\|H_h u - \Delta u\|_{\infty,\Omega_{1,h}}$	order
289	6.8212e-13	–	2.2737e-13	–
1089	2.8422e-12	-2.06	9.0949e-13	-2.00
4225	1.2278e-11	-2.11	3.6380e-12	-2.00
16641	4.9113e-11	-2.00	1.4552e-11	-2.00
66049	1.9645e-10	-2.00	5.8208e-11	-2.00
263169	8.4401e-10	-2.10	2.3283e-10	-2.00
1050625	3.4925e-09	-2.05	9.3132e-10	-2.00
4198401	1.3737e-08	-1.98	3.7253e-09	-2.00

Table 7: Convergence Rate for Quadratic Polynomial (H_h)

- Cubic Polynomial: $u = 11x^3 + 37x^2y + 73y^2 + 87xy + 71$

For cubic polynomial function, Table 8 displays a second order finite difference scheme of approximating ∇u. However, from Table 9, Hessian Recovery of overall nodes in domain converge at rate of $O(h)$, the convergence rate of Hessian Recovery for the interior subdomain is negative.

Dofs	$\|G_h u - \nabla u\|_{\infty,\Omega_h}$	order	$\|G_h u - \nabla u\|_{\infty,\Omega_{1,h}}$	order
289	3.7500e-01	–	9.6354e-02	–
1089	9.3750e-02	2.00	2.4089e-02	2.00
4225	2.3438e-02	2.00	6.0221e-03	2.00
16641	5.8594e-03	2.00	1.5055e-03	2.00
66049	1.4648e-03	2.00	3.7638e-04	2.00
263169	3.6621e-04	2.00	9.4096e-05	2.00
1050625	9.1553e-05	2.00	2.3524e-05	2.00
4198401	2.2889e-05	2.00	5.8810e-06	2.00

Table 8: Convergence Rate for Cubic Polynomial (G_h)

Dofs	$\|H_h u - \Delta u\|_{\infty,\Omega_h}$	order	$\|H_h u - \Delta u\|_{\infty,\Omega_{1,h}}$	order
289	8.7500e+00	–	2.9104e-11	–
1089	4.3750e+00	1.00	1.1642e-10	-2.00
4225	2.1875e+00	1.00	4.6566e-10	-2.00
16641	1.0938e+00	1.00	1.8626e-09	-2.00
66049	5.4688e-01	1.00	7.4506e-09	-2.00
263169	2.7344e-01	1.00	2.9802e-08	-2.00
1050625	1.3672e-01	1.00	1.1921e-07	-2.00
4198401	6.8361e-02	1.00	4.7684e-07	-2.00

Table 9: Convergence Rate for Cubic Polynomial (H_h)

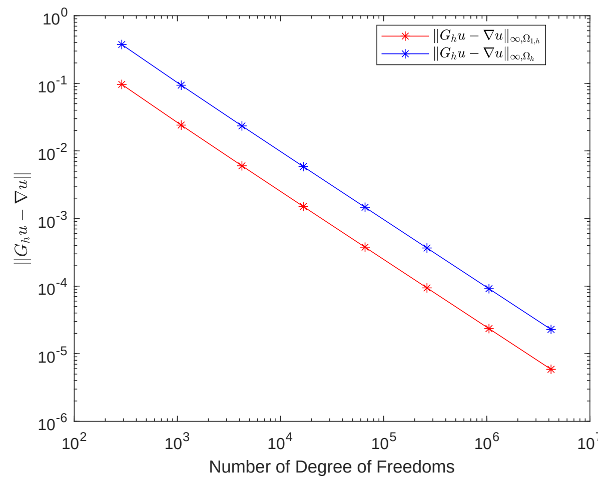

- Fourth Polynomial: $u = x^4 + 8x^3y + 4x^2y^2 + 4xy^3 + 2xy$

  According to Table 10, as the number of degree of freedoms reach to $(2^8+1)^2$, the convergence rate of Gradient Recovery will increase to 2. Also in Table 11, it depicts well when focused on the interior subdomain of Hessian Recovery, which means that the convergence rate of it is absolutely 2.

- Fifth Polynomial: $u = 3x^5 + 4y^5 + 2x^3 + 3y^2$

  Tables 12 and 13 imply that both Gradient Recovery and Hessian Recovery of interior subdomain cause similar error and similar convergence rate of 2, so those two curves overlap.

Dofs	$\|G_hu - \nabla u\|_{\infty,\Omega_h}$	order	$\|G_hu - \nabla u\|_{\infty,\Omega_{1,h}}$	order
289	3.5173e-01	–	8.6589e-02	–
1089	9.0190e-02	1.96	2.1647e-02	2.00
4225	2.2830e-02	1.98	5.5084e-03	1.97
16641	5.7427e-03	1.99	1.3892e-03	1.99
66049	1.4401e-03	2.00	3.4730e-04	2.00
263169	3.6057e-04	2.00	8.6824e-05	2.00
1050625	9.0212e-05	2.00	2.1730e-05	2.00
4198401	2.2562e-05	2.00	5.4354e-06	2.00

Table 10: Convergence Rate for Fourth Polynomial (G_h)

Dofs	$\|H_hu - \Delta u\|_{\infty,\Omega_h}$	order	$\|H_hu - \Delta u\|_{\infty,\Omega_{1,h}}$	order
289	8.2057e+00	–	4.6875e-02	–
1089	4.1764e+00	0.97	1.1719e-02	2.00
4225	2.1066e+00	0.99	2.9297e-03	2.00
16641	1.0579e+00	0.99	7.3242e-04	2.00
66049	5.3010e-01	1.00	1.8311e-04	2.00
263169	2.6534e-01	1.00	4.5776e-05	2.00
1050625	1.3274e-01	1.00	1.1444e-05	2.00
4198401	6.6388e-02	1.00	2.8610e-06	2.00

Table 11: Convergence Rate for Fourth Polynomial (H_h)

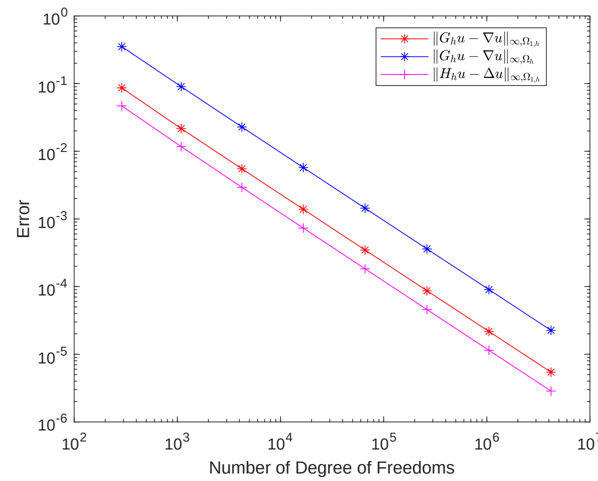

Dofs	$\|G_hu - \nabla u\|_{\infty,\Omega_h}$	order	$\|G_hu - \nabla u\|_{\infty,\Omega_{1,h}}$	order
289	4.0753e-01	–	1.1969e-01	–
1089	1.1678e-01	1.80	2.9911e-02	2.00
4225	3.1163e-02	1.91	7.7465e-03	1.95
16641	8.0436e-03	1.95	1.9707e-03	1.97
66049	2.0429e-03	1.98	4.9267e-04	2.00
263169	5.1475e-04	1.99	1.2317e-04	2.00
1050625	1.2919e-04	1.99	3.0859e-05	2.00
4198401	3.2362e-05	2.00	7.7231e-06	2.00

Table 12: Convergence Rate for Fifth Polynomial (G_h)

- Sixth Polynomial: $u = x^6 + y^6 + x^2y^4$
- Seventh Polynomial: $u = x^7 + x^5y^2 + x^3y^3 + y^7$

Dofs	$\|H_h u - \Delta u\|_{\infty,\Omega_h}$	order	$\|H_h u - \Delta u\|_{\infty,\Omega_{1,h}}$	order
289	1.3936e+01	–	1.3672e-01	–
1089	7.2302e+00	0.95	3.4180e-02	2.00
4225	3.6821e+00	0.97	8.6975e-03	1.97
16641	1.8580e+00	0.99	2.1935e-03	1.99
66049	9.3323e-01	0.99	5.4836e-04	2.00
263169	4.6768e-01	1.00	1.3709e-04	2.00
1050625	2.3411e-01	1.00	3.4313e-05	2.00
4198401	1.1712e-01	1.00	8.5998e-06	2.00

Table 13: Convergence Rate for Fifth Polynomial (H_h)

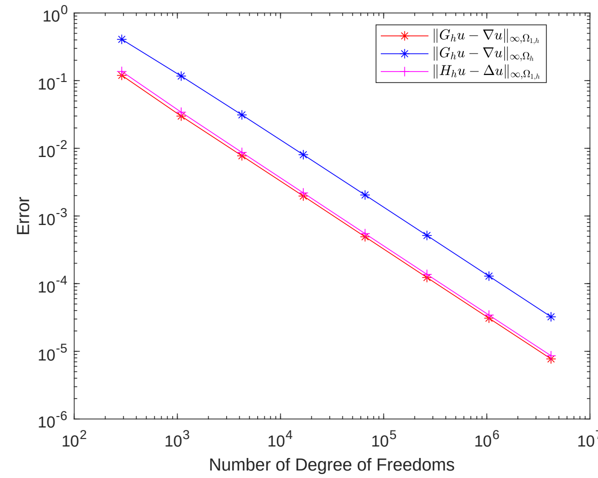

Dofs	$\|G_h u - \nabla u\|_{\infty,\Omega_h}$	order	$\|G_h u - \nabla u\|_{\infty,\Omega_{1,h}}$	order
289	2.4779e-01	–	7.3371e-02	–
1089	6.6636e-02	1.89	1.8324e-02	2.00
4225	1.8018e-02	1.89	4.8297e-03	1.92
16641	4.6986e-03	1.94	1.2394e-03	1.96
66049	1.1995e-03	1.97	3.0984e-04	2.00
263169	3.0302e-04	1.98	7.7461e-05	2.00
1050625	7.6151e-05	1.99	1.9428e-05	2.00
4198401	1.9087e-05	2.00	4.8650e-06	2.00

Table 14: Convergence Rate for Sixth Polynomial (G_h)

Dofs	$\|H_h u - \Delta u\|_{\infty,\Omega_h}$	order	$\|H_h u - \Delta u\|_{\infty,\Omega_{1,h}}$	order
289	9.4186e+00	–	1.1968e-01	–
1089	4.9723e+00	0.92	2.9910e-02	2.00
4225	2.5547e+00	0.96	7.7464e-03	1.95
16641	1.2948e+00	0.98	1.9707e-03	1.97
66049	6.5181e-01	0.99	4.9267e-04	2.00
263169	3.2701e-01	1.00	1.2317e-04	2.00
1050625	1.6378e-01	1.00	3.0860e-05	2.00
4198401	8.1962e-02	1.00	7.7266e-06	2.00

Table 15: Convergence Rate for Sixth Polynomial (H_h)

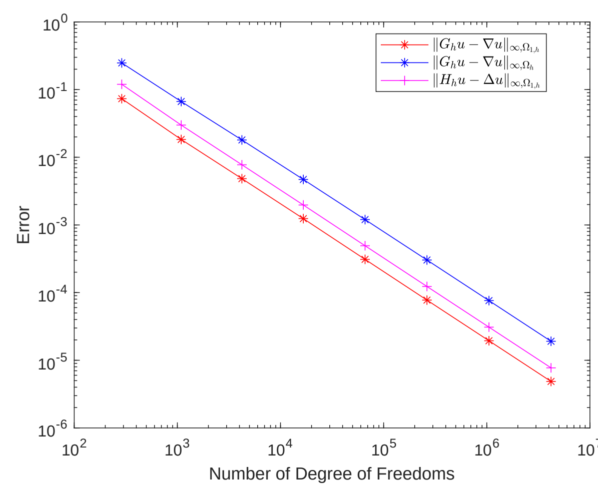

Considered the sixth-order polynomial function and seventh-order polynomial function together, from the four Tables 14, 15, 16 and 17, when the order of the polynomial increases, the mesh should be refined denser in order to get a second order finite difference scheme approximating ∇u and the second-order derivative of u.

Dofs	$\|G_h u - \nabla u\|_{\infty,\Omega_h}$	order	$\|G_h u - \nabla u\|_{\infty,\Omega_{1,h}}$	order
289	5.0165e-01	–	1.2935e-01	–
1089	1.3767e-01	1.87	3.2270e-02	2.00
4225	3.6054e-02	1.93	8.6333e-03	1.90
16641	9.2245e-03	1.97	2.2320e-03	1.95
66049	2.3329e-03	1.98	5.5799e-04	2.00
263169	5.8661e-04	1.99	1.3950e-04	2.00
1050625	1.4708e-04	2.00	3.5021e-05	1.99
4198401	3.6822e-05	2.00	8.7736e-06	2.00

Table 16: Convergence Rate for Seventh Polynomial (G_h)

Dofs	$\|H_h u - \Delta u\|_{\infty,\Omega_h}$	order	$\|H_h u - \Delta u\|_{\infty,\Omega_{1,h}}$	order
289	1.8123e+01	–	2.8041e-01	–
1089	9.7223e+00	0.90	7.0050e-02	2.00
4225	5.0365e+00	0.95	1.8423e-02	1.93
16641	2.5634e+00	0.97	4.7225e-03	1.96
66049	1.2931e+00	0.99	1.1806e-03	2.00
263169	6.4945e-01	0.99	2.9515e-04	2.00
1050625	3.2545e-01	1.00	7.4020e-05	2.00
4198401	1.6290e-01	1.00	1.8537e-05	2.00

Table 17: Convergence Rate for Seventh Polynomial (H_h)

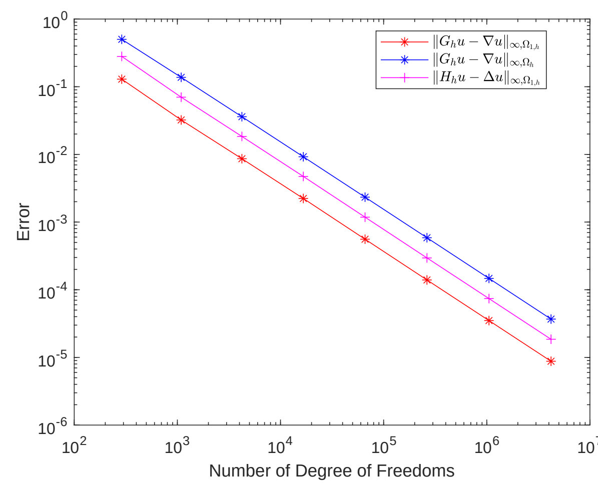

7.2 Regular Pattern

Meanwhile, Regular Pattern is still applied to examine the accuracy of the Gradient Recovery operator and Hessian Recovery operator.

- Smooth Function: $u = \sin(\pi x) \cdot \sin(\pi y)$ (Tables 18 and 19)
- Quadratic Polynomial: $u = x^2 + y^2$ (Tables 20 and 21)
- Cubic Polynomial: $u = 11x^3 + 37x^2 y + 73y^2 + 87xy + 71$ (Tables 22 and 23)
- Fourth Polynomial: $u = x^4 + 8x^3 y + 4x^2 y^2 + 4xy^3 + 2xy$ (Tables 24 and 25)

Dofs	$\|G_hu-\nabla u\|_{\infty,\Omega_h}$	order	$\|G_hu-\nabla u\|_{\infty,\Omega_{1,h}}$	order
289	5.9792e-02	–	3.7865e-02	–
1089	1.4823e-02	2.01	9.5084e-03	1.99
4225	3.6976e-03	2.00	2.4122e-03	1.98
16641	9.2388e-04	2.00	6.0703e-04	1.99
66049	2.3094e-04	2.00	1.5177e-04	2.00
263169	5.7732e-05	2.00	3.7944e-05	2.00
1050625	1.4433e-05	2.00	9.4929e-06	2.00
4198401	3.6082e-06	2.00	2.3741e-06	2.00

Table 18: Convergence Rate for Smooth Function (G_h)

Dofs	$\|H_hu-\Delta u\|_{\infty,\Omega_h}$	order	$\|H_hu-\Delta u\|_{\infty,\Omega_{1,h}}$	order
289	1.3836e+00	–	1.2155e-01	–
1089	6.9203e-01	1.00	3.0507e-02	1.99
4225	3.4604e-01	1.00	7.6997e-03	1.99
16641	1.7302e-01	1.00	1.9329e-03	1.99
66049	8.6513e-02	1.00	4.8325e-04	2.00
263169	4.3257e-02	1.00	1.2081e-04	2.00
1050625	2.1628e-02	1.00	3.0218e-05	2.00
4198401	1.0814e-02	1.00	7.5560e-06	2.00

Table 19: Convergence Rate for Smooth Function (H_h)

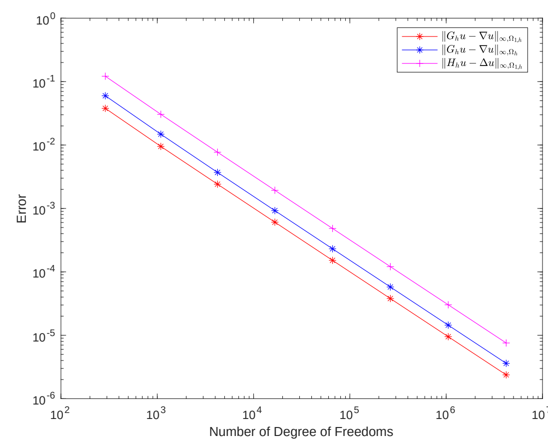

- Fifth Polynomial: $u = 3x^5 + 4y^5 + 2x^3 + 3y^2$ (Tables 26 and 27)
- Sixth Polynomial: $u = x^6 + y^6 + x^2y^4$ (Tables 28 and 29)
- Seventh Polynomial: $u = x^7 + x^5y^2 + x^3y^3 + y^7$ (Tables 30 and 31)

8 Elliptic Differential Partial Equation

In this section, Gradient Recovery and Hessian Recovery are applied for recovering the partial derivative of first-order and second-order in elliptic partial differential equations respectively to obtain solution u_h. Hessian Recovery there we use Method 2 to perform Hessian Recovery operator. Consider an elliptic partial differential equation with Dirichlet condition:

$$\begin{aligned} -\Delta u &= f, (x,y) \in \Omega \\ \Omega &= [0,1]^2 \\ u(x,y) &= u, (x,y) \in \Gamma \end{aligned} \tag{161}$$

Dofs	$\|G_h u - \nabla u\|_{\infty,\Omega_h}$	order	$\|G_h u - \nabla u\|_{\infty,\Omega_{1,h}}$	order
289	6.4837e-14	–	1.7764e-15	–
1089	1.4033e-13	-1.11	3.5527e-15	-1.00
4225	2.9132e-13	-1.05	1.0658e-14	-1.58
16641	5.9330e-13	-1.03	2.1316e-14	-1.00
66049	1.2932e-12	-1.12	4.2633e-14	-1.00
263169	2.4727e-12	-0.94	8.5265e-14	-1.00
1050625	5.1443e-12	-1.06	1.7053e-13	-1.00
4198401	9.9476e-12	-0.95	3.4106e-13	-1.00

Table 20: Convergence Rate for Quadratic Polynomial (G_h)

Dofs	$\|H_h u - \Delta u\|_{\infty,\Omega_h}$	order	$\|H_h u - \Delta u\|_{\infty,\Omega_{1,h}}$	order
289	1.0232e-12	–	3.9790e-13	–
1089	4.1780e-12	-2.03	1.5916e-12	-2.00
4225	1.8645e-11	-2.16	7.2760e-12	-2.19
16641	7.2305e-11	-1.96	2.9104e-11	-2.00
66049	3.0559e-10	-2.08	1.1642e-10	-2.00
263169	1.1860e-09	-1.96	4.6566e-10	-2.00
1050625	5.0932e-09	-2.10	1.8626e-09	-2.00
4198401	2.0373e-08	-2.00	7.4506e-09	-2.00

Table 21: Convergence Rate for Quadratic Polynomial (H_h)

8.1 Principle

Given a square area of Ω with the step size h, dividing the mesh (Figure 45) into N nodes. The number of interior nodes is M. Then we can discrete f into $-u_{xx} - u_{yy}$.

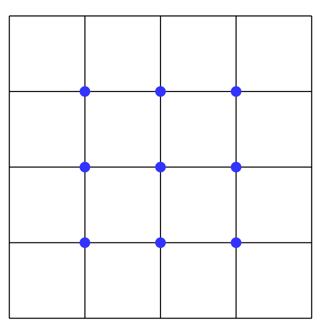

Figure 45: Mesh

Suppose z_i represents all nodes. Define $\Delta x = \Delta y = h$ (Figure 45) and solutions at every node are written as $u_h(z_i)$. Using Hessian Recovery to approximate second-order partial derivative, Δu

Dofs	$\|G_h u - \nabla u\|_{\infty,\Omega_h}$	order	$\|G_h u - \nabla u\|_{\infty,\Omega_{1,h}}$	order
289	3.7500e-01	–	9.1146e-02	–
1089	9.3750e-02	2.00	2.2786e-02	2.00
4225	2.3438e-02	2.00	5.6966e-03	2.00
16641	5.8594e-03	2.00	1.4242e-03	2.00
66049	1.4648e-03	2.00	3.5604e-04	2.00
263169	3.6621e-04	2.00	8.9010e-05	2.00
1050625	9.1553e-05	2.00	2.2252e-05	2.00
4198401	2.2889e-05	2.00	5.5631e-06	2.00

Table 22: Convergence Rate for Cubic Polynomial (G_h)

Dofs	$\|H_h u - \Delta u\|_{\infty,\Omega_h}$	order	$\|H_h u - \Delta u\|_{\infty,\Omega_{1,h}}$	order
289	8.7500e+00	–	7.2760e-11	–
1089	4.3750e+00	1.00	2.9104e-10	-2.00
4225	2.1875e+00	1.00	1.1642e-09	-2.00
16641	1.0938e+00	1.00	4.6566e-09	-2.00
66049	5.4688e-01	1.00	1.8626e-08	-2.00
263169	2.7344e-01	1.00	7.4506e-08	-2.00
1050625	1.3672e-01	1.00	2.9802e-07	-2.00
4198401	6.8361e-02	1.00	1.1921e-06	-2.00

Table 23: Convergence Rate for Cubic Polynomial (H_h)

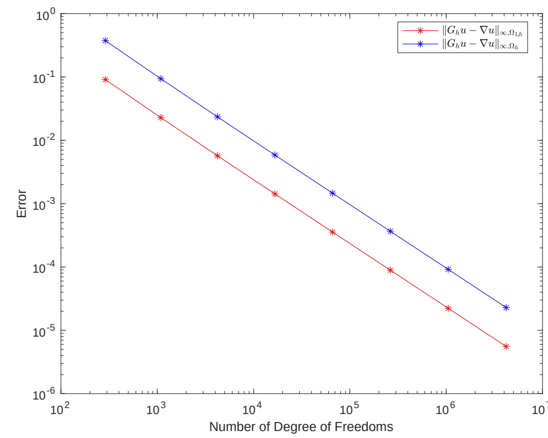

can be discreted into $H_{xx} + H_{yy}$.

$$\frac{\partial^2 u}{\partial x^2} \approx (H_h^{xx} u_h)(z_i) \tag{162}$$

$$\frac{\partial^2 u}{\partial y^2} \approx (H_h^{yy} u_h)(z_i) \tag{163}$$

Plug the equations above into Laplace equation. Thus, recovery difference scheme for Laplacian difference equation is

$$-(H_h^{xx} u_h)(z_i) - (H_h^{yy} u_h)(z_i) = f \tag{164}$$

Find the Laplacian difference equation at each point in Ω, there exists M equations. Transpose the system of liner equations to an matrix equation. Solve the equation finally we can get the solution like the form below:

$$u_h = \begin{bmatrix} u_h(z_1) & u_h(z_2) & \cdots & u_h(z_M) \end{bmatrix}^T \tag{165}$$

Dofs	$\|G_h u - \nabla u\|_{\infty,\Omega_h}$	order	$\|G_h u - \nabla u\|_{\infty,\Omega_{1,h}}$	order
289	3.5173e-01	–	1.0026e-01	–
1089	9.0190e-02	1.96	2.5065e-02	2.00
4225	2.2830e-02	1.98	6.3782e-03	1.97
16641	5.7427e-03	1.99	1.6085e-03	1.99
66049	1.4401e-03	2.00	4.0213e-04	2.00
263169	3.6057e-04	2.00	1.0053e-04	2.00
1050625	9.0212e-05	2.00	2.5161e-05	2.00
4198401	2.2562e-05	2.00	6.2936e-06	2.00

Table 24: Convergence Rate for Fourth Polynomial (G_h)

Dofs	$\|H_h u - \Delta u\|_{\infty,\Omega_h}$	order	$\|H_h u - \Delta u\|_{\infty,\Omega_{1,h}}$	order
289	8.2057e+00	–	6.2500e-02	–
1089	4.1764e+00	0.97	1.5625e-02	2.00
4225	2.1066e+00	0.99	3.9062e-03	2.00
16641	1.0579e+00	0.99	9.7656e-04	2.00
66049	5.3010e-01	1.00	2.4414e-04	2.00
263169	2.6534e-01	1.00	6.1035e-05	2.00
1050625	1.3274e-01	1.00	1.5259e-05	2.00
4198401	6.6388e-02	1.00	3.8147e-06	2.00

Table 25: Convergence Rate for Fourth Polynomial (H_h)

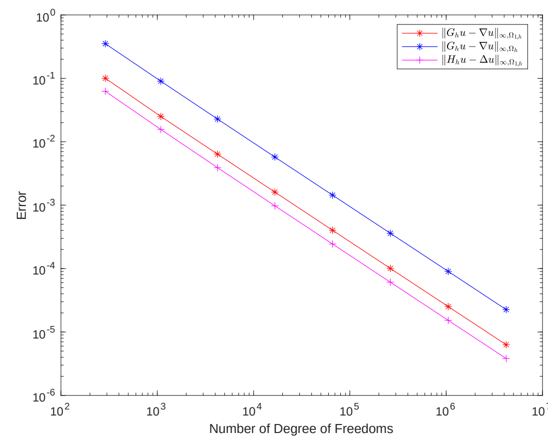

Define $u_h(z_i)$ as value of all the N nodes on the mesh. Finally, with boundary condition, an matrix equation will be attained.

$$(-H_h^{xx} - H_h^{yy})u_h(z_i) = \begin{bmatrix} f_1 \\ f_2 \\ \vdots \\ f_{M-1} \end{bmatrix} \tag{166}$$

Because the coefficients of $-H_h^{xx} - H_h^{yy}$ times boundary value are constant, so we can shift them to the right side of the equation. Solve the final matrix equation, u_h at interior nodes can be found.

8.2 Numerical Examples

To analysis accuracy of method using Gradient and Hessian Recovery to solve elliptic equations [3], error $\|u-u_h\|_{\infty,\Omega_h}$, $\|G_h u_h - \nabla u\|_{\infty,\Omega_h}$, $\|G_h u_h - \nabla u\|_{\infty,\Omega_{1,h}}$, $\|H_h u_h - \Delta u\|_{\infty,\Omega_h}$, $\|H_h u_h - \Delta u\|_{\infty,\Omega_{1,h}}$ and order will be calculated with seven exact functions u respectively in Regular Pattern and Cartesian

Dofs	$\|G_h u - \nabla u\|_{\infty,\Omega_h}$	order	$\|G_h u - \nabla u\|_{\infty,\Omega_{1,h}}$	order
289	5.5937e-01	–	1.1969e-01	–
1089	1.5058e-01	1.89	2.9911e-02	2.00
4225	3.9035e-02	1.95	7.7465e-03	1.95
16641	9.9356e-03	1.97	1.9707e-03	1.97
66049	2.5062e-03	1.99	4.9267e-04	2.00
263169	6.2934e-04	1.99	1.2317e-04	2.00
1050625	1.5769e-04	2.00	3.0859e-05	2.00
4198401	3.9466e-05	2.00	7.7231e-06	2.00

Table 26: Convergence Rate for Fifth Polynomial (G_h)

Dofs	$\|H_h u - \Delta u\|_{\infty,\Omega_h}$	order	$\|H_h u - \Delta u\|_{\infty,\Omega_{1,h}}$	order
289	1.9222e+01	–	1.3672e-01	–
1089	1.0151e+01	0.92	3.4180e-02	2.00
4225	5.2149e+00	0.96	8.6975e-03	1.97
16641	2.6428e+00	0.98	2.1935e-03	1.99
66049	1.3303e+00	0.99	5.4836e-04	2.00
263169	6.6740e-01	1.00	1.3709e-04	2.00
1050625	3.3426e-01	1.00	3.4319e-05	2.00
4198401	1.6727e-01	1.00	8.6296e-06	1.99

Table 27: Convergence Rate for Fifth Polynomial (H_h)

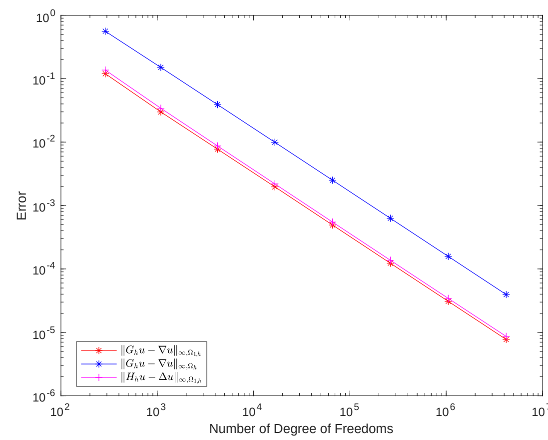

Pattern. f is defined by u, which is $-u_{xx} - u_{yy}$ after discretization. Ω_h is domain and $\Omega_{1,h}$ is the interior part of Ω_h which use Boundary 3 and $L = 0.1$.

8.2.1 Regular Pattern

After solving the equation, we draw six 3-D figures, three tables and one figure of comparison of convergence rate. The figure of comparison of convergence rate omit $\|H_h u_h - \Delta u\|_{\infty,\Omega_h}$ because the slope of it is $\frac{1}{2}$ while others are displayed as 1.

- Smooth Function: $u = \sin(\pi x) \cdot \sin(\pi y)$ (Tables 32, 33 and 34, Figure 46)

  In the below tables, we calculate error and convergence rate under degree of freedoms (Dofs) from $(2^4+1)^2$ to $(2^{11}+1)^2$. For $\|u - u_h\|_{\infty,\Omega_h}$, error decreases with the increase of Dofs and the rate is 2. For $\|G_h u_h - \nabla u\|_{\infty,\Omega_{1,h}}$ and $\|G_h u_h - \nabla u\|_{\infty,\Omega_h}$, error decreases with the increase of Dofs and the rate is also 2. But it is easily to observe that $\|G_h u_h - \nabla u\|_{\infty,\Omega_{1,h}}$ is smaller than $\|G_h u_h - \nabla u\|_{\infty,\Omega_h}$ at every Dofs. That is because at boundary nodes, the error between $G_h u_h$ and ∇u is larger than that on interior nodes. Therefore, if the domain is Ω_h, $\|u - u_h\|_\infty$

Dofs	$\|G_hu-\nabla u\|_{\infty,\Omega_h}$	order	$\|G_hu-\nabla u\|_{\infty,\Omega_{1,h}}$	order
289	2.6150e-01	–	7.6869e-02	–
1089	7.2961e-02	1.84	1.9197e-02	2.00
4225	1.9257e-02	1.92	5.0597e-03	1.92
16641	4.9459e-03	1.96	1.2984e-03	1.96
66049	1.2532e-03	1.98	3.2460e-04	2.00
263169	3.1541e-04	1.99	8.1149e-05	2.00
1050625	7.9117e-05	2.00	2.0354e-05	2.00
4198401	1.9812e-05	2.00	5.0967e-06	2.00

Table 28: Convergence Rate for Sixth Polynomial (G_h)

Dofs	$\|H_hu-\Delta u\|_{\infty,\Omega_h}$	order	$\|H_hu-\Delta u\|_{\infty,\Omega_{1,h}}$	order
289	9.4186e+00	–	9.5734e-02	–
1089	4.9723e+00	0.92	2.3928e-02	2.00
4225	2.5729e+00	0.95	6.1971e-03	1.95
16641	1.3126e+00	0.97	1.5766e-03	1.97
66049	6.6294e-01	0.99	3.9414e-04	2.00
263169	3.3314e-01	0.99	9.8534e-05	2.00
1050625	1.6699e-01	1.00	2.4689e-05	2.00
4198401	8.3600e-02	1.00	6.1874e-06	2.00

Table 29: Convergence Rate for Sixth Polynomial (H_h)

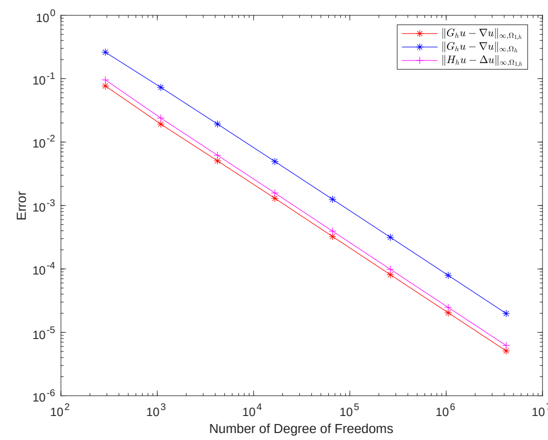

is determined by the boundary error. For $\|H_hu_h-\Delta u\|_{\infty,\Omega_{1,h}}$ and $\|H_hu_h-\Delta u\|_{\infty,\Omega_h}$, error decreases with the increase of Dofs. The rate of $\|H_hu_h-\Delta u\|_{\infty,\Omega_{1,h}}$ is 2 and $\|H_hu_h-\Delta u\|_{\infty,\Omega_h}$ is 1. $\|H_hu_h-\Delta u\|_{\infty,\Omega_{1,h}}$ is smaller than $\|H_hu_h-\Delta u\|_{\infty,\Omega_h}$ with the same reason above. However, the convergence rate is influenced greatly by the choice of domain.

Observing the figure of comparing convergence rate, it is apparent that $\|u-u_h\|_{\infty,\Omega_h}$ is the smallest. As both the operators G_h, H_h and numerical solution u_h are not exactly accurate, $\|G_hu_h-\nabla u\|_{\infty,\Omega_h}$, $\|G_hu_h-\nabla u\|_{\infty,\Omega_{1,h}}$ and $\|H_hu_h-\Delta u\|_{\infty,\Omega_h}$, $\|H_hu_h-\Delta u\|_{\infty,\Omega_{1,h}}$ are larger than $\|u-u_h\|_{\infty,\Omega_h}$ theoretically.

- Quadratic Polynomial: $u=x^2+y^2$ (Tables 35, 36 and 37, Figure 47)

  Quadratic Polynomial function can be excellent fitted by our method. Therefore, error in tables is approximate to zero. Meanwhile, convergence rate has no meaning because of the tiny error.

- Cubic Polynomial: $u=11x^3+37x^2y+73y^2+87xy+71$ (Tables 38, 39 and 40, Figure 48)

Dofs	$\|G_h u - \nabla u\|_{\infty,\Omega_h}$	order	$\|G_h u - \nabla u\|_{\infty,\Omega_{1,h}}$	order
289	5.0165e-01	–	1.4080e-01	–
1089	1.3767e-01	1.87	3.5132e-02	2.00
4225	3.6054e-02	1.93	9.4013e-03	1.90
16641	9.2245e-03	1.97	2.4309e-03	1.95
66049	2.3329e-03	1.98	6.0770e-04	2.00
263169	5.8661e-04	1.99	1.5192e-04	2.00
1050625	1.4708e-04	2.00	3.8141e-05	1.99
4198401	3.6822e-05	2.00	9.5554e-06	2.00

Table 30: Convergence Rate for Seventh Polynomial (G_h)

Dofs	$\|H_h u - \Delta u\|_{\infty,\Omega_h}$	order	$\|H_h u - \Delta u\|_{\infty,\Omega_{1,h}}$	order
289	1.8123e+01	–	2.0954e-01	–
1089	9.7223e+00	0.90	5.2349e-02	2.00
4225	5.0365e+00	0.95	1.3799e-02	1.92
16641	2.5634e+00	0.97	3.5411e-03	1.96
66049	1.2931e+00	0.99	8.8527e-04	2.00
263169	6.4945e-01	0.99	2.2132e-04	2.00
1050625	3.2545e-01	1.00	5.5511e-05	2.00
4198401	1.6290e-01	1.00	1.3909e-05	2.00

Table 31: Convergence Rate for Seventh Polynomial (H_h)

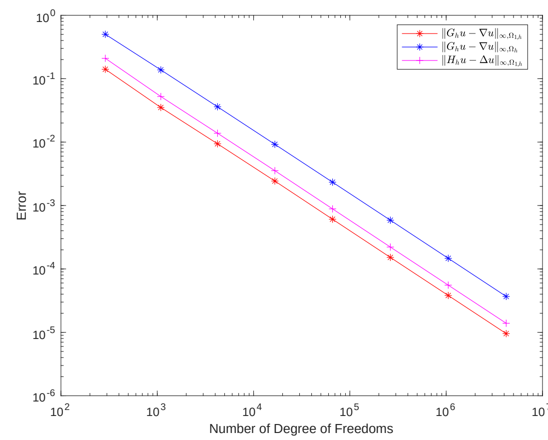

Dofs	$\|u - u_h\|_{\infty,\Omega_h}$	order
289	3.2190e-03	–
1089	8.0358e-04	2.00
4225	2.0082e-04	2.00
16641	5.0201e-05	2.00
66049	1.2550e-05	2.00
263169	3.1375e-06	2.00
1050625	7.8450e-07	2.00
4198401	1.9661e-07	2.00

Table 32: Convergence Rate for Smooth Function (u)

Dofs	$\|G_h u_h - \nabla u\|_{\infty,\Omega_h}$	order	$\|G_h u_h - \nabla u\|_{\infty,\Omega_{1,h}}$	order
289	4.9871e-02	–	2.8823e-02	–
1089	1.2311e-02	2.02	7.2454e-03	1.99
4225	3.0675e-03	2.00	1.8312e-03	1.98
16641	7.6622e-04	2.00	4.5997e-04	1.99
66049	1.9151e-04	2.00	1.1500e-04	2.00
263169	4.7876e-05	2.00	2.8750e-05	2.00
1050625	1.1968e-05	2.00	7.1910e-06	2.00
4198401	2.9906e-06	2.00	1.7968e-06	2.00

Table 33: Convergence Rate for Smooth Function (Gradient)

Similarly, Cubic Polynomial function can also be excellent fitted by our method. So tables and figures below are similar to those displayed in Quadratic Polynomial function expect the

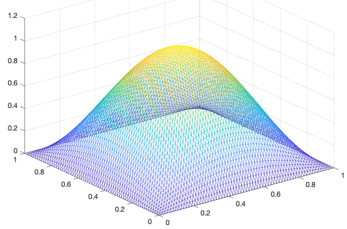

(a) FDM Solution u_h

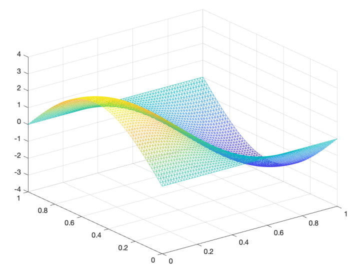

(b) $G_h^x u_h$

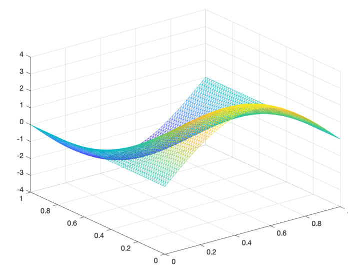

(c) $G_h^y u_h$

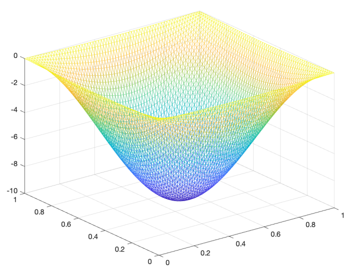

(d) $H_h^{xx} u_h$

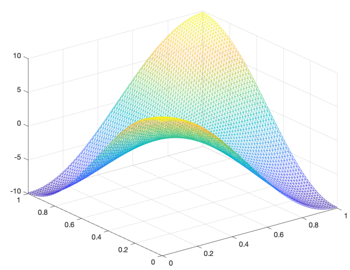

(e) $H_h^{xy} u_h$ and $H_h^{yx} u_h$

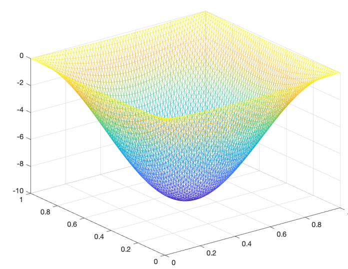

(f) $H_h^{yy} u_h$

Figure 46: Smooth Function

Dofs	$\|H_h u_h - \Delta u\|_{\infty,\Omega_h}$	order	$\|H_h u_h - \Delta u\|_{\infty,\Omega_{1,h}}$	order
289	1.3818e+00	–	9.4821e-02	–
1089	6.9181e-01	1.00	2.3762e-02	2.00
4225	3.4602e-01	1.00	5.9442e-03	2.00
16641	1.7302e-01	1.00	1.4863e-03	2.00
66049	8.6512e-02	1.00	3.7158e-04	2.00
263169	4.3256e-02	1.00	9.2896e-05	2.00
1050625	2.1628e-02	1.00	2.3224e-05	2.00
4198401	1.0814e-02	1.00	5.8073e-06	2.00

Table 34: Convergence Rate for Smooth Function (Hessian)

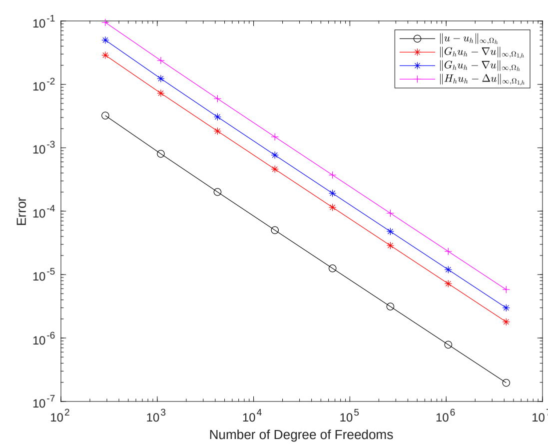

3-D figures.

Fourth Polynomial, Fifth Polynomial, Sixth Polynomial and Seventh Polynomial have the same conclusions as Smooth Function. However, in Fourth Polynomial and Fifth Polynomial, $\|G_h u_h - \nabla u\|_{\infty,\Omega_h}$ and $\|H_h u_h - \Delta u\|_{\infty,\Omega_h}$ are similar.

- Fourth Polynomial: $u = x^4 + 8x^3y + 4x^2y^2 + 4xy^3 + 2xy$ (Tables 41, 42 and 43, Figure 49)
- Fifth Polynomial: $u = 3x^5 + 4y^5 + 2x^3 + 3y^2$ (Tables 44, 45 and 46, Figure 50)

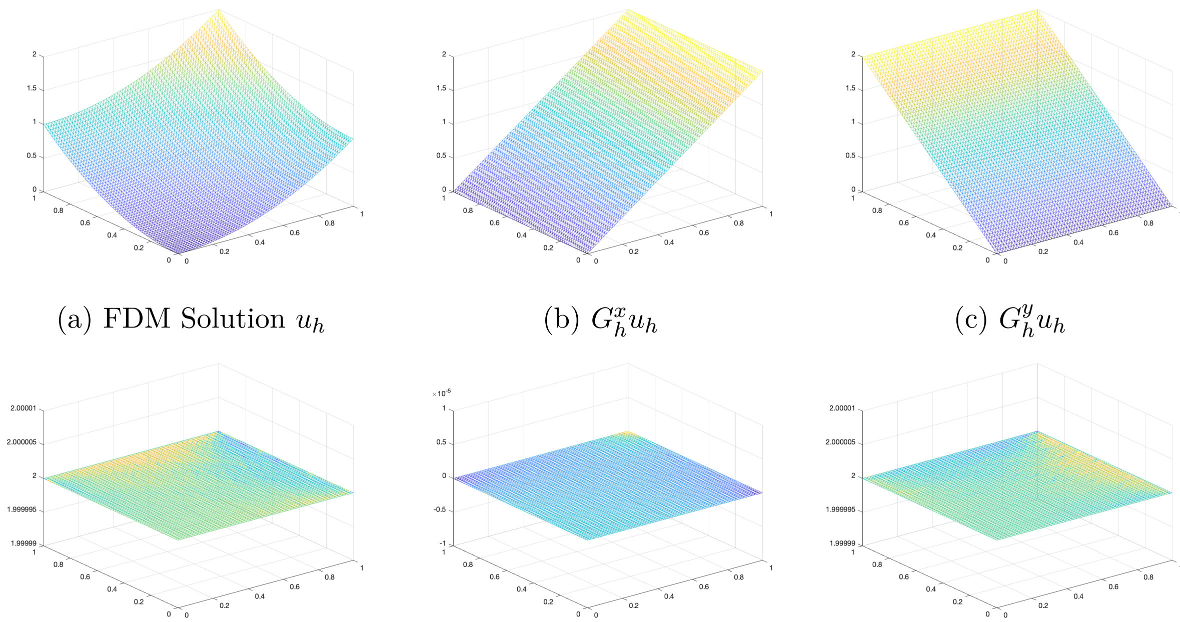

(a) FDM Solution u_h (b) $G_h^x u_h$ (c) $G_h^y u_h$

(d) $H_h^{xx} u_h$ (e) $H_h^{xy} u_h$ and $H_h^{yx} u_h$ (f) $H_h^{yy} u_h$

Figure 47: Quadratic Polynomial Function

Dofs	$\|u - u_h\|_{\infty,\Omega_h}$	order
289	2.8644e-14	–
1089	1.1591e-13	-2.02
4225	4.7040e-13	-2.02
16641	1.8926e-12	-2.01
66049	7.5877e-12	-2.00
263169	3.0346e-11	-2.00
1050625	1.2136e-10	-2.00
4198401	4.8543e-10	-2.00

Table 35: Convergence Rate for Quadratic Polynomial (u)

Dofs	$\|G_h u_h - \nabla u\|_{\infty,\Omega_h}$	order	$\|G_h u_h - \nabla u\|_{\infty,\Omega_{1,h}}$	order
289	1.5410e-13	–	9.9476e-14	–
1089	6.9367e-13	-2.17	4.0679e-13	-2.03
4225	2.9576e-12	-2.09	1.8119e-12	-2.16
16641	1.2406e-11	-2.07	7.6206e-12	-2.07
66049	4.9639e-11	-2.00	3.0390e-11	-2.00
263169	2.0101e-10	-2.02	1.2135e-10	-2.00
1050625	8.0519e-10	-2.00	4.8715e-10	-2.01
4198401	3.2309e-09	-2.00	1.9551e-09	-2.00

Table 36: Convergence Rate for Quadratic Polynomial (Gradient)

- Sixth Polynomial: $u = x^6 + y^6 + x^2y^4$ (Tables 47, 48 and 49, Figure 51)
- Seventh Polynomial: $u = x^7 + x^5y^2 + x^3y^3 + y^7$ (Tables 50, 51 and 52, Figure 52)

8.2.2 Cartesian Pattern

Conclusions in Cartesian Pattern are similar to those in Regular Pattern. But there are also some differences. First, in Smooth Function, $\|u - u_h\|_{\infty,\Omega_h}$ is not the smallest. Second, in Smooth

Dofs	$\|H_h u_h - \Delta u\|_{\infty,\Omega_h}$	order	$\|H_h u_h - \Delta u\|_{\infty,\Omega_{1,h}}$	order
289	1.0516e-12	–	3.8369e-13	–
1089	4.6612e-12	-2.15	2.7285e-12	-2.83
4225	2.6830e-11	-2.53	1.5461e-11	-2.50
16641	1.4097e-10	-2.39	4.0018e-11	-1.37
66049	6.9485e-10	-2.30	1.8917e-10	-2.24
263169	3.3615e-09	-2.27	9.3132e-10	-2.30
1050625	1.5600e-08	-2.21	4.1910e-09	-2.17
4198401	7.1479e-08	-2.20	1.8626e-08	-2.15

Table 37: Convergence Rate for Quadratic Polynomial (Hessian)

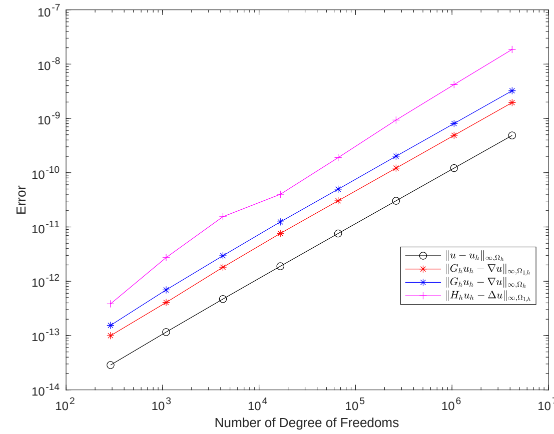

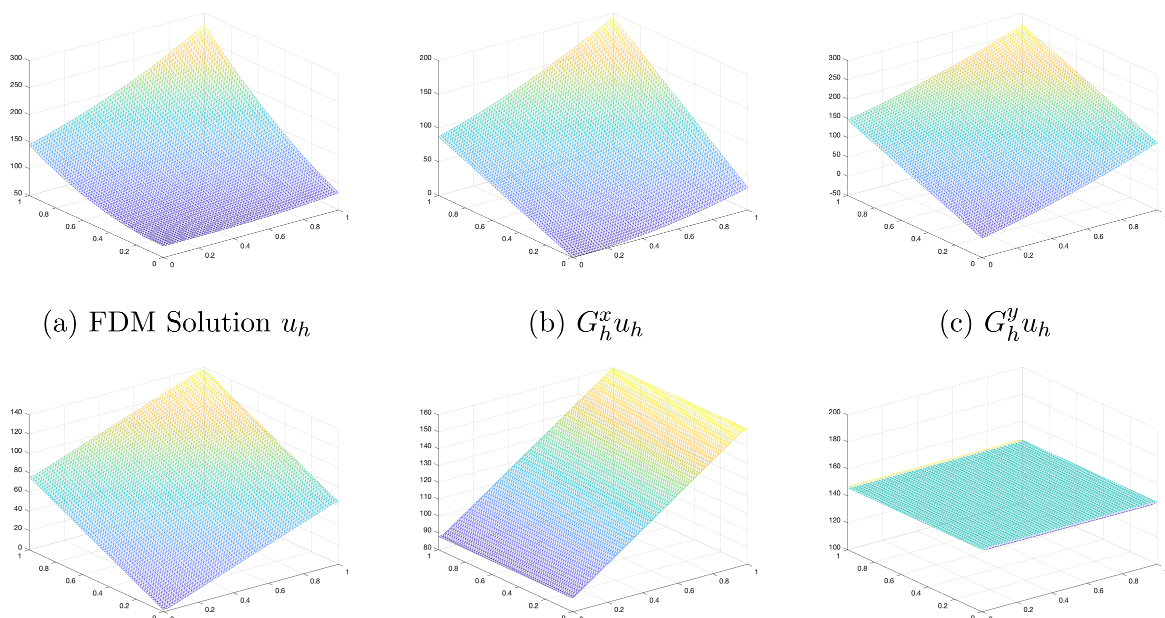

(a) FDM Solution u_h

(b) $G_h^x u_h$

(c) $G_h^y u_h$

(d) $H_h^{xx} u_h$

(e) $H_h^{xy} u_h$ and $H_h^{yx} u_h$

(f) $H_h^{yy} u_h$

Figure 48: Cubic Polynomial Function

Function, Fourth Polynomial and Fifth Polynomial, difference between $\|G_h u_h - \nabla u\|_{\infty,\Omega_h}$ and $\|H_h u_h - \Delta u\|_{\infty,\Omega_h}$ is small.

- Smooth Function: $u = \sin(\pi x) \cdot \sin(\pi y)$ (Tables 53, 54 and 55, Figure 53)
- Quadratic Polynomial: $u = x^2 + y^2$ (Tables 56, 57 and 58, Figure 54)
- Cubic Polynomial: $u = 11x^3 + 37x^2 y + 73y^2 + 87xy + 71$ (Tables 59, 60 and 61, Figure 55)

Dofs	$\|u-u_h\|_{\infty,\Omega_h}$	order
289	5.5422e-12	–
1089	2.2624e-11	-2.03
4225	9.1603e-11	-2.02
16641	3.6829e-10	-2.01
66049	1.4749e-09	-2.00
263169	5.8989e-09	-2.00
1050625	2.3589e-08	-2.00
4198401	9.4347e-08	-2.00

Table 38: Convergence Rate for Cubic Polynomial (u)

Dofs	$\|G_hu_h-\nabla u\|_{\infty,\Omega_h}$	order	$\|G_hu_h-\nabla u\|_{\infty,\Omega_{1,h}}$	order
289	3.7500e-01	–	9.1146e-02	–
1089	9.3750e-02	2.00	2.2786e-02	2.00
4225	2.3438e-02	2.00	5.6966e-03	2.00
16641	5.8594e-03	2.00	1.4242e-03	2.00
66049	1.4648e-03	2.00	3.5604e-04	2.00
263169	3.6621e-04	2.00	8.9027e-05	2.00
1050625	9.1553e-05	2.00	2.2323e-05	2.00
4198401	2.2889e-05	2.00	5.8478e-06	1.93

Table 39: Convergence Rate for Cubic Polynomial (Gradient)

Dofs	$\|H_hu_h-\Delta u\|_{\infty,\Omega_h}$	order	$\|H_hu_h-\Delta u\|_{\infty,\Omega_{1,h}}$	order
289	8.7500e+00	–	8.0036e-11	–
1089	4.3750e+00	1.00	4.0745e-10	-2.35
4225	2.1875e+00	1.00	2.5611e-09	-2.65
16641	1.0938e+00	1.00	6.9849e-09	-1.45
66049	5.4688e-01	1.00	3.5390e-08	-2.34
263169	2.7344e-01	1.00	1.4901e-07	-2.07
1050625	1.3672e-01	1.00	5.9605e-07	-2.00
4198401	6.8362e-02	1.00	4.0531e-06	-2.77

Table 40: Convergence Rate for Cubic Polynomial (Hessian)

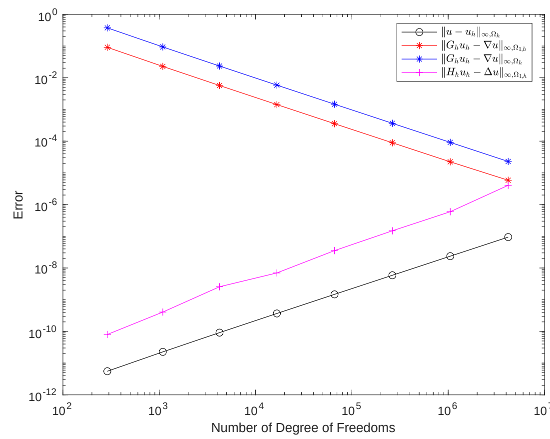

Dofs	$\|u-u_h\|_{\infty,\Omega_h}$	order
289	5.7380e-04	–
1089	1.4378e-04	2.00
4225	3.5965e-05	2.00
16641	8.9927e-06	2.00
66049	2.2483e-06	2.00
263169	5.6216e-07	2.00
1050625	1.4091e-07	2.00
4198401	3.6706e-08	1.94

Table 41: Convergence Rate for Fourth Polynomial (u)

Dofs	$\|G_hu_h-\nabla u\|_{\infty,\Omega_h}$	order	$\|G_hu_h-\nabla u\|_{\infty,\Omega_{1,h}}$	order
289	3.5195e-01	–	9.9448e-02	–
1089	9.0218e-02	1.96	2.4859e-02	2.00
4225	2.2833e-02	1.98	6.3285e-03	1.97
16641	5.7431e-03	1.99	1.5964e-03	1.99
66049	1.4401e-03	2.00	3.9910e-04	2.00
263169	3.6058e-04	2.00	9.9774e-05	2.00
1050625	9.0213e-05	2.00	2.4970e-05	2.00
4198401	2.2562e-05	2.00	6.2409e-06	2.00

Table 42: Convergence Rate for Fourth Polynomial (Gradient)

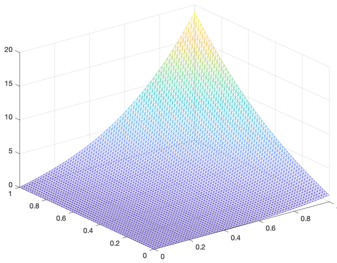

(a) FDM Solution u_h

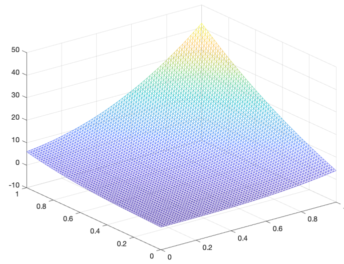

(b) $G_h^x u_h$

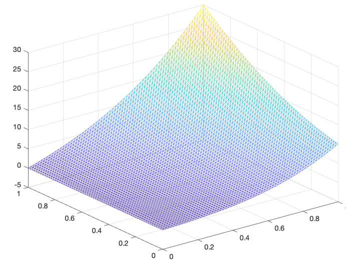

(c) $G_h^y u_h$

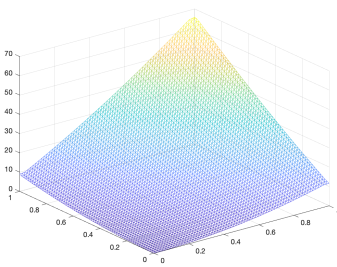

(d) $H_h^{xx} u_h$

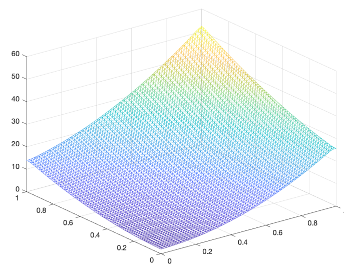

(e) $H_h^{xy} u_h$ and $H_h^{yx} u_h$

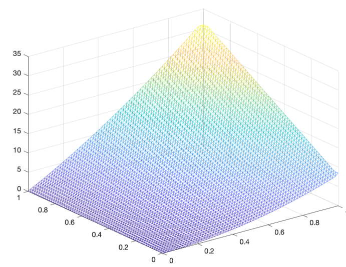

(f) $H_h^{yy} u_h$

Figure 49: Fourth-order Polynomial Function

Dofs	$\|H_h u_h - \Delta u\|_{\infty,\Omega_h}$	order	$\|H_h u_h - \Delta u\|_{\infty,\Omega_{1,h}}$	order
289	8.2088e+00	–	6.8165e-02	–
1089	4.1772e+00	0.97	1.7020e-02	2.00
4225	2.1068e+00	0.99	4.2952e-03	1.99
16641	1.0580e+00	0.99	1.0795e-03	1.99
66049	5.3011e-01	1.00	2.6986e-04	2.00
263169	2.6534e-01	1.00	6.7467e-05	2.00
1050625	1.3274e-01	1.00	1.6886e-05	2.00
4198401	6.6389e-02	1.00	4.2617e-06	1.99

Table 43: Convergence Rate for Fourth Polynomial (Hessian)

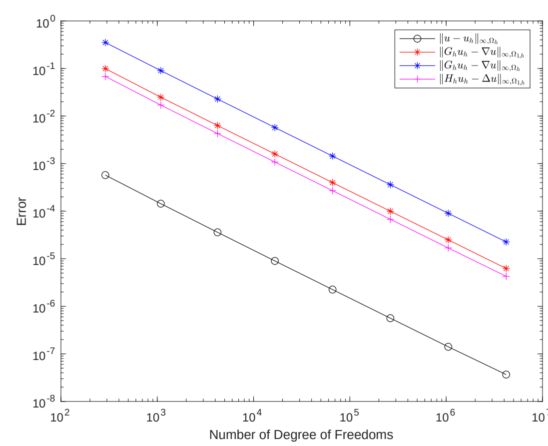

- Fourth Polynomial: $u = x^4 + 8x^3y + 4x^2y^2 + 4xy^3 + 2xy$ (Tables 62, 63 and 64, Figure 56)

- Fifth Polynomial: $u = 3x^5 + 4y^5 + 2x^3 + 3y^2$ (Tables 65, 66 and 67, Figure 57)
- Sixth Polynomial: $u = x^6 + y^6 + x^2y^4$ (Tables 68, 69 and 70, Figure 58)
- Seventh Polynomial: $u = x^7 + x^5y^2 + x^3y^3 + y^7$ (Tables 71, 72 and 73, Figure 59)

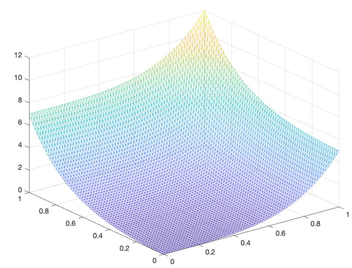

(a) FDM Solution u_h

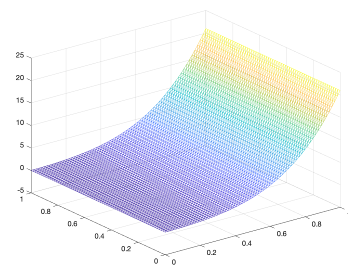

(b) $G_h^x u_h$

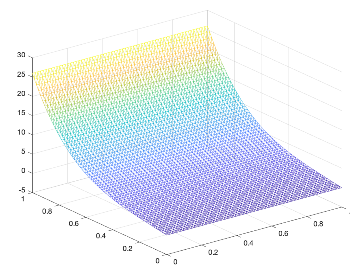

(c) $G_h^y u_h$

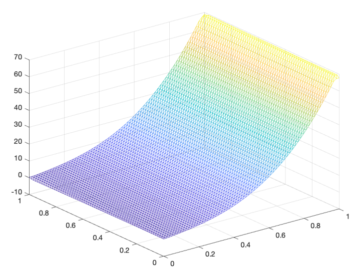

(d) $H_h^{xx} u_h$

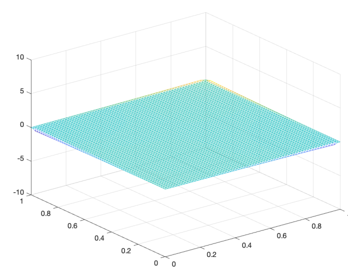

(e) $H_h^{xy} u_h$ and $H_h^{yx} u_h$

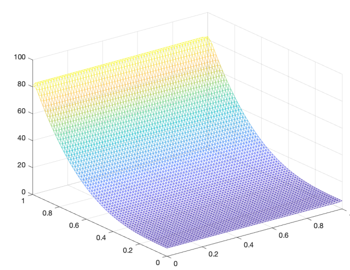

(f) $H_h^{yy} u_h$

Figure 50: Fifth-order Polynomial Function

Dofs	$\|u - u_h\|_{\infty,\Omega_h}$	order
289	1.0397e-02	–
1089	2.6055e-03	2.00
4225	6.5236e-04	2.00
16641	1.6311e-04	2.00
66049	4.0781e-05	2.00
263169	1.0195e-05	2.00
1050625	2.5492e-06	2.00
4198401	6.3880e-07	2.00

Table 44: Convergence Rate for Fifth Polynomial (u)

Dofs	$\|G_h u_h - \nabla u\|_{\infty,\Omega_h}$	order	$\|G_h u_h - \nabla u\|_{\infty,\Omega_{1,h}}$	order
289	5.6045e-01	–	1.0508e-01	–
1089	1.5071e-01	1.89	2.6331e-02	2.00
4225	3.9052e-02	1.95	6.8745e-03	1.94
16641	9.9376e-03	1.97	1.7567e-03	1.97
66049	2.5064e-03	1.99	4.3918e-04	2.00
263169	6.2938e-04	1.99	1.0980e-04	2.00
1050625	1.5769e-04	2.00	2.7524e-05	2.00
4198401	3.9466e-05	2.00	6.8881e-06	2.00

Table 45: Convergence Rate for Fifth Polynomial (Gradient)

Dofs	$\|H_h u_h - \Delta u\|_{\infty,\Omega_h}$	order	$\|H_h u_h - \Delta u\|_{\infty,\Omega_{1,h}}$	order
289	1.9234e+01	–	1.2591e-01	–
1089	1.0154e+01	0.92	3.0701e-02	2.04
4225	5.2156e+00	0.96	8.8198e-03	1.80
16641	2.6430e+00	0.98	2.3697e-03	1.90
66049	1.3304e+00	0.99	5.9217e-04	2.00
263169	6.6741e-01	1.00	1.4803e-04	2.00
1050625	3.3426e-01	1.00	3.7353e-05	1.99
4198401	1.6727e-01	1.00	9.3952e-06	1.99

Table 46: Convergence Rate for Fifth Polynomial (Hessian)

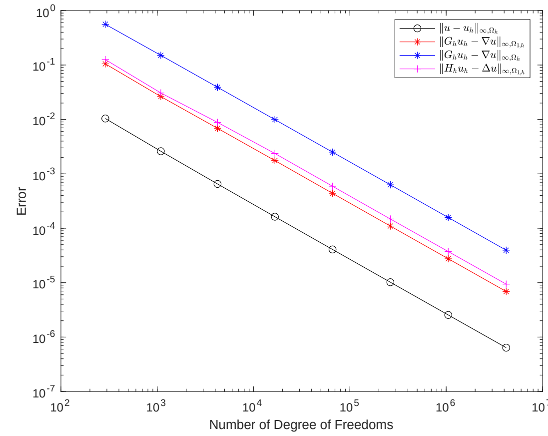

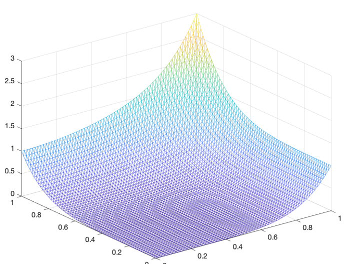

(a) FDM Solution u_h

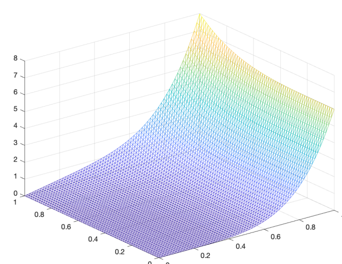

(b) $G_h^x u_h$

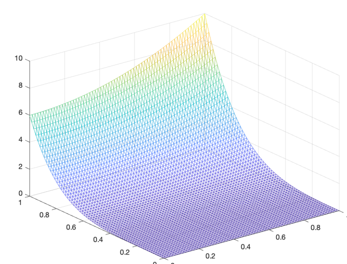

(c) $G_h^y u_h$

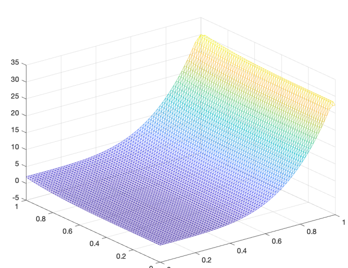

(d) $H_h^{xx} u_h$

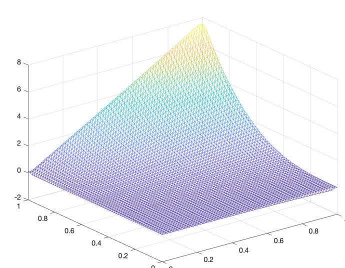

(e) $H_h^{xy} u_h$ and $H_h^{yx} u_h$

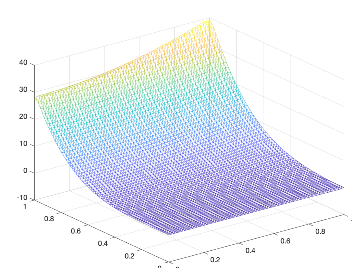

(f) $H_h^{yy} u_h$

Figure 51: Sixth-order Polynomial Function

Dofs	$\|u-u_h\|_{\infty,\Omega_h}$	order
289	5.6722e-03	–
1089	1.4228e-03	2.00
4225	3.5617e-04	2.00
16641	8.9070e-05	2.00
66049	2.2270e-05	2.00
263169	5.5677e-06	2.00
1050625	1.3920e-06	2.00
4198401	3.4816e-07	2.00

Table 47: Convergence Rate for Sixth Polynomial (u)

Dofs	$\|G_hu_h-\nabla u\|_{\infty,\Omega_h}$	order	$\|G_hu_h-\nabla u\|_{\infty,\Omega_{1,h}}$	order
289	2.6224e-01	–	6.5276e-02	–
1089	7.3056e-02	1.84	1.6268e-02	2.00
4225	1.9269e-02	1.92	4.3131e-03	1.92
16641	4.9474e-03	1.96	1.1111e-03	1.96
66049	1.2534e-03	1.98	2.7775e-04	2.00
263169	3.1543e-04	1.99	6.9437e-05	2.00
1050625	7.9120e-05	2.00	1.7425e-05	1.99
4198401	1.9813e-05	2.00	4.3640e-06	2.00

Table 48: Convergence Rate for Sixth Polynomial (Gradient)

Dofs	$\|H_hu_h-\Delta u\|_{\infty,\Omega_h}$	order	$\|H_hu_h-\Delta u\|_{\infty,\Omega_{1,h}}$	order
289	9.5006e+00	–	1.1916e-01	–
1089	4.9946e+00	0.93	2.9135e-02	2.03
4225	2.5735e+00	0.96	8.2126e-03	1.83
16641	1.3128e+00	0.97	2.1878e-03	1.91
66049	6.6298e-01	0.99	5.4674e-04	2.00
263169	3.3315e-01	0.99	1.3667e-04	2.00
1050625	1.6699e-01	1.00	3.4450e-05	1.99
4198401	8.3601e-02	1.00	8.6508e-06	1.99

Table 49: Convergence Rate for Sixth Polynomial (Hessian)

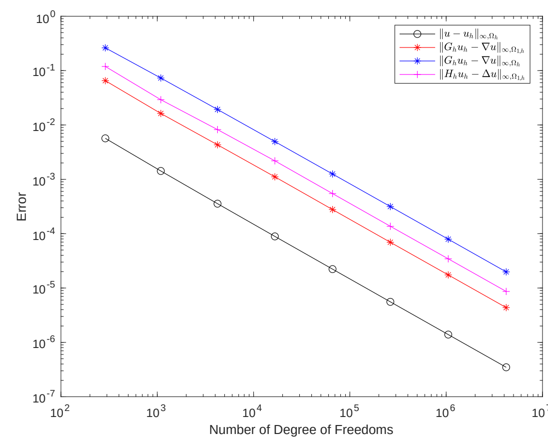

Dofs	$\|u-u_h\|_{\infty,\Omega_h}$	order
289	9.1762e-03	–
1089	2.3204e-03	1.98
4225	5.8076e-04	2.00
16641	1.4524e-04	2.00
66049	3.6315e-05	2.00
263169	9.0789e-06	2.00
1050625	2.2698e-06	2.00
4198401	5.6762e-07	2.00

Table 50: Convergence Rate for Seventh Polynomial (u)

Dofs	$\|G_hu_h-\nabla u\|_{\infty,\Omega_h}$	order	$\|G_hu_h-\nabla u\|_{\infty,\Omega_{1,h}}$	order
289	5.1476e-01	–	1.2028e-01	–
1089	1.3953e-01	1.88	2.9970e-02	2.00
4225	3.6300e-02	1.94	8.0519e-03	1.90
16641	9.2562e-03	1.97	2.0879e-03	1.95
66049	2.3370e-03	1.99	5.2195e-04	2.00
263169	5.8712e-04	1.99	1.3048e-04	2.00
1050625	1.4714e-04	2.00	3.2772e-05	1.99
4198401	3.6830e-05	2.00	8.2114e-06	2.00

Table 51: Convergence Rate for Seventh Polynomial (Gradient)

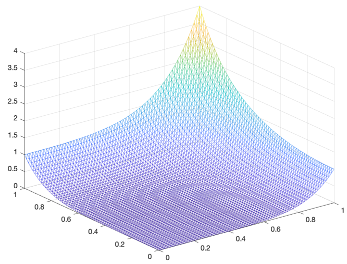

(a) FDM Solution u_h

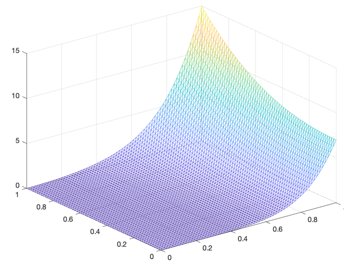

(b) $G_h^x u_h$

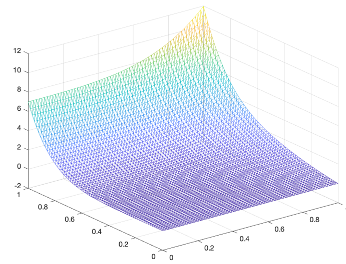

(c) $G_h^y u_h$

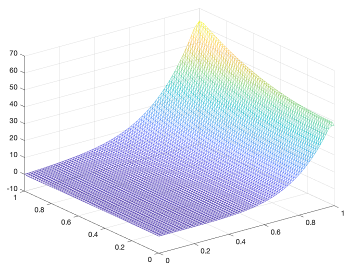

(d) $H_h^{xx} u_h$

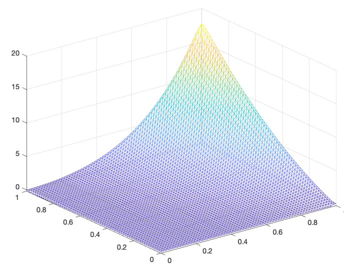

(e) $H_h^{xy} u_h$ and $H_h^{yx} u_h$

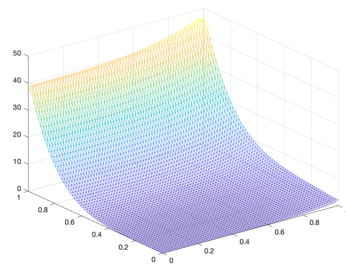

(f) $H_h^{yy} u_h$

Figure 52: Seventh-order Polynomial Function

Dofs	$\|H_h u_h - \Delta u\|_{\infty,\Omega_h}$	order	$\|H_h u_h - \Delta u\|_{\infty,\Omega_{1,h}}$	order
289	1.8307e+01	–	2.5876e-01	–
1089	9.7742e+00	0.91	6.3226e-02	2.03
4225	5.0502e+00	0.95	1.7848e-02	1.82
16641	2.5669e+00	0.98	4.7601e-03	1.91
66049	1.2940e+00	0.99	1.1895e-03	2.00
263169	6.4967e-01	0.99	2.9735e-04	2.00
1050625	3.2550e-01	1.00	7.4965e-05	1.99
4198401	1.6292e-01	1.00	1.8823e-05	1.99

Table 52: Convergence Rate for Seventh Polynomial (Hessian)

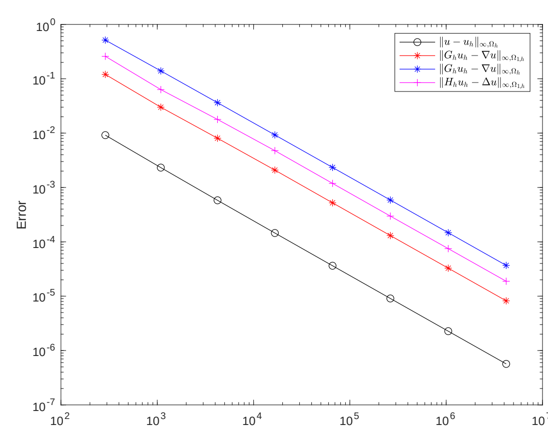

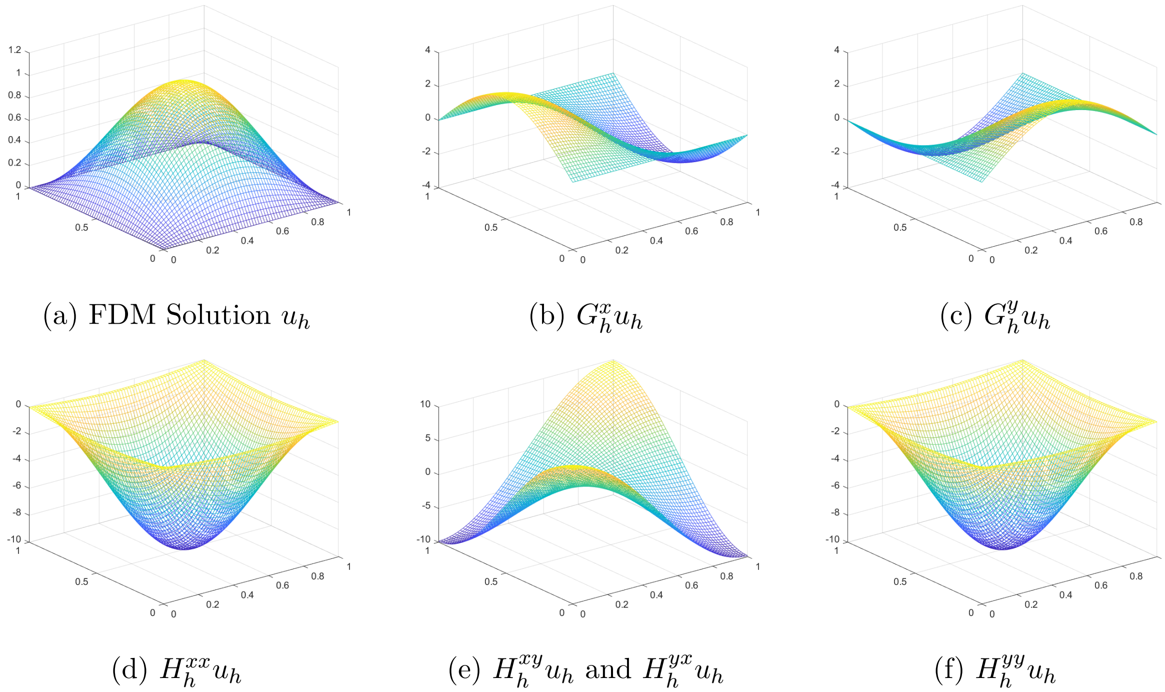

(a) FDM Solution u_h (b) $G_h^x u_h$ (c) $G_h^y u_h$

(d) $H_h^{xx} u_h$ (e) $H_h^{xy} u_h$ and $H_h^{yx} u_h$ (f) $H_h^{yy} u_h$

Figure 53: Smooth Function

Dofs	$\|u - u_h\|_{\infty,\Omega_h}$	order
289	1.6237e-02	–
1089	4.0267e-03	2.01
4225	1.0047e-03	2.00
16641	2.5104e-04	2.00
66049	6.2752e-05	2.00
263169	1.5687e-05	2.00
1050625	3.9219e-06	2.00
4198401	9.8061e-07	2.00

Table 53: Convergence Rate for Smooth Function (u)

Dofs	$\|G_h u_h - \nabla u\|_{\infty,\Omega_h}$	order	$\|G_h u_h - \nabla u\|_{\infty,\Omega_{1,h}}$	order
289	3.1804e-02	–	9.3309e-03	–
1089	7.6658e-03	2.05	2.3316e-03	2.00
4225	1.8985e-03	2.01	5.9397e-04	1.97
16641	4.7349e-04	2.00	1.4975e-04	1.99
66049	1.1830e-04	2.00	3.7437e-05	2.00
263169	2.9571e-05	2.00	9.3591e-06	2.00
1050625	7.3924e-06	2.00	2.3420e-06	2.00
4198401	1.8477e-06	2.00	5.8540e-07	2.00

Table 54: Convergence Rate for Smooth Function (Gradient)

Dofs	$\|H_h u_h - \Delta u\|_{\infty,\Omega_h}$	order	$\|H_h u_h - \Delta u\|_{\infty,\Omega_{1,h}}$	order
289	1.9043e+00	–	2.7328e-02	–
1089	9.6473e-01	0.98	6.7826e-03	2.01
4225	4.8395e-01	1.00	1.7579e-03	1.95
16641	2.4217e-01	1.00	4.4677e-04	1.98
66049	1.2111e-01	1.00	1.1168e-04	2.00
263169	6.0558e-02	1.00	2.7919e-05	2.00
1050625	3.0279e-02	1.00	6.9959e-06	2.00
4198401	1.5140e-02	1.00	2.0336e-06	1.78

Table 55: Convergence Rate for Smooth Function (Hessian)

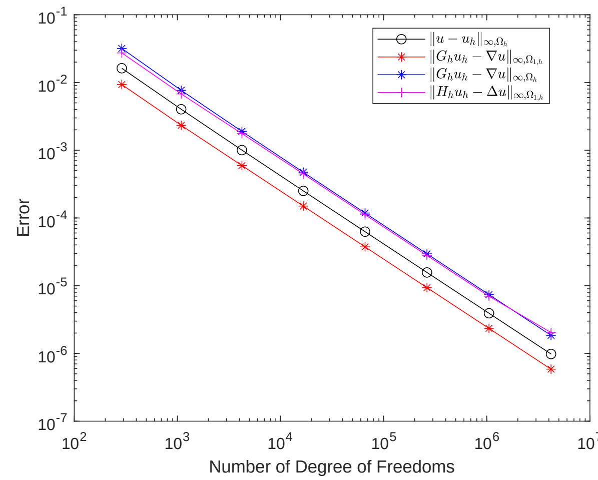

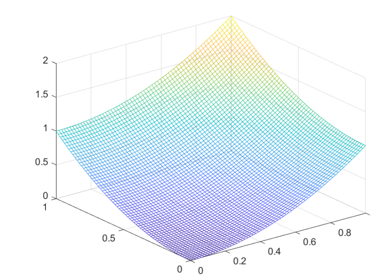

(a) FDM Solution u_h

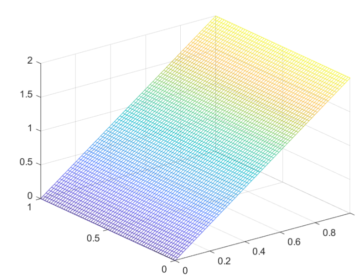

(b) $G_h^x u_h$

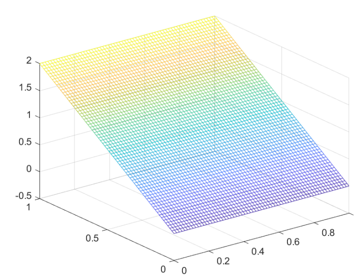

(c) $G_h^y u_h$

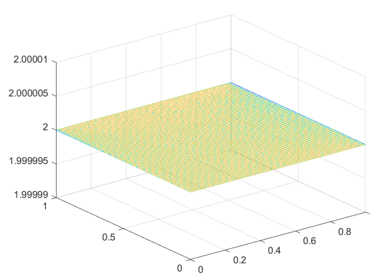

(d) $H_h^{xx} u_h$

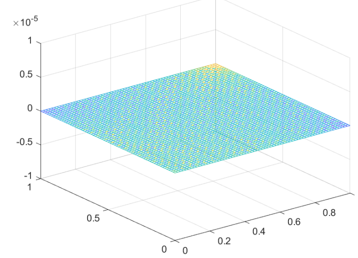

(e) $H_h^{xy} u_h$ and $H_h^{yx} u_h$

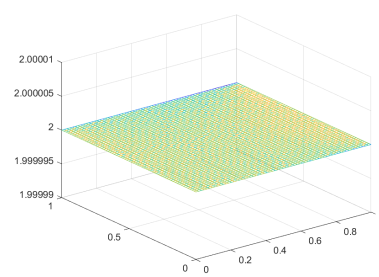

(f) $H_h^{yy} u_h$

Figure 54: Quadratic Polynomial Function

Dofs	$\|u - u_h\|_{\infty,\Omega_h}$	order
289	8.6597e-15	–
1089	3.5749e-14	-2.05
4225	1.3356e-13	-1.90
16641	5.3535e-13	-2.00
66049	2.1233e-12	-1.99
263169	8.4798e-12	-2.00
1050625	3.3851e-11	-2.00
4198401	1.3554e-10	-2.00

Table 56: Convergence Rate for Quadratic Polynomial (u)

Dofs	$\|G_h u_h - \nabla u\|_{\infty,\Omega_h}$	order	$\|G_h u_h - \nabla u\|_{\infty,\Omega_{1,h}}$	order
289	8.7041e-14	–	3.0198e-14	–
1089	2.9488e-13	-1.76	1.1813e-13	-1.97
4225	1.0694e-12	-1.86	5.1159e-13	-2.11
16641	4.0998e-12	-1.94	2.3057e-12	-2.17
66049	1.4893e-11	-1.86	8.7468e-12	-1.92
263169	5.9742e-11	-2.00	3.3907e-11	-1.95
1050625	2.3124e-10	-1.95	1.3617e-10	-2.01
4198401	9.5963e-10	-2.05	5.5809e-10	-2.04

Table 57: Convergence Rate for Quadratic Polynomial (Gradient)

Dofs	$\|H_h u_h - \Delta u\|_{\infty,\Omega_h}$	order	$\|H_h u_h - \Delta u\|_{\infty,\Omega_{1,h}}$	order
289	8.5265e-13	–	1.7053e-13	–
1089	3.8085e-12	-2.16	1.7337e-12	-3.35
4225	2.0464e-11	-2.43	7.3896e-12	-2.09
16641	1.1278e-10	-2.46	1.1187e-10	-3.92
66049	4.1655e-10	-1.89	4.1655e-10	-1.90
263169	3.3251e-09	-3.00	3.2451e-09	-2.96
1050625	1.7870e-08	-2.43	1.7870e-08	-2.46
4198401	2.0931e-07	-3.55	2.0768e-07	-3.54

Table 58: Convergence Rate for Quadratic Polynomial (Hessian)

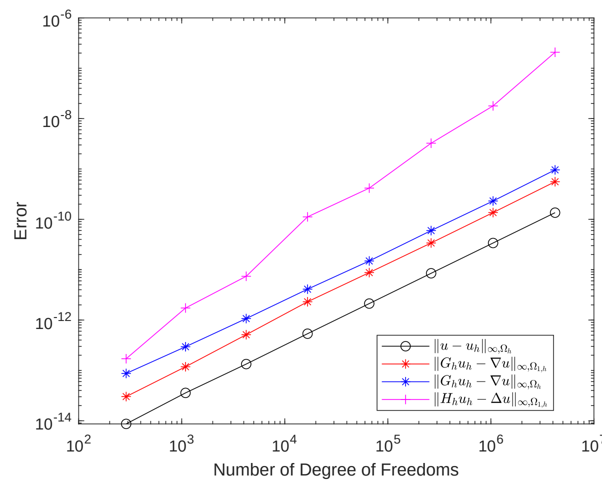

Dofs	$\|u - u_h\|_{\infty,\Omega_h}$	order
289	1.6911e-12	–
1089	6.5370e-12	-1.95
4225	2.5580e-11	-1.97
16641	1.0314e-10	-2.01
66049	4.1143e-10	-2.00
263169	1.6399e-09	-1.99
1050625	6.5599e-09	-2.00
4198401	2.6245e-08	-2.00

Table 59: Convergence Rate for Cubic Polynomial (u)

Dofs	$\|G_h u_h - \nabla u\|_{\infty,\Omega_h}$	order	$\|G_h u_h - \nabla u\|_{\infty,\Omega_{1,h}}$	order
289	3.7500e-01	–	9.6354e-02	–
1089	9.3750e-02	2.00	2.4089e-02	2.00
4225	2.3438e-02	2.00	6.0221e-03	2.00
16641	5.8594e-03	2.00	1.5055e-03	2.00
66049	1.4648e-03	2.00	3.7638e-04	2.00
263169	3.6621e-04	2.00	9.4101e-05	2.00
1050625	9.1552e-05	2.00	2.3543e-05	2.00
4198401	2.2889e-05	2.00	5.9611e-06	1.98

Table 60: Convergence Rate for Cubic Polynomial (Gradient)

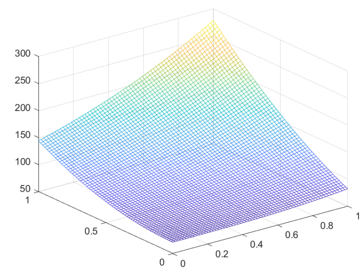

(a) FDM Solution u_h

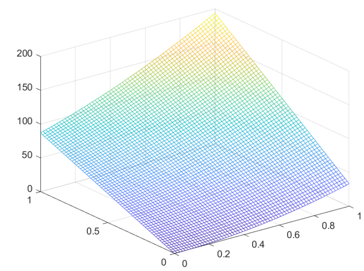

(b) $G_h^x u_h$

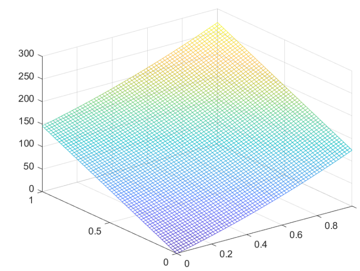

(c) $G_h^y u_h$

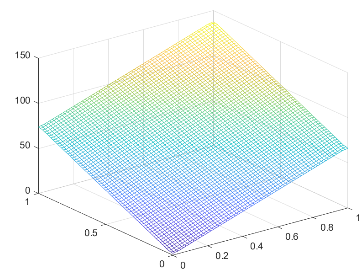

(d) $H_h^{xx} u_h$

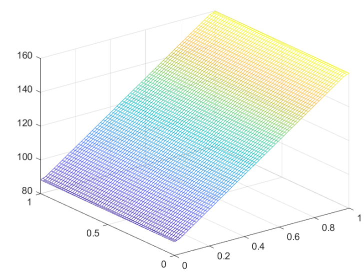

(e) $H_h^{xy} u_h$ and $H_h^{yx} u_h$

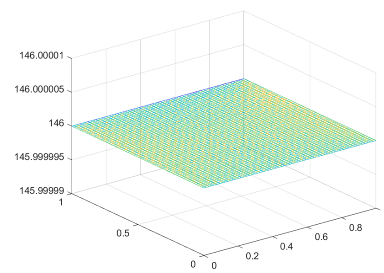

(f) $H_h^{yy} u_h$

Figure 55: Cubic Polynomial Function

Dofs	$\|H_h u_h - \Delta u\|_{\infty,\Omega_h}$	order	$\|H_h u_h - \Delta u\|_{\infty,\Omega_{1,h}}$	order
289	8.7500e+00	–	3.0923e-11	–
1089	4.3750e+00	1.00	2.1100e-10	-2.77
4225	2.1875e+00	1.00	1.3388e-09	-2.67
16641	1.0938e+00	1.00	1.0361e-08	-2.95
66049	5.4687e-01	1.00	1.2992e-07	-3.65
263169	2.7344e-01	1.00	5.4389e-07	-2.07
1050625	1.3672e-01	1.00	3.0808e-06	-2.50
4198401	6.8376e-02	1.00	5.9620e-05	-4.27

Table 61: Convergence Rate for Cubic Polynomial (Hessian)

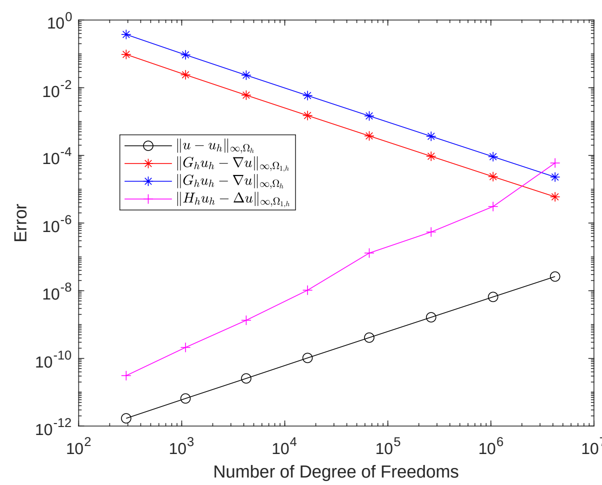

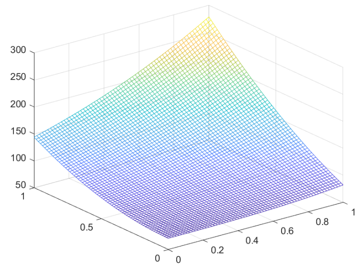

(a) FDM Solution u_h

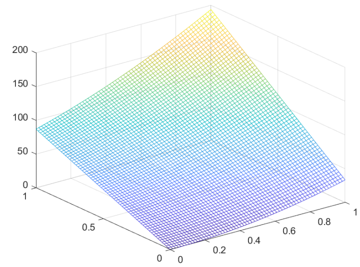

(b) $G_h^x u_h$

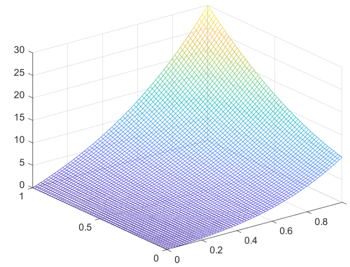

(c) $G_h^y u_h$

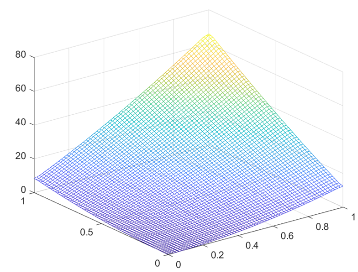

(d) $H_h^{xx} u_h$

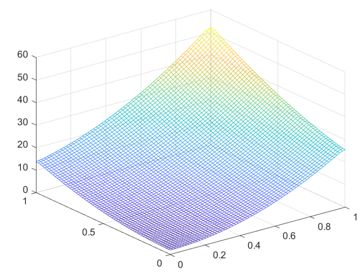

(e) $H_h^{xy} u_h$ and $H_h^{yx} u_h$

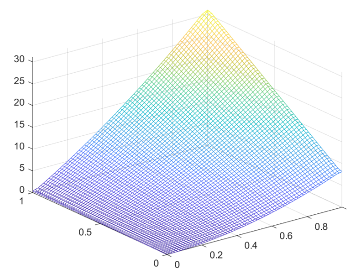

(f) $H_h^{yy} u_h$

Figure 56: Fourth-order Polynomial Function

Dofs	$\|u - u_h\|_{\infty,\Omega_h}$	order
289	3.6675e-03	–
1089	9.1268e-04	2.01
4225	2.2797e-04	2.00
16641	5.6972e-05	2.00
66049	1.4240e-05	2.00
263169	3.5598e-06	2.00
1050625	8.9005e-07	2.00
4198401	2.2292e-07	2.00

Table 62: Convergence Rate for Fourth Polynomial (u)

Dofs	$\|G_h u_h - \nabla u\|_{\infty,\Omega_h}$	order	$\|G_h u_h - \nabla u\|_{\infty,\Omega_{1,h}}$	order
289	3.5346e-01	–	8.1449e-02	–
1089	9.0403e-02	1.97	2.0358e-02	2.00
4225	2.2857e-02	1.98	5.1973e-03	1.97
16641	5.7462e-03	1.99	1.3132e-03	1.98
66049	1.4405e-03	2.00	3.2829e-04	2.00
263169	3.6063e-04	2.00	8.2072e-05	2.00
1050625	9.0219e-05	2.00	2.0545e-05	2.00
4198401	2.2563e-05	2.00	5.1388e-06	2.00

Table 63: Convergence Rate for Fourth Polynomial (Gradient)

Dofs	$\|H_h u_h - \Delta u\|_{\infty,\Omega_h}$	order	$\|H_h u_h - \Delta u\|_{\infty,\Omega_{1,h}}$	order
289	8.2305e+00	–	8.3227e-02	–
1089	4.1826e+00	0.98	2.0242e-02	2.04
4225	2.1082e+00	0.99	5.3447e-03	1.92
16641	1.0583e+00	0.99	1.3840e-03	1.95
66049	5.3020e-01	1.00	3.4424e-04	2.01
263169	2.6536e-01	1.00	8.6309e-05	2.00
1050625	1.3275e-01	1.00	2.1756e-05	1.99
4198401	6.6390e-02	1.00	5.9120e-06	1.88

Table 64: Convergence Rate for Fourth Polynomial (Hessian)

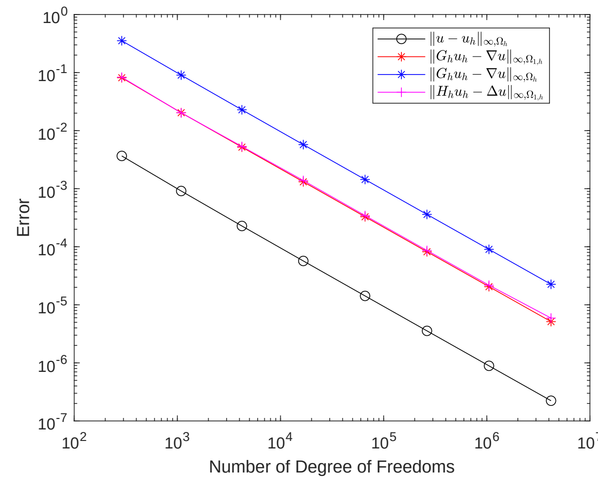

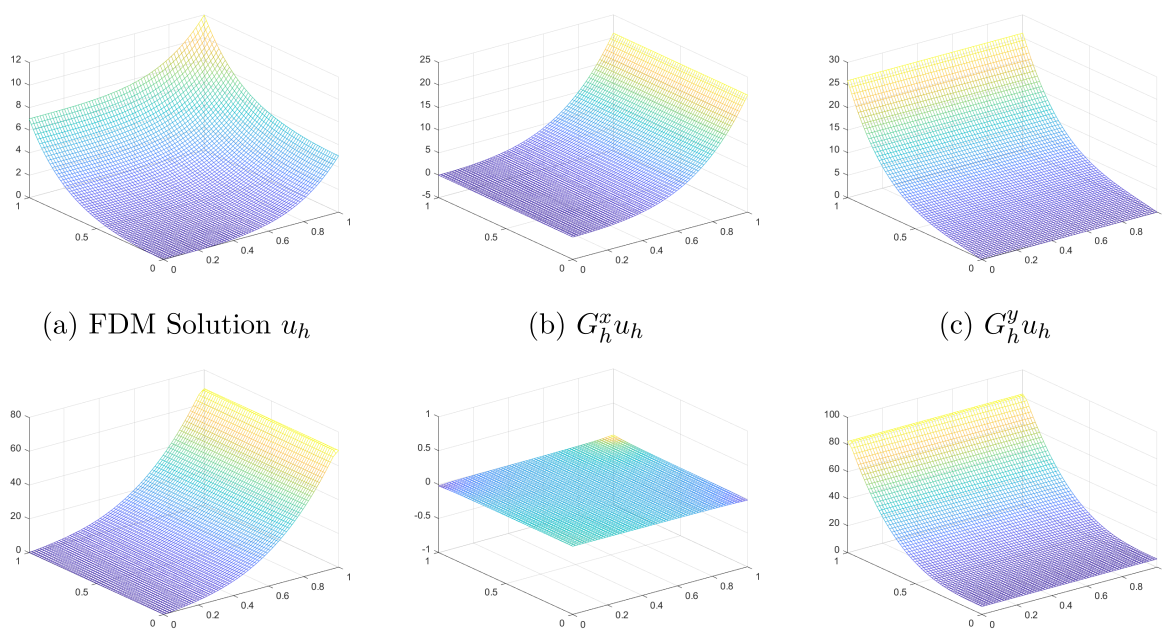

(a) FDM Solution u_h

(b) $G_h^x u_h$

(c) $G_h^y u_h$

(d) $H_h^{xx} u_h$

(e) $H_h^{xy} u_h$ and $H_h^{yx} u_h$

(f) $H_h^{yy} u_h$

Figure 57: Fifth-order Polynomial Function

Dofs	$\|u-u_h\|_{\infty,\Omega_h}$	order
289	1.0537e-02	–
1089	2.6153e-03	2.01
4225	6.5290e-04	2.00
16641	1.6314e-04	2.00
66049	4.0783e-05	2.00
263169	1.0195e-05	2.00
1050625	2.5490e-06	2.00
4198401	6.3765e-07	2.00

Table 65: Convergence Rate for Fifth Polynomial (u)

Dofs	$\|G_hu_h-\nabla u\|_{\infty,\Omega_h}$	order	$\|G_hu_h-\nabla u\|_{\infty,\Omega_{1,h}}$	order
289	4.0736e-01	–	1.0559e-01	–
1089	1.1675e-01	1.80	2.6354e-02	2.00
4225	3.1160e-02	1.91	6.8776e-03	1.94
16641	8.0430e-03	1.95	1.7567e-03	1.97
66049	2.0428e-03	1.98	4.3920e-04	2.00
263169	5.1475e-04	1.99	1.0980e-04	2.00
1050625	1.2919e-04	1.99	2.7524e-05	2.00
4198401	3.2362e-05	2.00	6.8898e-06	2.00

Table 66: Convergence Rate for Fifth Polynomial (Gradient)

Dofs	$\|H_hu_h-\Delta u\|_{\infty,\Omega_h}$	order	$\|H_hu_h-\Delta u\|_{\infty,\Omega_{1,h}}$	order
289	1.4137e+01	–	1.3039e-01	–
1089	7.2869e+00	0.96	2.9376e-02	2.15
4225	3.6973e+00	0.98	8.7696e-03	1.74
16641	1.8619e+00	0.99	2.3779e-03	1.88
66049	9.3426e-01	0.99	5.8476e-04	2.02
263169	4.6794e-01	1.00	1.5409e-04	1.92
1050625	2.3417e-01	1.00	3.8074e-05	2.02
4198401	1.1714e-01	1.00	1.1085e-05	1.78

Table 67: Convergence Rate for Fifth Polynomial (Hessian)

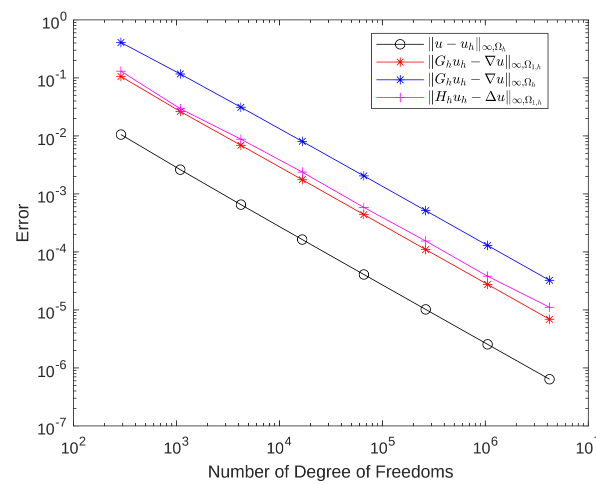

Dofs	$\|u-u_h\|_{\infty,\Omega_h}$	order
289	7.2553e-03	–
1089	1.8050e-03	2.01
4225	4.4958e-04	2.01
16641	1.1236e-04	2.00
66049	2.8088e-05	2.00
263169	7.0219e-06	2.00
1050625	1.7555e-06	2.00
4198401	4.3891e-07	2.00

Table 68: Convergence Rate for Sixth Polynomial (u)

Dofs	$\|G_hu_h-\nabla u\|_{\infty,\Omega_h}$	order	$\|G_hu_h-\nabla u\|_{\infty,\Omega_{1,h}}$	order
289	2.5723e-01	–	5.8793e-02	–
1089	6.7856e-02	1.92	1.4596e-02	2.01
4225	1.8010e-02	1.91	3.8789e-03	1.91
16641	4.6975e-03	1.94	1.0011e-03	1.95
66049	1.1994e-03	1.97	2.5029e-04	2.00
263169	3.0301e-04	1.98	6.2571e-05	2.00
1050625	7.6149e-05	1.99	1.5706e-05	1.99
4198401	1.9087e-05	2.00	3.9343e-06	2.00

Table 69: Convergence Rate for Sixth Polynomial (Gradient)

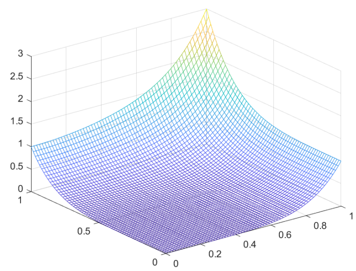

(a) FDM Solution u_h

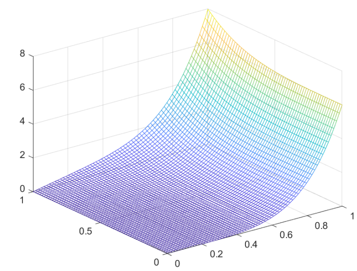

(b) $G_h^x u_h$

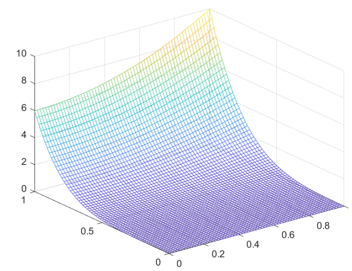

(c) $G_h^y u_h$

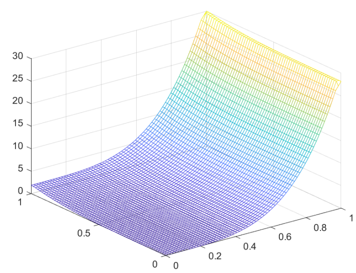

(d) $H_h^{xx} u_h$

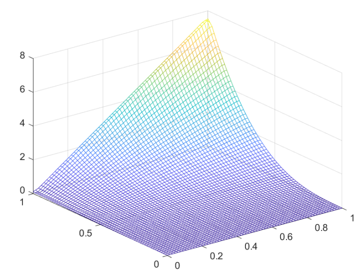

(e) $H_h^{xy} u_h$ and $H_h^{yx} u_h$

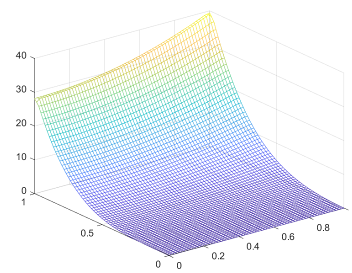

(f) $H_h^{yy} u_h$

Figure 58: Sixth-order Polynomial Function

Dofs	$\|H_h u_h - \Delta u\|_{\infty,\Omega_h}$	order	$\|H_h u_h - \Delta u\|_{\infty,\Omega_{1,h}}$	order
289	9.5552e+00	–	1.2587e-01	–
1089	5.0082e+00	0.93	2.8504e-02	2.14
4225	2.5640e+00	0.97	8.5152e-03	1.74
16641	1.2972e+00	0.98	2.2879e-03	1.90
66049	6.5240e-01	0.99	5.6433e-04	2.02
263169	3.2716e-01	1.00	1.4946e-04	1.92
1050625	1.6382e-01	1.00	3.6794e-05	2.02
4198401	8.1971e-02	1.00	1.0966e-05	1.75

Table 70: Convergence Rate for Sixth Polynomial (Hessian)

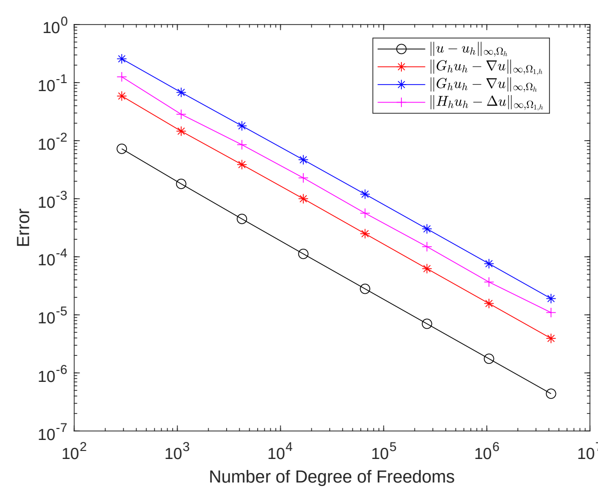

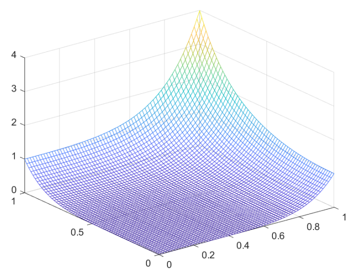

(a) FDM Solution u_h

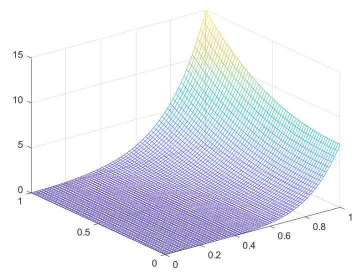

(b) $G_h^x u_h$

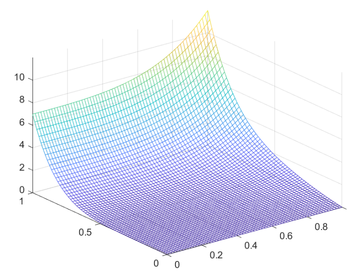

(c) $G_h^y u_h$

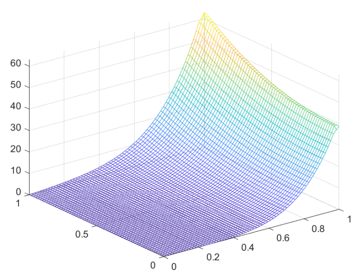

(d) $H_h^{xx} u_h$

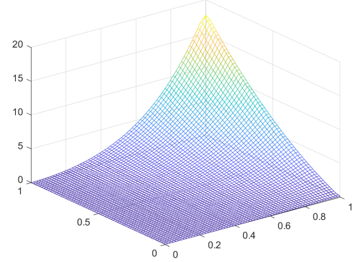

(e) $H_h^{xy} u_h$ and $H_h^{yx} u_h$

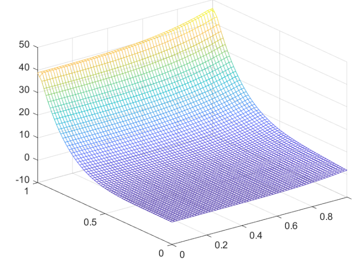

(f) $H_h^{yy} u_h$

Figure 59: Seventh-order Polynomial Function

Dofs	$\|u - u_h\|_{\infty,\Omega_h}$	order
289	1.3039e-02	–
1089	3.2480e-03	2.01
4225	8.1065e-04	2.00
16641	2.0259e-04	2.00
66049	5.0647e-05	2.00
263169	1.2662e-05	2.00
1050625	3.1654e-06	2.00
4198401	7.9140e-07	2.00

Table 71: Convergence Rate for Seventh Polynomial (u)

Dofs	$\|G_h u_h - \nabla u\|_{\infty,\Omega_h}$	order	$\|G_h u_h - \nabla u\|_{\infty,\Omega_{1,h}}$	order
289	5.2456e-01	–	1.0207e-01	–
1089	1.4072e-01	1.90	2.5305e-02	2.01
4225	3.6461e-02	1.95	6.8034e-03	1.90
16641	9.2776e-03	1.97	1.7662e-03	1.95
66049	2.3394e-03	1.99	4.4160e-04	2.00
263169	5.8747e-04	1.99	1.1040e-04	2.00
1050625	1.4718e-04	2.00	2.7732e-05	1.99
4198401	3.6836e-05	2.00	6.9496e-06	2.00

Table 72: Convergence Rate for Seventh Polynomial Function (Gradient)

Dofs	$\|H_h u_h - \Delta u\|_{\infty,\Omega_h}$	order	$\|H_h u_h - \Delta u\|_{\infty,\Omega_{1,h}}$	order
289	1.8454e+01	–	2.7056e-01	–
1089	9.8121e+00	0.91	6.0797e-02	2.15
4225	5.0601e+00	0.96	1.8520e-02	1.71
16641	2.5694e+00	0.98	4.9364e-03	1.91
66049	1.2946e+00	0.99	1.2145e-03	2.02
263169	6.4983e-01	0.99	3.2536e-04	1.90
1050625	3.2554e-01	1.00	7.9620e-05	2.03
4198401	1.6293e-01	1.00	2.4013e-05	1.73

Table 73: Convergence Rate for Seventh Polynomial Function (Hessian)

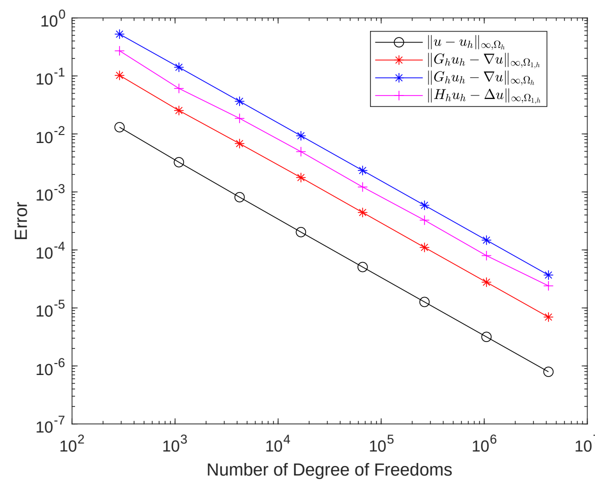

9 Concluding Remarks

In this project, we define five uniform meshes: Regular Pattern, Chevron Pattern, Criss-cross Pattern, Union-Jack Pattern and Cartesian Pattern at first. Then we mainly present two methods of PPR which called Gradient Recovery and Hessian Recovery and attain two operators, G_h and H_h. Performing them into elliptic partial differential equations, the numerical solution u_h is attained. Among the courses, we test the convergence of the operators and two methods.

Five uniform meshes are divided into two types, Regular Pattern, Chevron Pattern, Criss-cross Pattern, Union-Jack Pattern for the triangular pattern and Cartesian Pattern for the rectangular pattern in the following processes.

Gradient Recovery is explored for using surrounding nodes information to recover the gradient of a certain node. Therefore, we need to find the patch about the node in order to obtain enough data. According to relative articles and experience, it is necessary to impose boundary strategy due to possible deterioration of recovered gradient value in boundary. Thus, we can secure enough information for the recovery later. To simplify our algorithm, (x, y) coordinate is altered to (ξ, η). Consequently, the node needs to be mapped to origin, which signify the recovered gradient is only connected with the coefficient of primary terms. After gaining nodes of the patch, least square method is employed to compute the coefficient of quadratic equations $P_2(x, y)$ and calculate its first-order partial derivative, namely Gradient Recovery. Furthermore, we perform manual results of the recovered gradient and compare it with results in Mathematica. Meanwhile, we compute Taylor Expansion by Mathematica and observe symmetry and rules of both recovered gradient coefficients and Taylor Expansion. Through calculating convergence rate, we discover that gradient recovery operator is superconvergent. Simultaneously, the Taylor Expansion procured from Mathematica also proves that the operator belongs to second-order precision.

Based on Gradient Recovery, we further put forward Hessian Recovery, which is rather significant for solving elliptic partial differential equations. There exists two methods of Hessian Recovery. The first one applies gradient recovery on $G_h^x u$ and $G_h^y u$. The other one directly calculates the second-order partial derivative of $P_2(x, y)$. In our report, we adopt the second method and conduct following exploration. In Matlab, Hessian Recovery operators converge at rate of $O(h^2)$. In the meantime, the outcome of Mathematica demonstrates superconvergence as well. To guarantee the correctness of both Gradient Recovery operator and Hessian Recovery operator, some numerical examples are offered.

We employ these two operators to approximate the first-order and second-order partial derivative and take advantage of them to obtain numerical solution of elliptic partial differential equations. During the solving process, as a finite difference scheme, Hessian Recovery replaces the traditional method when solving Laplace equation. According to relative articles, we construct algorithm using Matlab and finally explore convergence rate of this method. For numerical solution and recovered gradient, the convergence rate indicates that the method converges at second-order accuracy. Recovered Hessian converges to the exact Hessian at rate of $O(h)$ in domain. However, in interior subdomain, it converges at rate of $O(h^2)$. For verifying the correctness of both Gradient Recovery and Hessian Recovery, some numerical examples are offered.

In the practical applications, polynomial preserving recovery has been adopted by commercial software, including ANSYS, Abaqus, COMSOL Multiphysics, Diffpack, LS-DYNA, etc. Moreover, it can extent the field of partial differential equations and further study adaptive meshes.

References

[1] Hailong Guo, Zhimin Zhang, and Ren Zhao. Hessian recovery for finite element methods. 2014.

[2] Hailong Guo, Zhimin Zhang, Ren Zhao, and Qingsong Zou. Polynomial preserving recovery on boundary. *Journal of Computational and Applied Mathematics*, 307:119 – 133, 2016.

[3] R. Zhao, W. Du, F. Shi, and Y. Cao. Recovery based finite difference scheme on unstructured mesh. *Applied Mathematics Letters*, 129, 2022.